# Advancing Precipitation and Transboundary Flood Forecasting in Monsoon Climates

Md S Sikder

A dissertation

submitted in partial fulfillment of the

requirements for the degree of

Doctor of Philosophy

University of Washington

2018

Reading Committee:

Faisal Hossain, Chair

Erkan Istanbulluoglu

Roger A. Pielke Sr.

Program Authorized to Offer Degree:

Department of Civil and Environmental Engineering

University of Washington

## Abstract

Advancing Precipitation and Transboundary Flood Forecasting in Monsoon Climates

Md S Sikder

Chair of the Supervisory Committee:
Professor Faisal Hossain
Department of Civil and Environmental Engineering

About a billion people are directly or indirectly affected by annual monsoon flooding in South and Southeast Asia. Skillful flood forecasting is crucial in this densely populated part of the world, where most of the countries share large international river basins. Flood forecasting is a challenging task for the downstream nations in this region due to lack of upstream in-situ data. Data from global numerical weather prediction (NWP) models are now common to the operational flood forecasting agencies as an alternative to in-situ data. Many of these agencies use the NWP model as a “black box” and the impact of model configurations in operational flood forecasting system has not been extensively studied for monsoon climates. Therefore, it is appropriate to study the performance of this NWP models in monsoon flood forecasting to enhance the current systems.

Due to the current lack of structured guidance for operational users of weather and climate data for flood forecasting, performance of the general circulation model (GCM), regional NWP model (Weather Research and Forecasting), and global NWP model (Global Forecasting System) were studied for monsoon regimes. Investigation shows that the GCM are not suitable for operational application at seasonal timescales, where climatology outperforms in persistence based forecasting. Next, regional NWP model (WRF) model configuration was optimized for the monsoon climate before using it for flow forecasting. Through a comprehensive investigation of possible model configurations, three different cloud microphysics and cumulus parameterization schemes were identified as optimal for monsoon climates. Investigations revealed that a generalized forecasting approach is indeed feasible for the operational NWP-based flood forecaster in South and Southeast Asia.

Finally, the most user-ready element of this study was derived from a comparison between the regional NWP model (WRF) and global NWP model (GFS) forecasted flow. The results indicate that the improvement due to the use of a regional NWP model like WRF for flow forecasting in large river basins with strong monsoon driven seasonality is marginal compared to that obtained from global NWP-based (GFS) flow forecasting. An easy to apply and computationally efficient bias correction scheme has been developed for operational application of weather forecast forcing from global NWP that can bypass the routine need for dynamic downscaling by regional NWP model. This bias correction scheme further improved skill in flow forecasting thereby making real-world application of global NWP weather forecast forcing computationally efficient in resource-constrained setting of forecasting agencies of South and Southeast Asia.

# TABLE OF CONTENTS

# LIST OF FIGURES

# LIST OF TABLES

# ACKNOWLEDGEMENTS

I would like to express my sincere gratitude to my academic advisor Dr. Faisal Hossian for his continuous support, encouragement, and patience. His guidance, thoughtful insight, and enthusiasm over the last four years helped me to accomplish my research objective. He always encourages me to do research for the benefit of the people, rather than publishing article in journals. I am greatly indebted to my advisor for giving me the opportunity to research with him and pursue my goal.

I would also like to thank my dissertation committee members, Dr. Roger A. Pielke Sr., Dr. Erkan Istanbulluoglu, and Dr. Alison Duvall for their valuable time, interest, the energy and for providing their feedback that greatly helped to improve the dissertation. In addition, I would like to thank Dr. Rebecca B. Neumann, for her time and support during my PhD qualifying exam.

Fanatical support for my final two years of graduate education at UW was provided by the NASA Earth and Space Science Fellowship (NNX16AO68H). I am extremely thankful to Dr. David Green for accepting my research proposal for this grant.

I would like to thank the members of the Sustainability, Satellites, Water and Environment (SASWE) Research Group for their cooperation. Thanks to Xiaodong Chen for providing technical support regarding Linux and WRF model in many occasions. Also, an especial thanks to Asif Mahmood and Nishan Biswas for their continuous support and encouragement during this study. I would like to thank Matthew Bonnema, Shahryar Ahmad, Hisham Eldardiry for

their support. I am also thankful to former SASWE group members, Mehedi Maswood and Naveed Iqbal for their encouragement in my journey.

I am grateful to all my family members, especially my parents for their great inspiration and support all through the work. I would like to thank my uncle Shahidur Rahman and Nurul Hossain Khan for their encouragement to pursue the doctoral degree.

Finally, during writing this dissertation, two of the chapters have been published in peer-reviewed journals. I would like to acknowledge the publishers, American Meteorological Society and John Wiley and Sons for granting permission to reproduce these articles in this dissertation. These articles are;

Chapter 2:

Sikder, S., X. Chen, F. Hossain, J. B. Roberts, F. Robertson, C. K. Shum, and F. J. Turk (2016), Are General Circulation Models Ready for Operational Streamflow Forecasting for Water Management in the Ganges and Brahmaputra River Basins? Journal of Hydrometeorology, 17(1), 195-210, doi:10.1175/JHM-D-14-0099.1.

Chapter 3:

Sikder, S. and F. Hossain (2016), Assessment of the weather research and forecasting model generalized parameterization schemes for advancement of precipitation forecasting in monsoon-driven river basins, Journal of Advances in Modeling Earth Systems, 8(3), 1210-1228, doi:10.1002/2016MS000678.

# DEDICATION

To my mother, for her endless love, support, and inspiration.

# Chapter 1. INTRODUCTION

## 1.1 BACKGROUND OF THE STUDY

Flood is a common natural disaster all over the world [*Yucel et al.,* 2015], and vary frequent in areas with monsoon climate (Figure 1.1) due to copious amounts of rain during that season [*Kale,* 2014]. Lack of knowledge about the real-time hydrological state of the upstream area makes flood more catastrophic in international river basins than other places. By analyzing the riverine flood data from 1985-2005, *Bakker* [2009] have shown that the number of the international river basin floods (i.e., transboundary flood) is only 10% of the total riverine floods. With this small number of occurrences, transboundary floods are responsible for 32% of total causalities, and the affected individuals could be high as 60%. *UN-Water* [2008] reported that 40% of the global population lives in the 263 shared or transboundary lake or river basins (Figure 1.1). This large population is directly or indirectly affected by the transboundary floods. The situation is worse in large transboundary river deltas in monsoon climates, such as the Bengal and Mekong deltas [*Maswood and Hossain,* 2015]. Reluctance of real time hydro-meteorological data sharing among the developing nations in such flood prone area makes the downstream nations more vulnerable to the flood hazard.

Flood forecasting with an early warning system is one of the most economic and effective ways to mitigating flood, which is a good measure to reduce the transboundary flood hazard [*CEGIS,* 2007]. Such system requires forecasted or at least real time meteorological data of the upstream region. Further geophysical data (i.e. DEM, soil and vegetation, river network, cross-section) are required to develop a physically-based (i.e., conventional model based approach) flood forecasting and warning system. A common physically-based flood forecasting system can

be divided into three major components along with warning generation and transmission (Figure 1.2). The first component is preparing real-time or generating forecast of the necessary meteorological data (e.g., precipitation, temperature), used by the hydrological model of the next component. The calibrated hydrological model uses the meteorological forcing and produces flow forecast at the basin outflow, located near the boundary of an international river. In the last component, a calibrated hydrodynamic model uses this forecasted flow as model boundary. The hydrodynamic model generates forecasted water level at various locations of the downstream river network. Finally, the forecasted water levels and generated inundation maps using these water levels are used to prepare the flood warning. Setting up of such flood forecasting system in the downstream of a transboundary river is still a challenge for the forecaster due to insufficient real-time in-situ data of the upstream [*Hossain et al.,* 2014a]. Thus, many feasible alternatives for acquiring real time and forecasted hydro-meteorological data for ungauged-transboundary river basin is an active research topic.

Several investigations of flood forecasting using the real-time satellite data indicate that the use of the real-time space-borne data (i.e., precipitation, water level) for flood forecasting in ungauged river basin is now feasible. Satellite altimetry has shown a promising performance to predict downstream river levels from upstream water level data [*Hossain et al.,* 2014b; 2014c; *Biancamaria et al.,* 2011]. In numerical model based approach (Figure 1.2), the first step for a flood forecasting is the precipitation estimation or prediction. This type of forecasting system can utilize the near real-time precipitation from the satellite. *Wardah et al.* [2008] have demonstrated the performance of the geostationary satellite precipitation product for flash flood forecasting. They were able to achieve an extra 2 hours lead time in forecasting using the satellite-based Artificial Neural Network (ANN) rain estimation coupled with a hydrological model. However,

the maximum possible lead time of a flood forecasting system with real time data is limited up to the time of concentration of the basin (Figure 1.3).

The most obvious and feasible alternative to increase the lead time beyond the time of concentration is the use of numerical atmospheric models like the General Circulation models (GCM) or Numerical Weather Prediction (NWP) models [*Yucel el al.,* 2015; *Nam et al.,* 2014; *Cloke and Pappenberger,* 2009]. In general, these global scale models are coarse in resolution. Further downscaling (i.e., statistical or dynamical) is required to make these products more usable. The regional NWP model is a tool to dynamically downscale the global NWP products. The finer scale of the regional NWP models allows one to predict the mesoscale phenomena, spatial features of various forms of precipitation, like convective precipitation. Studies have shown that the use of the regional NWP model can improve the forecast quality [*Kumar et al.,* 2016; *Givati et al.,* 2012]. Many studies have been conducted for real time flood forecasting using the regional NWP along with hydrologic and hydrodynamic models [e.g., *Liu et al.,* 2015; *Liguori et al.,* 2012; *Roberts et al.,* 2009; *Verbunt et al.,* 2006; *Jasper et al.,* 2002].

However, forecasting precipitation using the NWP models remains difficult [*Yucel el al.,* 2015; *Ebert,* 2001]. One of the leading reasons is the improper representation of the atmospheric processes, like convection [*Yucel and Onen,* 2014; *Lowrey and Yang,* 2008] through model parameterization due to incomplete understanding of processes. As precipitation is the most important meteorological input for the hydrological models [*Coe,* 2000], the skill of the forecasted flow depends on the quality of the NWP forecasted quantitative precipitation forecast (QPF) [*Yucel and Onen,* 2014; *Hapuarachchi et al.,* 2011]. The uncertainty of the QPF is propagated to the forecasted flood level through hydrologic-hydrodynamic models [*Nam et al.,* 2014; *Bartholmes and Todini,* 2005].

Many operational agencies in South and Southeast Asia in monsoon climates are currently using [*Shrestha et al.,* 2015] or have a plan [*World Bank,* 2016] to use dynamically downscaled NWP products for flood forecasting. However, there is a lack of detailed end to end studies about the performance of using this NWP products for flood forecasting in monsoon climate. Most of the studies with the NWP model are based on a storm or a set of storm events where the storms come with intense or heavy precipitation [e.g., *Ahasan and Khan,* 2013; *Hsiao et al.,* 2013; *Hong and Lee,* 2009; *Rao et al.,* 2007]. The NWP model performance need to be assessed throughout the monsoon period, including during no rain scenarios to prevent a false alarm by an operational flood forecasting system. In most cases, these operational agencies of South and Southeast Asia use the regional NWP model (e.g., Weather Research and Forecasting-WRF) as a "black box" to downscale the global NWP products (e.g., Global Forecast System-GFS). Therefore, it is appropriate to study the impact of using these NWP products for flood forecasting in that area to reduce the uncertainty of QPF and identify the optimized approach.

In this study, the performance of different numerical modelling based approaches of flood forecasting in monsoon climate has been evaluated. The goal is to identify a simple, user-ready, and skillful model based flood forecasting approach to assist the operational agencies of that flood prone area. First, the efficiency of the forecasted flow derived from statistically downscaled General Circulation Models (herein, North American Multi-Model Ensemble-NMME) forecasted meteorological data was evaluated. This is followed by a systematic study to optimize the performance of the forecasted precipitation of a regional NWP model (i.e., WRF) in monsoon climate. Finally, the forecasted meteorological data from the optimized regional NWP model and its parent global NWP model (here, GFS) have been used to derive forecasted flow. The performance of the forecasted flows from WRF and GFS have been compared with each

other to evaluate the impact of using the regional NWP model for monsoon flood forecasting. In the end, a simple and operationally suitable forecast approach for South and Southeast Asia is proposed. The research questions addressed in this dissertation are;

1) Is GCM forecasts skillful enough to use it in the operational flood forecasting system in monsoon climate?
2) Is it feasible to derive a generalized dynamic downscaling approach using the WRF model to forecast precipitation in the river basins with monsoon climate?
3) Can we develop a generalized approach of downscaling global NWP precipitation using WRF model skillful enough to for operational flood forecasting?

## 1.2 OBJECTIVE OF THE STUDY

The general objectives of this study are;

1) To evaluate the performance of numerical model based flood forecasting system in monsoon climate, using freely available space-borne data, numerical model, and model output by:
    a. evaluating the performance of statistically downscaled GCM products
    b. optimizing the dynamic downscaling process of the global NWP model (GFS) using a regional NWP model (WRF) for monsoon climate
    c. evaluating the performance of NWP (global and regional) in flood forecasting
2) To assess the feasibility of the developed flood forecasting approach for operational flood forecasting in monsoon weather, and set a guideline for the flood forecasting agencies of South and Southeast Asia.

## 1.3 OUTLINE OF THE DISSERTATION

**Chapter 2:** Are General Circulation Models Ready for Operational Streamflow Forecasting for Water Management in the Ganges and Brahmaputra River Basins?

The performance of forecasted flow derived from GCM forecasted meteorological data has been evaluated in this chapter. Here, the North American Multi-Model Ensemble (NMME) forecasted precipitation, temperature and wind speed have been used to force a calibrated Variable Infiltration Capacity (VIC) model [a hydrologic model; *Siddique-E-Akbor et al.*, 2014]. The results demonstrated that the GCMs (i.e., NMME) are not suitable for operational flood forecasting in South Asian monsoon weather. The Finding of this chapter has been published in AMS *Journal of Hydrometeorology* [*Sikder et al.*, 2016].

**Chapter 3:** Assessment of the Weather Research and Forecasting Model Generalized Parameterization Schemes for Advancement of Precipitation Forecasting in Monsoon-Driven River Basins.

Sensitivity of the WRF model performance in monsoon climate for combinations of different model parameterization schemes and model resolution was assessed in this chapter. Three different combinations of model parameterization schemes were identified among the tested, which are suitable for 9-27 km WRF model in such climate. The result of this sensitivity analysis has been published in *Journal of Advances in Modeling Earth Systems* [*Sikder and Hossain*, 2016].

**Chapter 4:** Sensitivity of Initial Condition and Cloud Microphysics to Forecasting of Monsoon Rainfall in South Asia.

Evaluation of the WRF model performance in different states continues in this chapter. The sensitivity of different model initialization techniques indicates that the simple model initialization in worthy in monsoon weather. While, complex techniques introduced more

uncertainty in the forecast. The findings of this chapter have been submitted in the *Meteorological Applications*.

**Chapter 5:** Improving Operational Flood Forecasting in Monsoon Climates with Bias-Corrected Quantitative Forecasting of Precipitation.

In the chapter, the performance of the flow derived from the WRF forecasted precipitation has been evaluated and compared with the GFS forecast. The results indicate that the value of using WRF for monsoon flood forecasting is marginal when compared to that obtained from the global (GFS) forecast. A simple bias correction technique was developed, which showed promising performance in flow forecasting as a computationally efficient solution in real-time. The summary of the results of this study has been submitted in the *International Journal of River Basin Management.*

**Chapter 6:** Conclusions and Recommendations.

This concluding chapter contains the summary of the findings, based on the results from chapter 2 to chapter 5. The chapter also includes the recommendations and directions for further studies to enhance the NWP based flood forecasting system in monsoon weather.

## 1.4 FIGURES

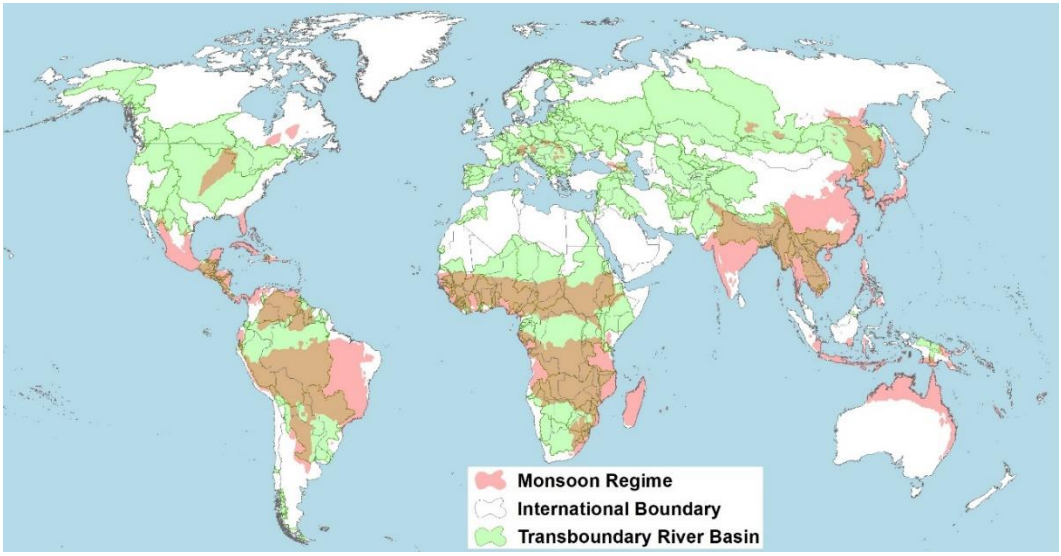


Figure 1.1. Transboundary river basins around the world along with the summer monsoon regime defined by *Zhang and Wang* [2008] [after *Jacques et al.*, 2013].

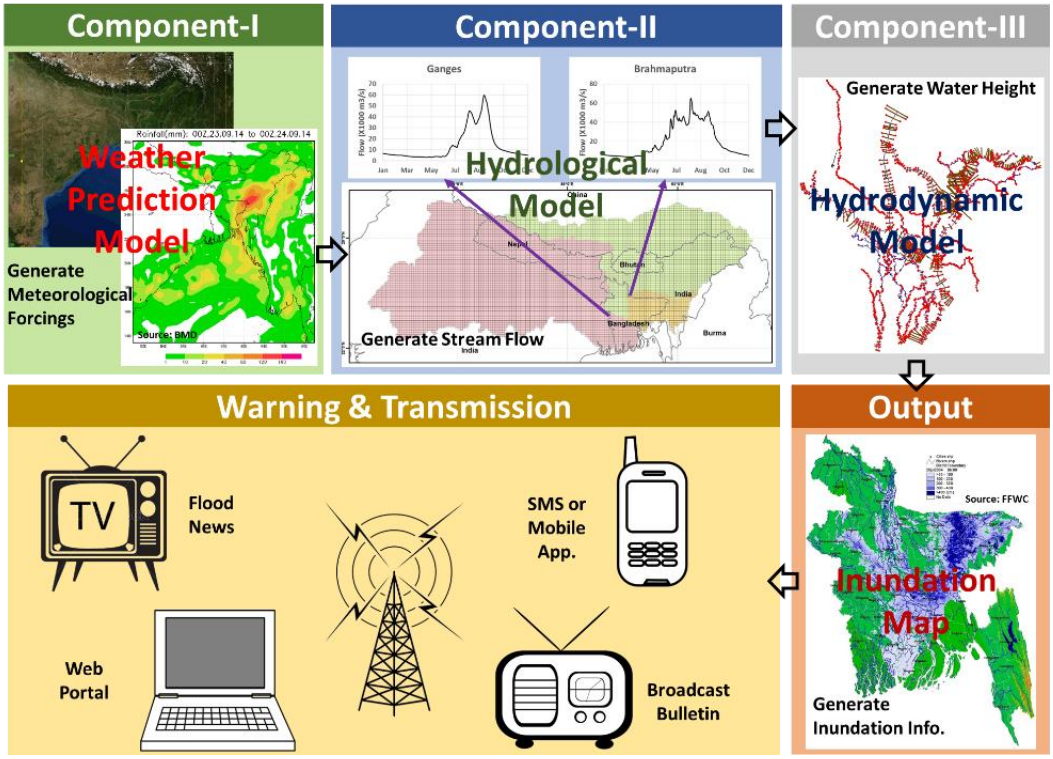


Figure 1.2. Framework of a numerical model based flood forecasting and early warning system.

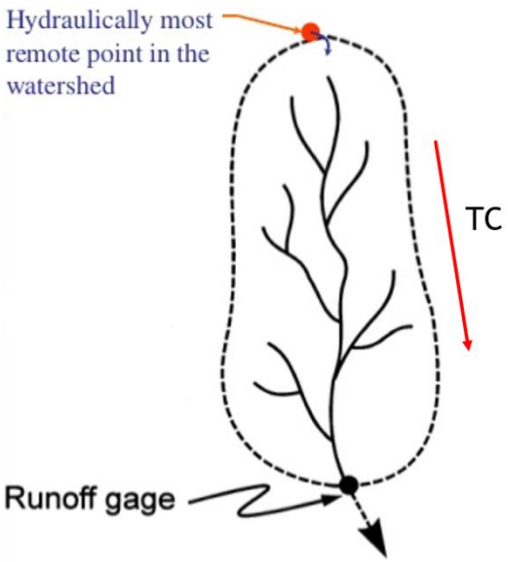


Figure 1.3. Time of concentration (TC) of river basin; time needed to travel the most remote water droplets to the basin outlet.

# Chapter 2. ARE GENERAL CIRCULATION MODELS READY FOR OPERATIONAL STREAMFLOW FORECASTING FOR WATER MANAGEMENT IN THE GANGES AND BRAHMAPUTRA RIVER BASINS?

Note: This chapter has been published in its current form as an article in *Journal of Hydrometeorology* [*Sikder et al.,* 2016]; the main differences are in section numbering and some reference information. 

**Abstract:** This study asks the question of whether GCMs are ready to be operationalized for streamflow forecasting in South Asian river basins, and if so, at what temporal scales and for which water management decisions are they likely to be relevant? The authors focused on the Ganges, Brahmaputra, and Meghna basins for which there is a gridded hydrologic model calibrated for the 2002–10 period. The North American Multi-model Ensemble (NMME) suite of eight GCM hindcasts was applied to generate precipitation forecasts for each month of the 1982–2012 (30 year) period at up to 6 months of lead time, which were then downscaled according to the bias-corrected statistical downscaling (BCSD) procedure to daily time steps. A global retrospective forcing dataset was used for this downscaling procedure. The study clearly revealed that a regionally consistent forcing for BCSD, which is currently unavailable for the region, is one of the primary conditions to realize reasonable skill in streamflow forecasting. In terms of relative RMSE (normalized by reference flow obtained from the global retrospective forcings used in downscaling), streamflow forecast uncertainty (RMSE) was found to be 38%–50% at monthly scale and 22%–35% at seasonal (3 monthly) scale. The Ganges River (regulated) experienced higher uncertainty than the Brahmaputra River (unregulated). In terms of anomaly

correlation coefficient (ACC), the streamflow forecasting at seasonal (3 monthly) scale was found to have less uncertainty (>0.3) than at monthly scale (<0.25). The forecast skill in the Brahmaputra basin showed more improvement when the time horizon was aggregated from monthly to seasonal than the Ganges basin. Finally, the skill assessment for the individual seasons revealed that the flow forecasting using NMME data had less uncertainty during monsoon season (July–September) in the Brahmaputra basin and in post-monsoon season (October–December) in the Ganges basin. Overall, the study indicated that GCMs can have value for management decisions only at seasonal or annual water balance applications at best if appropriate historical forcings are used in downscaling. The take-home message of this study is that GCMs are not yet ready for prime-time operationalization for a wide variety of multiscale water management decisions for the Ganges and Brahmaputra River basins.

## 2.1 INTRODUCTION

General circulation models (GCMs) are most commonly applied as tools for making long-term (~50–100 years) projections on future climate based on natural and anthropogenic scenarios [*IPCC,* 2013]. At the heart of their projection-making ability lies a four-dimensional framework (x, y, z, and t) to model the land, ocean, and atmosphere processes of the entire Earth in a coupled manner. This requires a comprehensive computational platform to model the physics, albeit with certain parameterizations, to achieve realistic solutions of the future state of Earth's climate. Historically, GCMs have been used mostly for addressing climate issues [*Yuan et al.,* 2015; *Wilby et al.,* 1998) in the framework of a boundary value problem [*Pielke,* 1998]. There is now an ongoing discussion if such models, with proper initialization, especially for the ocean and land states, can also be used to operationally forecast future climate variability at seasonal to

interannual time scales [*Salas et al.,* 2012, *Kundzewicz and Stakhiv,* 2010). For example, to predict streamflow at monthly to seasonal scales using a hydrologic model, GCMs can potentially provide vital information about the soil condition to initialize the model as well as the atmospheric boundary to force the model [*Yuan et al.,* 2015].

South Asia represents a clear case where such short-term climate forecasts (of mostly precipitation) could play a vital role in the water management and planning decisions for water agencies. More than 700 million people of South Asian nations, comprising India, Pakistan, Nepal, Bhutan, Bangladesh, Myanmar, Thailand, Cambodia, and Vietnam, depend on the climate-sensitive Himalayan glaciers for a significant supply of water (Table 2.1). There are several societal issues that make the operational use of seasonal-scale precipitation forecast from GCMs urgent for this populous region. First, year-round cropping to support the green revolution and food demand of South Asian nations means that the agricultural lands are never left fallow with three major growing seasons (e.g., spring–summer, summer–fall, and winter–spring). Consequently, these agricultural lands not only depend on the monsoon rains during the summer–fall (May–October) growing seasons, but they also heavily depend on the glacier and snow-fed groundwater (deep and shallow) during the non-monsoon growing seasons when streamflow or surface water availability is either low or receding [*Byerlee,* 1992]. Second, South Asia is vulnerable to uncoordinated human activity in the upstream (higher elevation) regions, such as extraction, diversion, and dam impoundment of river waters. Some pertinent examples are the Farakka Barrage [on the Ganges River; *Mirza,* 1998], the Gozaldoba Barrage (on the Teesta River, a tributary of the Brahmaputra; *Nishat and Faisal,* 2000), the now-shelved Tipaimukh Dam on the Meghna River in India [Sinha, 1995], and the much-discussed Indian River Linking Project [IRLP; *Misra et al.,* 2007]. This anthropogenic variability due to the

artificial redistribution of water (with no coordination with downstream water planning agencies) is compounded further by the seasonal variability of flow due to the monsoon. Overall, the coevolving human and natural drivers present a challenge for water managers, particularly those tasked with water resources planning and improving irrigation practices at seasonal or interseasonal time scales. Thus, forecasting surface water availability can be useful for making proactive decisions on water management [*Hossain et al.,* 2014b].

To grasp the need for forecasts of water availability along with a clear understanding of regional-scale human impacts, consider the case of the Institute of Water Modeling (IWM) in Bangladesh. The IWM functions as a trust organization for the Government of Bangladesh and is the main technical partner for water-related decision-making activity for the Ministry of Water Resources of Bangladesh [see *Hossain et al.,* 2014a]. One of the pressing needs for the IWM is to provide guidance to farmers who operate low-lift pumps for groundwater extraction (during December–April) and those who depend on surface water irrigation schemes in the Ganges tributaries (during October–December). A key surface water irrigation scheme in Bangladesh is based on one of the major tributaries of the Ganges River (known as Gorai) as it enters Bangladesh in the northwest (Fig. 2.1a). On the other hand, most groundwaterbased irrigation occurs in the Brahmaputra basin (which is mostly unregulated) in the northern part of Bangladesh (Fig. 2.1a). In both cases, skillful forecast of surface water availability is needed a few months ahead. For the Ganges River, Indian stakeholder agencies in the upstream area begin extensive diversion and withdrawal of flow during the non-monsoon period, which causes the downstream flow hydrograph to rapidly recede at downstream locations in Bangladesh. The converse is true for Brahmaputra River, which is a fast-flowing and rain-fed river basin. Thus, any precipitation forecast–based projection of water availability via hydrologic modeling can be

directly useful for season-to-season irrigation planning in Bangladesh if there is skill in the forecast. However, a hydrologic model without an upstream regulation component may not be able to pick up the human-altered recession in the downstream location, and thus, a simple bias adjustment of recession flow (i.e., subtracting or adding to flow approximately the flux that is being withdrawn in the upstream) during the non-monsoon period may be required to make the most of precipitation forecasts. This is in fact a common practice used by water managers.

A few other agencies in the region that have very similar decision-making needs are the Indus River System Authority (IRSA) in Pakistan, which provides guidance on the operation of water regulation structures of Indus basin, and the Central Water Commission (CWC) in India. Operational agencies are now aware that the stand-alone use of physics-based numerical models (e.g., GCMs and hydrologic and hydraulic models) that mimic the physical laws of nature may not be sufficient to project water availability that is now increasingly dominated by human decisions made by competing users and nations [see, e.g., *Vogel,* 2011]. However, forecasts of surface water availability from numerical models remains an objective, physically based starting point for an agency to add a water management component based on proxy information on how the water is likely to be regulated by the competing user located in the upstream (transboundary) region.

Based on the above tenet, this study investigates the question of whether GCMs are ready to be operationalized for streamflow forecasting for water management in South Asian river basins, and if so, at what temporal scales and water management decisions are they likely to be relevant? GCMs are essentially tailored for topdown and global-to-regional assessments and decisionmaking [*Wilby et al.,* 1998]. Water management decisions by agencies at seasonal time scales are typically made at smaller spatial scales than the scale at which GCMs are generally

applied. GCM-idealized physics processes (parameterizations) are designed for function at the computational scales on the order of 100 km and are tuned to produce realistic and energetically consistent large-scale climate. Thus, there are significant uncertainties in scaling issues and the degree to which these parameterizations can deliver realistic means and distributions of hydrometeorological variables at their finest scales relevant for decision-making. At issue is how effectively these quantities can be downscaled to drive applications (e.g., hydrologic or agricultural) models whose processes operate at much finer scales. Before GCMs can be operationally implemented for short-term (seasonal scale) decision-making for water management by South Asian agencies, a rigorous assessment of the skill of GCM is essential. End-users are particularly interested in performance metrics, including uncertainties, when evaluating whether to operationalize any new forecast product on the fly.

It should be noted that the development of streamflow forecasting systems for South Asia and in other regions has been ongoing for a number of years given the frequent occurrence of large-scale flooding and drought problems (i.e., first in the Ganges and Brahmaputra basins in Bangladesh and more recently in the Indus basin in Pakistan). Many of these systems typically have a flood-centric focus and not necessarily a water management-centric objective. For example, *Shrestha et al.* [2014] have demonstrated the forecasting of daily mean streamflow at an unregulated river location in the upper Indus using numerical weather prediction initial states from the European Centre for Medium-Range Weather Forecasts (ECMWF) to drive a hydrologic model. *Webster* [2013] has called for a need to improve weather forecasts in the developing world. *Hopson and Webster* [2010] have developed an automated system for streamflow forecasting in Bangladesh at 1–10 days by propagating calibrated ECMWF precipitation forecast ensembles through a hydrologic model. The platform for such a system

was provided by *Jian et al.* [2009], who explored the large-scale controls on streamflow at intraseasonal time scales. For gaining an understanding of the rich heritage of using climate signals in extending forecasts of hydrologic prediction systems in the United States, the reader is referred to the review of literature provided in *Hamlet and Lettenmaier* [1999a; 1999b] and *Wood et al.* [2002]. More recently, *Yuan et al.* [2015] have reviewed current climate model–based hydrologic forecasting.

Given the dominance of a monsoonal system where the majority of the precipitation occurs over a 3–5 month period, the surface water availability (flow in major rivers) is highly seasonal and skewed. At major river locations in downstream regions, such as Hardinge Bridge on the Ganges River or Bahadurabad on the Brahmaputra River (Fig. 2.1a), there exists multi-decadal records of streamflow (spanning at least 30 years or more). Such records allow the construction of flow climatology that is already used for decision-making by water management agencies at seasonal to annual time scales. Although GCMs are typically optimized to produce climate forecasts and not weather forecasts, it is nevertheless worthwhile to assess the value added by GCM-based streamflow forecasting beyond the traditional use of flow climatology.

In this study, we focus exclusively on the Ganges, Brahmaputra, and Meghna (GBM) river basins for which we have a comprehensive and calibrated hydrologic model, the three-layer Variable Infiltration Capacity model [VIC-3L; *Liang et al.*, 1994]. This model was used to convert the hydrometeorological (climate) forecast (of precipitation, temperature, and wind speed) into forecasts of surface water availability, primarily streamflow. In the remaining sections, we provide a brief overview of the North American Multi-model Ensemble (NMME) experiment protocol [*Kirtman et al.*, 2014]. This is followed by a discussion of the study region and an overview of the streamflow predictability using VIC-3L to accurately capture streamflow

dynamics. A discussion of the necessary skill corrections and downscaling of the seasonal forecasts follows. Finally, we present our findings on the forecast skill of precipitation and streamflow to evaluate how ready GCMs are for prime-time use by South Asian agencies. We openly discuss the key issues that need a resolution to raise the application readiness of GCM-based forecasting of water availability for water managers of South Asia. This study presents an application-oriented investigation aimed at judging the application readiness level (ARL) of GCMs for seasonal-scale transboundary water management in South Asia.

## 2.2 NMME FOR PRECIPITATION FORECASTING

We have applied the suite of general circulation models that have recently been organized under the auspices of the NMME initiative. As advocated by a recent U.S. National Academies report [*NRC*, 2010], a collaborative and coordinated implementation strategy for the NMME prediction system is currently delivering real-time, global, seasonal-to-interannual predictions on the NOAA Climate Prediction Center (CPC) operational schedule [*Kirtman et al.*, 2014].

It is expected that multi-model ensembles provide improved forecasts through not only systematic error cancellation but improved sampling of the true forecast distribution [*Hagedorn et al.*, 2005; *Funk et al.*, 2014]. The NMME protocol consists of 9-month lead (at minimum) dynamical forecasts from nine participating GCMs. A detailed list of experimental setup, available models, number of ensembles, and hindcast period can be found in *Kirtman et al.* [2014]. Here, Table 2.2 provides an adapted [from *Kirtman et al.*, 2014] and updated list of the models that are currently (as of March 2015) providing real-time forecasts and are used for constructing the multi-model ensemble forecasts. Briefly, both real-time forecasts and a set of hindcasts generally covering the period 1981–2010 are available through the International

Research Institute (IRI) for Climate and Society data portal. Archived forecast variables include precipitation, sea surface temperature (SST), and 2-m air temperature. As the NMME progresses during its second phase, a more expansive set of archived variables is being made available [*Kirtman et al.*, 2014]. Thus, the choice of NMME for our skill assessment was deemed appropriate given the increasing versatility (beyond just a few hydrometeorological variables) that NMME is expected to afford in the upcoming years. The total multi-model ensemble utilized in this study consists of 96 members obtained from eight of the contributing models. In section 5, we discuss the treatment of NMME-forecasted hydrometeorological variables for the development of downscaled scenarios necessary for resolving surface water availability at hydrologically relevant scales.

## 2.3 STUDY REGION

The study region is the GBM basin of South Asia. The total catchment area of the GBM basin is about 1.72 X $10^6$ $km^2$. The countries within the GBM basin are Bangladesh, India, Nepal, Bhutan, and China. The geographical location of the GBM basin is between 21˚ and 31˚N and 73˚ and 97˚E. The Ganges, Brahmaputra, and Meghna Rivers are the three major rivers in the GBM basin. The Himalayan and Vindhya ranges are the sources of these three rivers [*Nishat and Rahman,* 2009]. The catchment areas of different countries within the GBM basin are furnished in Table 2.3 (http://www.jrcb. gov.bd/). A map showing the region is in Fig. 2.1a.

The GBM basin exhibits extremes in surface water availability. Annual rainfall in the GBM ranges from 990 to 11,500 mm [*Shah,* 2001]. Streamflow in the downstream regions of the Brahmaputra and Ganges Rivers can vary from 5,000 in winter to 80,000 $m^3s^{-1}$ during the monsoon season [*Mirza,* 1998]. The Himalayan Range covers about 15,000 glaciers, which store

about 12,000 $km^3$ of freshwater [*Dyurgerov and Meier,* 2005]. Thus, annual water distribution in the GBM basin is highly dominated by the storage of precipitation over a long period in the Himalayas [*Chowdhury and Ward,* 2004]. In contrast, the Vindhya Range in the south, at elevations spanning 450–11,00 m, contributes significant amounts of orographic precipitation to nourish the southern tributaries of the Ganges–Yamuna system. The GBM river system is the third-largest (behind the Amazon and Congo) freshwater outlet to the world's oceans [*Chowdhury and Ward,* 2004].

## 2.4 VIC-3L

The Variable Infiltration Capacity model, first developed by *Liang et al.* [1994], was used as the macroscale distributed hydrological model. VIC is a large-scale, semidistributed macroscale hydrological model. It is capable of solving full water and energy balances. The minimum set of input forcing data that are required for simulation of the hydrologic fluxes is 1) precipitation, 2) temperature (minimum and maximum), and 3) wind speed. The basic features of VIC are as follows:

1) The land surface is modeled as a (lumped) grid of large (e.g., 12.5 km), flat, uniform cells.

2) Inputs to the model are time series of daily or subdaily meteorological drivers (e.g., rainfall, snow, air temperature, and wind speed).

3) Land–atmosphere fluxes, and the water and energy balances at the land surface, are simulated at a daily or subdaily time step. Water can only enter a grid cell via the atmosphere.

4) Grid cells are simulated independently of each other, and the entire simulation is run for each grid cell separately, one grid cell at a time, rather than for each time step, looping over all grid cells.

5) Routing of streamflow is performed separately from the land surface simulation, using a separate model. In this study, we used the routing model of *Lohmann et al.* [1998, 1996].

Previous applications of VIC in nearby and similar environments are reported in the work of *Costa-Cabral et al.* [2008] for the Mekong basin, *Shrestha et al.* [2014] for the Indus basin, and *Wu et al.* [2012] for the South Asian region. Flow routing was carried out at the locations of streamflow gauging (at Bahadurabad station in the Brahmaputra River and Hardinge Bridge in the Ganges River). The streamflow simulation using in situ forcing data (gridded from in situ weather station measurements that were available only from 2002 to 2010) is shown in Fig. 2.1b along with in situ (i.e., observed) flow measurements. Table 2.4 provides a summary of the performance of the calibrated VIC-3L against streamflow observations. On the other hand, the in situ flow-calibrated VIC-3L could be applied over a much longer period (30 years) because of availability of long-term retrospective global forcings archived by *Sheffield et al.* [2006, 2012] that were used for downscaling of GCM forecast forcings. Hydrologic simulation from 1982 to 2012 was therefore used in the skill assessment of flow forecasting relative to the retrospective global forcing. For further details on the calibration, validation, and in situ dataset preparation, the reader is referred to *Siddique-E-Akbor et al.* [2014].

Given the hydrological characteristics of the GBM basin dominated by a strong monsoonal signal each year (during June–September), streamflow in large rivers shows well-defined seasonality, particularly at lower regions of the basin with higher drainage area. Figures 2.1c and 2.1d show the simulation of streamflow for the Ganges River using in situ records that the water

resources and planning division of IWM in Bangladesh already use for seasonal-scale decision-making on water management. It should be kept in mind that this conventional decision-making on water management for the whole region of Bangladesh is afforded only at few locations where a continuous record of flow gauging exists since the 1960s for building and updating flow climatology. Thus, a spatially distributed model, if it is demonstrated to have skill at these select locations, can be a platform for estimating forecast climatology at ungauged locations (or at a collection of grid cells) where there is no measurement and yet water management decisions need to be made based on mean annual or seasonal flow or flow duration curves.

Our VIC-3L simulation of streamflow using the 1982– 2012 retrospective global forcing of *Sheffield et al.* [2006], which is used as the baseline for downscaling GCM outputs, indicates that the VIC-simulated streamflow captures quite well the interannual and interseasonal variability (for 17 out of 26 years where in situ flow data were available from 1985 to 2010; Figs. 2.1c,d). The performance metrics of VIC-3L using this baseline forcing is comparable to those obtained with in situ forcing data for the same study period (see Table 2.4 and Figs. 2.1c,d). The long-term anomaly (Figs. 2.2a,b) of the simulated streamflow from global forcing [*Sheffield et al.*, 2006] indicated that the reference forcing (used for downscaling of GCM forecast forcing) can capture the inter-annual variability for most years. For example, both basins were able to capture the extreme flooding events of 1988 and 1998 in lower regions of the Ganges and Brahmaputra basins. The annual anomaly of the Brahmaputra basin from Sheffield global forcing (SGF) matched well qualitatively (as a trend) with the observed anomaly up to 1998 and again during 2004–09 (Fig. 2.2a). For the Ganges at the Hardinge Bridge location, the SGF yielded better agreement in picking up observed flow anomaly after 1994, which is an intriguing but

unverifiable coincidence as the Ganges water sharing treaty between the governments of India and Bangladesh was signed in 1996 (Fig. 2.2b).

In general, we observe that the accuracy of the simulated flow during the 1982–2012 time period using the retrospective global forcing is significantly reduced (Table 2.4) as the simulation reflects the uncertainty due to both VIC and the SGF dataset. If we assume that VIC is able to perfectly represent the rainfall–runoff process of the basins, the quality of the simulated streamflow using the global retrospective forcing can be attributed to the uncertainty of the global forcing dataset only (Table 2.5). Comparing the values reported in Table 2.4 with those shown in Table 2.5 indicates that high uncertainty is introduced into the simulated flow because of uncertainty in the retrospective global forcing data. As an initial proof-of-concept study to assess prime-time readiness of GCM for operational streamflow forecasts, we circumvented this problem by treating the streamflow generated from global forcing–derived flow as reference flow in all subsequent skill assessment. The justification for this is that GCM forecasting forcings will not be able to exceed the skill obtained from the global forcing used in the downscaling. In this way, the uncertainty involved in the GCM downscaling using the retrospective global forcing of *Sheffield et al.* [2006] can be avoided to analyze scenarios of what if forcings to downscale GCM were perfect. Nevertheless, in the truest operational sense, we have observed, as will be shown later, that GCM-based streamflow forecasting is not ready for prime time, even for the basic water management applications (such as seasonal to annual water balance decision-making) until the quality of the historical forcing used for downscaling is improved through the creation of a more regionally consistent in situ forcing dataset. In other words, a future study of GCM forecast forcings downscaled on the basis of a more regionally relevant dataset would be worthwhile.

## 2.5 INTERANNUAL VARIABILITY AND DEVELOPMENT OF DOWNSCALED SCENARIOS

Prior to use of the NMME seasonal forecasts, GCM simulations require careful evaluation and must be downscaled to the resolution of the VIC-3L system. GCMs are typically run at a more coarse resolution than numerical weather prediction models. As such, a primary objective of GCMs is to capture the slowly evolving, large-scale components of oceanic and atmospheric dynamics. To understand the relationship between the local-scale GBM rainfall with that at the regional and global scale, an analysis has been performed using the area-average rainfall anomalies.

### 2.5.1 *Large-Scale Relationships*

A record of precipitation variability from the Asian Precipitation–Highly-Resolved Observational Data Integration Toward Evaluation of Water Resources (APHRODITE) dataset [*Yatagai et al.,* 2012] has been used to construct a standardized precipitation index (SPI) of GBM area-average rainfall. Global precipitation and SST estimates have been obtained from the Global Precipitation Climatology Project [GPCP; *Adler et al.,* 2003] and the *Reynolds et al.* [2007] Optimum Interpolation Sea Surface Temperature (OISST) dataset. Figures 2.3a and 2.3b are used to illustrate the relationships between the GBM regional-average SPI, rainfall within the GBM itself, and global-scale SST and precipitation. During most months (including January and July as illustrated), the SPI is significantly correlated ($p = 0.10$) with most locations in the GBM region. The remainder of Fig. 2.3a depicts strong correlations with SST and precipitation throughout the tropics; these patterns are reminiscent of those associated with well-known phenomena such as El Niño–Southern Oscillation (ENSO). It is known that tropical SST variability influences atmospheric convection, and together they can influence remote regions

through teleconnection patterns [*Alexander et al.,* 2002; *Klein et al.,* 1999]. Note that the connection to the GBM regional precipitation anomalies appears stronger for January than July.

It is precisely these large-scale climate anomalies and their remote teleconnections that provide a significant source of seasonal forecasting skill. In Fig. 2.3b, the same teleconnections are examined between observed SPI interannual variability and forecasted precipitation and sea surface temperature. The correlations are based on the NCEP Climate Forecast System, version 2 (CFSv2), 24-ensemble mean forecast. It is evident that the seasonal climate model forecasts are able to capture similar structures, as observed. However, the amplitudes and locations of the teleconnection patterns can vary systematically from those in Fig. 2.3a. For example, the model-forecast SST teleconnections are more narrowly constrained along the equator and somewhat eastward. There is also a strong precipitation teleconnection over the northwestern tropical Pacific (near Japan) that is not found in the observations.

### 2.5.2 *Raw Forecast Skill*

The inability to fully capture these large-scale relationships has direct influence on the ability of the model to properly translate forcing from remote tropical regions to higher latitudes. The result can be subpar performance of direct model forecasts in these tele-connected regions despite reasonably skillful forecasts within the tropics. While it is possible to apply multivariate corrections (e.g., canonical correlation analysis) trained using the hindcast datasets, it is beyond the scope of this study. Rather, this study will focus on the native forecast skill of the NMME forecasts. Figure 2.4 provides an analysis of the probabilistic forecast skill of the raw NMME forecasts. The debiased ranked probability skill score (RPSS) is computed for both rainfall and temperature forecasts following *Müller et al.* [2005]. The RPSS is evaluated at each point within the GBM basin individually, and the area-average RPSS is shown as a function of verifying

month and forecast lead. A positive value of the RPSS indicates the percentage improvement of the NMME forecast of identifying the observed tercile bin—below-, near-, or above-normal monthly average—against that of climatology (i.e., assuming equal chances for each tercile). As shown, only marginal improvement is found on average within the basin against a climatological forecast. The highest, but very modest, skill is found for the shortest lead time. We should note that the evaluation of the RPSS for individual point locations is a very stringent test, as it is expected most skill present is only found at the large, coarse resolution of the GCM. These results indicate a potentially significant shortcoming for providing distributed model forecasts for point locations. Further, it implies that at least some bias correction, particularly one that can improve the probabilistic forecast, may be needed.

### 2.5.3 *Bias Correction and Spatial Disaggregation*

For application to the VIC-3L, the NMME forecasts must be downscaled to the daily, 0.58 forcing of the model grid. The NMME forecasts are archived at monthly, 1˚ resolution. As with long-term climate projections, a downscaling approach must be employed. Here, we take the approach of bias-corrected statistical downscaling (BCSD), as established in *Wood et al.* [2002]. It is known that coupled general circulation models do not adequately capture the climatological cycle for atmospheric, land, and oceanic variables and require systematic error corrections [*Becker et al.,* 2013]. Following *Wood et al.* [2002], systematic error correction of the monthly forecasts has been implemented through use of a cumulative distribution function (CDF) matching technique. The model distributions of precipitation and temperature are CDF matched to those of the *Sheffield et al.* [2006] meteorological forcing dataset (SGF) for the years 1982–2012. Gamma distributions are used for the nonzero precipitation estimates while a Gaussian distribution is used for temperature variables. To downscale from the 1˚ NMME resolution, a

local scaling approach is applied to the bias-corrected NMME forecasts. The local scaling factor is equal to the ratio of the climatological high-resolution estimate against that obtained by resampling of the coarse-resolution climatology to the locations of the finer-resolution grid. After correcting monthly mean biases and applying the local scaling factor, daily forcing is obtained by randomly drawing a year (for the appropriate forecast month) from the historical archive of the SGF dataset. The daily values are multiplicatively scaled (zero-bounded quantities) or shifted (nonzero-bounded quantities) to match the bias-corrected NMME forecast at each grid point. If a daily rainfall value results in a value higher than that observed in the historical archive, then its total value is equally spread among its neighboring days. Because only daily average temperature is forecast by NMME, daily minimum and maximum temperatures were obtained by shifting the SGF average by the same amount, resulting in their average matching the monthly mean, as in *Wood et al.* [2002]. Wind speed is left unadjusted, as the NMME forecasts do not typically provide this variable. The BCSD approach is applied to every forecast lead for every verifying forecast month.

## 2.6 Results and Discussion

We applied the NMME suite of GCMs as an ensemble of precipitation forecasts that were made for each month of our study period (1982–2012; 372 months) and at up to 6 months of lead time. First, the forecast skill of precipitation data was assessed against the SGF dataset. Here the SGF was used as the reference data for performance analysis, because, as noted earlier, the same dataset was used to downscale the NMME data from monthly to daily scale. As our original input data (NMME data) are in monthly scale, we first show the skill of the forecast at monthly scales. The skill of the NMME precipitation was determined in terms of relative root-mean-

square error (RMSE). Also, to quantify the correlation between the observed (SGF) and the NMME forecast, the anomaly correlation coefficient (ACC) was used [*Wilks,* 2011; *Miyakoda et al.,* 1972]. Both matrices were calculated for the entire Ganges and Brahmaputra basins for the time period of 1982–2012.

Figure 2.5 shows the relative RMSE (normalized by the SGF) trend of the NMME precipitation forecast over the entire Ganges and Brahmaputra basins. It is quite clear that there is no significantly consistent trend of the relative RMSE with lead time. In addition, the difference between the RMSE values at different lead times is not significant, indicating a lack of sensitivity to the precipitation forecast horizon. However, a modestly increasing trend in RMSE (or loss of skill at longer lead times) is visible in both basins. The uncertainly of the NMME precipitation forecast in Brahmaputra basin is generally lower (<30%) than the Ganges basin (44%–48%; Fig. 2.5). The ACC trend shows a similar type of assessment for the NMME precipitation forecast (Fig. 2.6). The pattern of the ACC versus lead time is weakly correlated (<0.35) to lead time. In general, when the ACC values are below 0.6, skill is considered unsatisfactory [*Murphy and Epstein,* 1989].

Next, we performed similar assessment for streamflow forecasting at monthly time scales. The ensembles of forecast hydrograph are shown for both river locations and for specific lead times (Fig. 2.7). The reference streamflow (i.e., obtained from SGF data) is found to be bound within the forecast ensembles for most of the period when the flow is lean (November–May). In general, the Ganges River at Hardinge Bridge yields higher variability in forecast (Fig. 2.7b), while for Brahmaputra (at Bahadurabad), the forecast simulations exhibit higher precision. Forecasts in general are challenged during the late monsoon season (August–October) for the Ganges River (Fig. 2.7b) and during the monsoon season (June–September) for the Brahmaputra

River (Fig. 2.7a). The precipitation forecast yielded a probabilistic streamflow forecast that also enveloped the reference flow during the rising or receding periods of the highly seasonal flow regimes of the rivers. It should be noted that the spread of the forecast streamflow from all eight ensembles at monthly time scales was very small to yield a discernible envelope. In terms of relative RMSE (normalized by reference streamflow from SGF; Fig. 2.8, left), streamflow forecast uncertainty (RMSE) was found to be 38%–50% of the reference flow, with a more consistent trend against lead time compared to precipitation skill (i.e., RMSE rises while ACC decreases reasonably consistently as lead time increases). However, as mentioned earlier, the low ACC observed (<0.35) is indicative of poor skill at the monthly time scale. This indicates that water management based on forecasting at monthly time scales will not be appropriate for the two river basins yet.

The comparison between relative RMSE of the NMME-derived outflow (normalized by in situ observed flow and reference streamflow from SGF) is shown in Fig. 2.9 to help us understand the combined role of uncertainty due to hydrologic model and downscaling approach based on SGF data. The relative RMSE with respect to the in situ observed flow is almost flat against the lead time, which is inconsistent and points to needed improvements in downscaling using more robust and regionally appropriate forcing datasets and hydrologic model accuracy. The RMSE values normalized by the reference streamflow from SGF are slightly lower than the in situ RMSE and show a more sensitive trend to lead time. This likely proves that the use of good-quality in situ historical forcings in NMME downscaling may improve the true forecast performance. Again, we do observe that the skill values are quite high (>45%) at monthly time scales, to warrant any useful decision-making.

To explore a more appropriate time scale (than monthly) for the eventual use (operationalization) of streamflow forecast, the seasonal (3-monthly average flow) scale was analyzed. For this purpose, the year was subdivided into four seasons; January–March, April–June, July–September, and October–December. The overall performance of the seasonal analysis is shown in Fig. 2.10. The relative RMSE that was normalized by reference flow from SGF showed much more sensitivity to lead time (Fig. 2.10, left). The uncertainty in terms of relative RMSE ranged from 22% to 35% of reference flow at seasonal time scales, which is lower than the uncertainty at monthly time scales. The Brahmaputra basin showed relatively better performance in terms of relative RMSE as well as the ACC (Fig. 2.10, right). The ACC for Bahadurabad in the Brahmaputra River showed a clear decreasing trend after a 2-month lead. Also, the performance of the Brahmaputra basin significantly increases in the seasonal scale than the monthly scale in both benchmarks (Figs. 2.8, 2.10).

Last, Figs. 2.11 and 2.12 show the performance of individual seasons with respect to the reference streamflow from SGF in terms of relative RMSE and ACC, respectively. In relative RMSE standards, July–September showed the worst performance (<35%) and January–March showed the best (>10%) for both basins (Fig. 2.11). But the ACC showed that July–September in the Brahmaputra basin and October–December in the Ganges basin is more skillful than the other seasons (Fig. 2.12). In both cases, the ACC remained lower than 0.6, even at seasonal time scales.

## 2.7 CONCLUSIONS

The key features of the study findings can be summarized as follows. In terms of relative RMSE (normalized by reference flow from global forcing), streamflow forecast uncertainty was found to be higher (38%–50%) at monthly time scales and lower (22%–35%) at seasonal time scales. The Ganges River experienced higher uncertainty than the Brahmaputra River in terms of relative RMSE. Skill of the NMME flow forecast in terms of ACC showed similar outcomes, where the seasonal forecast yielded better correlation with the reference flow than the monthly scale. The forecast skill in the Brahmaputra basin showed more improvement in seasonal time scales than the Ganges basin after switching from the monthly scale. Forecast of streamflow during the late monsoon period (August–October) was found to be a little challenging for the lack of NMME precipitation forecast skill during the peak season over the Ganges basin. Overall, the ACC in both monthly and seasonal scales remained well below 0.6.

Earlier we asked whether GCMs are ready to be operationalized for streamflow forecasting in South Asian river basins, and if so, at what temporal scales and water management decisions are they likely to be relevant? Based on the summary of the findings reported above, which are mostly relative to assuming that reference flow from global forcing is perfectly representative of in situ conditions, our take-home message is that, despite skill improvement of streamflow forecast in seasonal scale for water balance applications, GCMs are not yet ready for prime-time operationalization for a wide variety of multiscale water management decisions for the Ganges and Brahmaputra River basins. In tracing the source of what is likely required to be improved a priori before revisiting these two questions, we have identified the hydrologic model and downscaling approach using a more regionally consistent forcing dataset.

Toward continuous improvement of operational readiness of GCM streamflow forecasting, future studies, in addition to creating better forcings for downscaling and models, need to address the current limitations. A primary hurdle in the way of raising skill of operational forecasting is lack of better hydrologic records and regionally consistent forcing datasets for downscaling across the entire basin [*Sikder and Hossain,* 2015; *Hossain and Katiyar,* 2006]. Assessment of GCM forecasting as well as hydrologic model improvements should be assessed at locations that represent smaller drainage areas within the GBM, lower response time (more flashiness), and less seasonality in the flow patterns of flow. For example, the Meghna basin in the northeast suffers from flash flood during spring season. Another issue to address is that of hydromorphology [*Hossain,* 2014; *Vogel,* 2011], which encompasses the difficult issue of artificial redistribution of surface water by competing upstream parties and cannot be resolved wholly using physical models forced with GCM forecast forcings alone. This is where a satellite-based observational system that routinely monitors the state of surface water (height, surface area, and volume changes) at high space–time resolution and provides clues on water redistribution can potentially be integrated in water forecast modules. Recent work on radar altimeters by *Hossain et al.* [2014b] indicates that the expanding constellation of surface water–relevant satellites may indeed make the monitoring of water management in regulated basins much more feasible. Future assessments of operational readiness of GCMs for seasonal streamflow forecasting in large river systems should therefore also involve the coupling of water management component assimilating surface water measurements from satellites with a hydrologic model so that the variability due to human activity can be teased out as much as possible.

As noted earlier, the South Asian region is vulnerable to uncertainty in water resources availability that often manifests as shortage (drought or upstream and unilateral extraction by dams or diversion projects), excess (floods), and crop-damaging natural disasters (cyclones and river flooding). Among various options to build resilience against this vulnerability, one of the most costeffective strategies with a proven benefit-to-cost ratio is to institutionalize a forecasting system that can forecast and warn of the changing dynamics of water cycle parameters [*Negri et al.,* 2005]. For example, recent rural household surveys in Bangladesh have revealed that a doubling of the flood forecasting range from 3 to 7 days can potentially minimize losses further from 3% to 20% for the Bangladesh economy [*CEGIS,* 2007]. A comprehensive water availability forecasting system during the season when water is limited or in excess can provide routine and early information to beneficiaries such as farmers and water supply managers. For all these reasons, the systematic improvement of the downscaling procedure using regionally consistent historical forcings and improved hydrologic models should be a high priority to make better use of gradually improving GCMs in the future. When GCMs are ready for operationalization, water balance–based management decisions at seasonal time scales should be practiced before pushing the envelope toward monthly time scales, which seems quite impossible according to our study given the current state of the art.

Given the findings with GCM for operational flow forecasting, the next logical step was to investigate the application of NWP models and QPF. The next set of 3 chapters explore this topic with chapter 3 exploring the performance of regional NWP and the optimization of its configuration for monsoon climates.

## 2.8 TABLES

Table 2.1. Summary of water resources vulnerability indicators for South Asian nations.

| Country | Population density ($km^{-2}$) | GDP per capita/HDI[a] | Water vulnerability index[a] | Major issues of water vulnerability[b] |
|---|---|---|---|---|
| Bangladesh | 1060 | $406/137 | 0.45 | FL, DR, CYC, GWCONT, GLM |
| Pakistan | 202 | $632/134 | 0.60 | FL, DR, CYC |
| India | 334 | $640/126 | 0.50 | FL, DR, CYC, GLM, GWCONT |
| Nepal | 179 | $252/138 | 0.40 | GLB, GLM |
| Afghanistan | 40 | $202/NA | 0.60 | DR, GLM |
| Myanmar | 74 | $702/132 | 0.30 | FL, CYC |
| Vietnam | 259 | $1170/113 | 0.31 | FL, GW CONT |

[a] HDI is the Human Development Index rank (out of all nations).
[b] FL, flood; DR, drought; CYC, cyclone; GW CONT, groundwater contamination (arsenic); GLM, glacier melt; and GLB, glacier burst. Water vulnerability varies from 0 to 1, with 1 being highly vulnerable water resources.

Table 2.2. List of NMMEs utilized in this study.

| Model | Hindcast period | Ensemble size | Maximum lead (months) | Version |
|---|---|---|---|---|
| Canadian Coupled Global Climate Model | 1981 - 2010 | 10 | 11.5 | Fourth Generation (CanCM4) |
| Community Climate System Model | 1982 - 2010 | 6 | 11.5 | 3 (CCSM3) |
| | 1982 - 2010 | 10 | 11.5 | 4 (CCSM4) |
| Geophysical Fluid Dynamics Laboratory Climate Model | 1982 - 2010 | 10 | 11.5 | 2.1 (GFDL CM2.1) |
| | 1981- 2010 | 12 | 11.5 | 2.5 (GFDL CM2.5_FLOR-A06) |
| | 1981 - 2010 | 12 | 11.5 | 2.5 (GFDL CM2.5_FLOR-B01) |
| Goddard Earth Observing System Model | 1981 - 2010 | 12 | 8.5 | 5 (GEOS-5) |
| Climate Forecast System | 1982 - 2010 | 24 | 9.5 | 2 (CFSv2) |

Table 2.3. Geographic and hydrologic model properties of the GBM basins.

| River basin | Area ($km^2$) | Model gridcell resolution (km) | No. of grids | Peak elev (m MSL) |
|---|---|---|---|---|
| Ganges | 1,087,300 | 12.5 | 5506 | 3892 |
| Brahmaputra | 552,000 | 25.0 | 1550 | 8848 |
| Meghna | 82,000 | 12.5 | 1171 | 600 |

Table 2.4. Performance of VIC-3L during 2002–10 using in situ gridded and SGF data (shown in parentheses). Performance metrics are shown for streamflow simulation against observed measurements at two downstream locations of GBM basins shown in Fig. 2.1.

| Basin | Season | RMSE ($m^3/s^{-1}$) | Correlation | Efficiency |
|---|---|---|---|---|
| Brahmaputra location: Bahadurabad | Dry (Nov-May) | 7,847 (7,340) | 0.74 (0.73) | 0.45 (0.39) |
| | Wet (Jun-Oct) | 16,230 (14,615) | 0.84 (0.75) | 0.70 (0.40) |
| | Full year | 12,088 (11,013) | 0.92 (0.88) | 0.83 (0.75) |
| Ganges location: Hardinge Bridge | Dry (Nov-May) | 4,510 (4,045) | 0.86 (0.85) | 0.23 (0.54) |
| | Wet (Jun-Oct) | 10,733 (12,931) | 0.80 (0.54) | 0.46 (0.25) |
| | Full year | 7,750 (8,919) | 0.88 (0.75) | 0.73 (0.55) |

Table 2.5. Performance of streamflow using SGF, relative to flow simulated using in situ gridded forcing data (i.e., considering no model uncertainty from VIC-3L during 2002–10). Metrics are shown for 2002–10 to allow for comparison with Table 2.4 to understand the combined effect of model and input uncertainty.

| Basin | Season | RMSE ($m^3/s^{-1}$) | Correlation | Efficiency |
|---|---|---|---|---|
| Brahmaputra location: Bahadurabad | Dry (Nov-May) | 3,523 | 0.74 | 0.45 |
| | Wet (Jun-Oct) | 13,153 | 0.76 | 0.29 |
| | Full year | 8,926 | 0.88 | 0.62 |
| Ganges location: Hardinge Bridge | Dry (Nov-May) | 1,429 | 0.88 | 0.76 |
| | Wet (Jun-Oct) | 15,602 | 0.57 | 0.33 |
| | Full year | 10,156 | 0.74 | 0.54 |

## 2.9 FIGURES

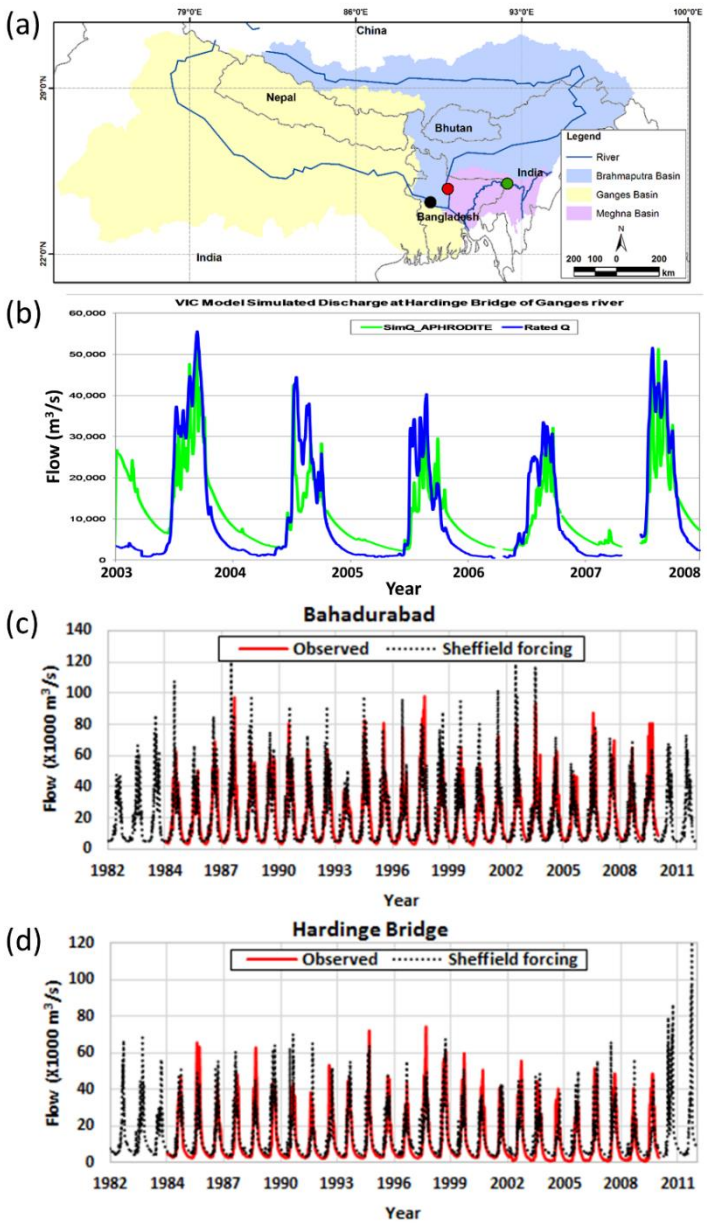


Figure 2.1. (a) The GBM basins that are currently modeled by VIC-3L to simulate surface runoff streamflow. The solid circles represent streamflow locations at the Ganges (black), Brahmaputra (red), and Meghna (green) Rivers. (b) Discharge simulation by VIC-3L using in situ and gridded forcing (green line) and observed (blue line) data at the Ganges River [Hardinge Bridge location, black circle in (a); after *Siddique-E-Akbor et al.*, [2014]]. (c) Streamflow simulated by the SGF data for the Brahmaputra River at Bahadurabad for 1982–2012. (d) As in (c), but for the Ganges River at Hardinge Bridge location. Note that performance metrics are shown in Table 2.3.

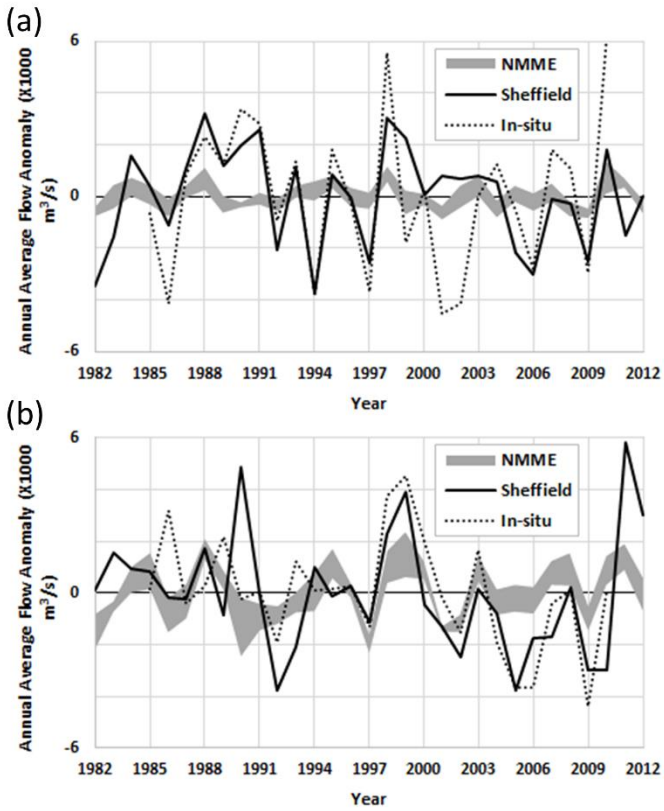


Figure 2.2. (a) Annual average anomaly of in situ observed flow, outflow simulated using the SGF data, and outflow from six different lead times of average NMME at Bahadurabad in the Brahmaputra River. (b) As in (a), but for Hardinge Bridge in the Ganges River.

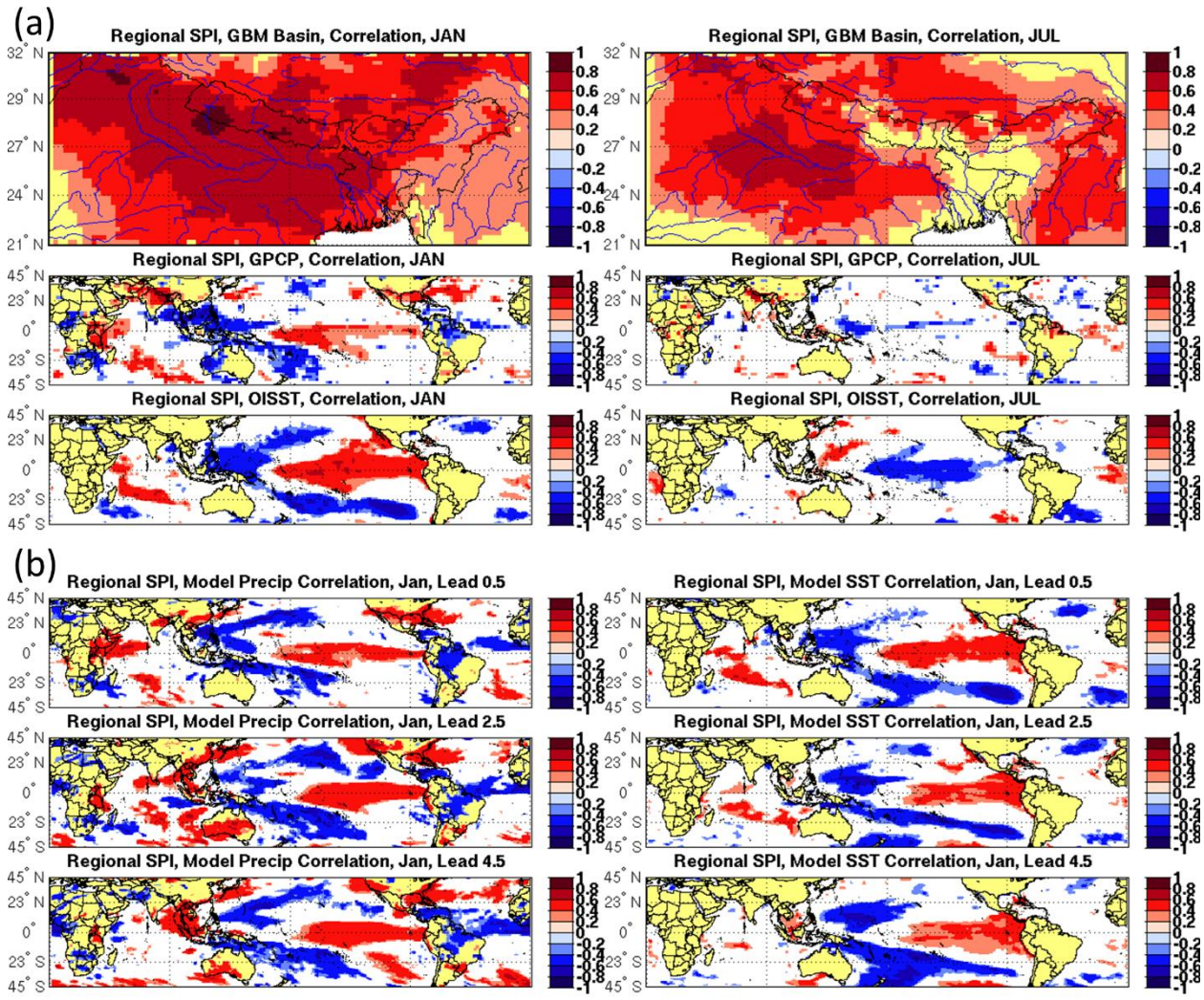


Figure 2.3. (a) Observed area-average SPI correlations with observed rainfall (significant at the p 5 0.10 level) at each point over (top) the GBM basin, with large-scale precipitation from (middle) GPCP and (bottom) SST. Both (left) January and (right) July are illustrated. (b) The observed January area-average SPI correlations with the NMME seasonal forecasts (significant at the p 5 0.10 level) for (left) precipitation and (right) SST at lead times of (top) 0.5, (middle) 2.5, and (bottom) 4.5 months. Note the similarity of tropical precipitation and SST signals with those in (a).

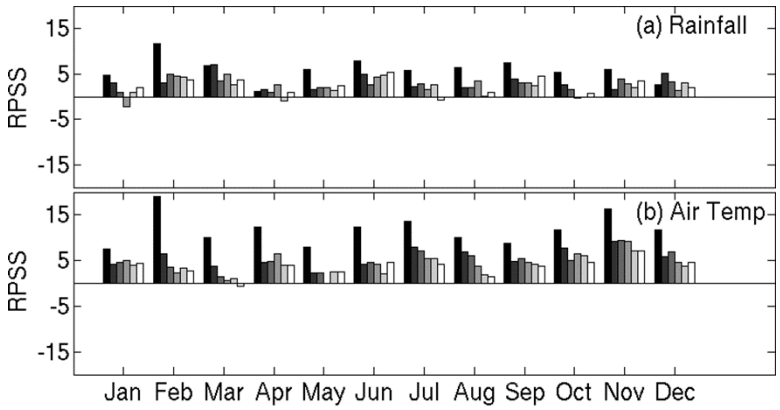


Figure 2.4. The GBM area-average RPSS for (a) rainfall and (b) air temperature are shown for all 12 verifying months. Within each grouping by month, the bars indicate the ranked probability skill with increasing forecast lead from 0.5 (black) to 5.5 (white) months (from left to right). The RPSS is computed against the use of climatological tercile (e.g., below, near, and above normal) probabilities.

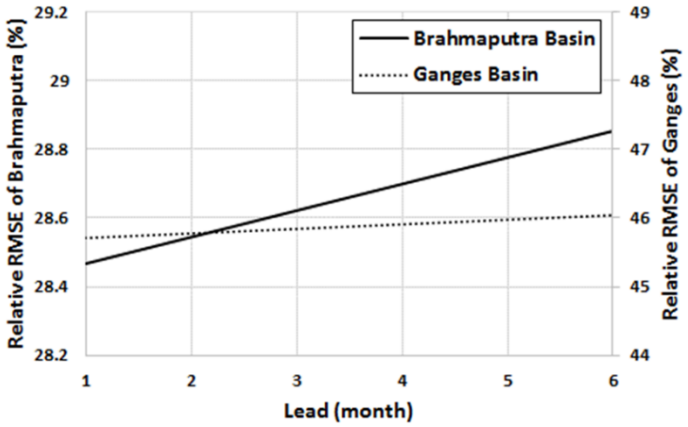


Figure 2.5. Relative RMSE (normalized by SGF) trend of NMME precipitation forecast (during 1982–2012) over the entire Ganges and Brahmaputra basin as a function of lead time (months). Note that the trend is idealized as a linear regression mainly to observe sensitivity to lead time.

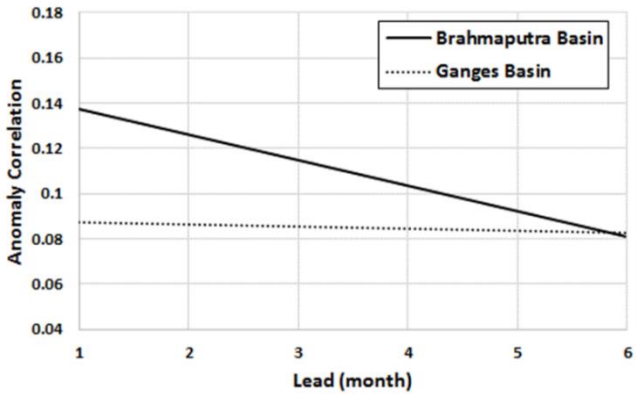


Figure 2.6. ACC trend of NMME precipitation forecast (during 1982–2012) as a function of lead time (months) when compared to Princeton global forcing data over the entire Ganges and Brahmaputra basin. Note that the trend is idealized as a linear regression mainly to observe sensitivity to lead time.

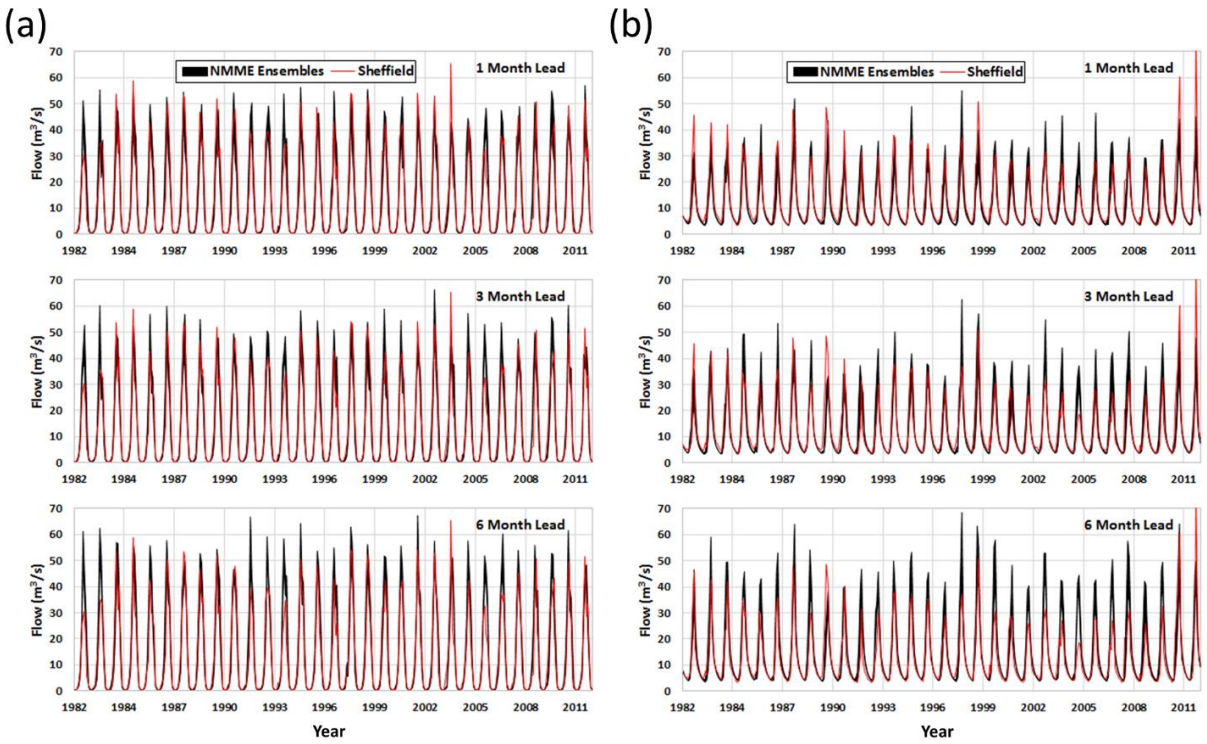


Figure 2.7. (a) Monthly average forecast hydrograph showing all eight ensemble members lumped as an envelope of black lines at Bahadurabad (Brahmaputra River). The red line is the hydrograph simulated using SGF. There is no clear distinction in performance in terms of hydrograph spread at increasing lead times. (b) As in (a), but for Hardinge Bridge (Ganges River).

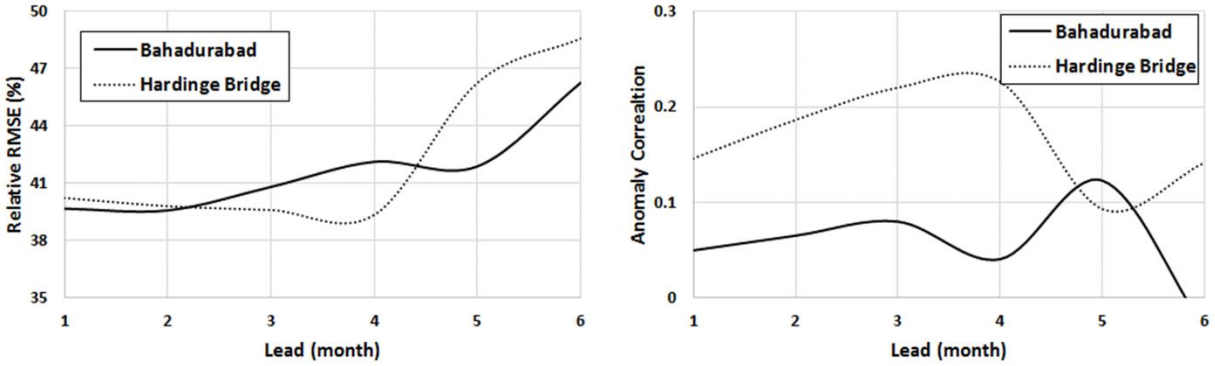


Figure 2.8. (left) Relative RMSE (normalized by the streamflow from SGF) and (right) ACC of the streamflow from NMME average for Brahmaputra at Bahadurabad and Ganges at Hardinge Bridge in monthly scale (1982–2012; 372 months).

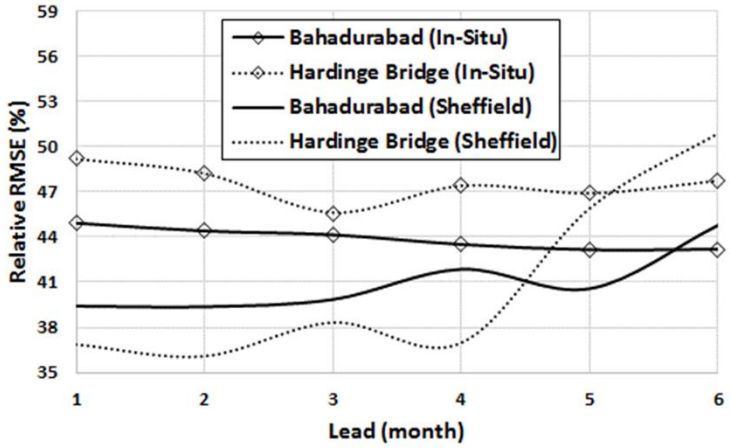


Figure 2.9. Relative RMSE of the outflow from NMME average. Normalized by in situ flow and outflow from Princeton forcing (Sheffield) in monthly scale (1985–2010; 312 months).

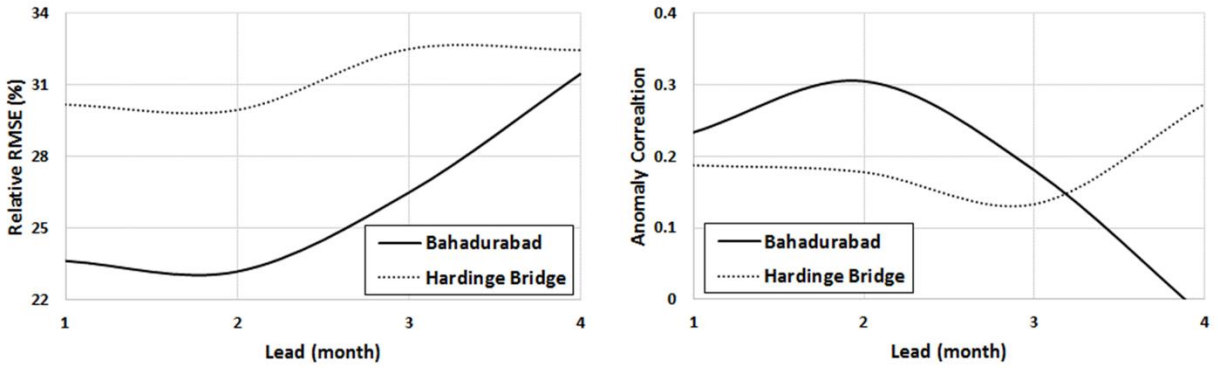


Figure 2.10. As in Fig. 2.8, but for seasonal scale (3-month average of January–March, April–June, July–September, and October–December; 1982–2012; 124 seasons). Note that Brahmaputra yields a slightly more consistent trend with respect to lead time.

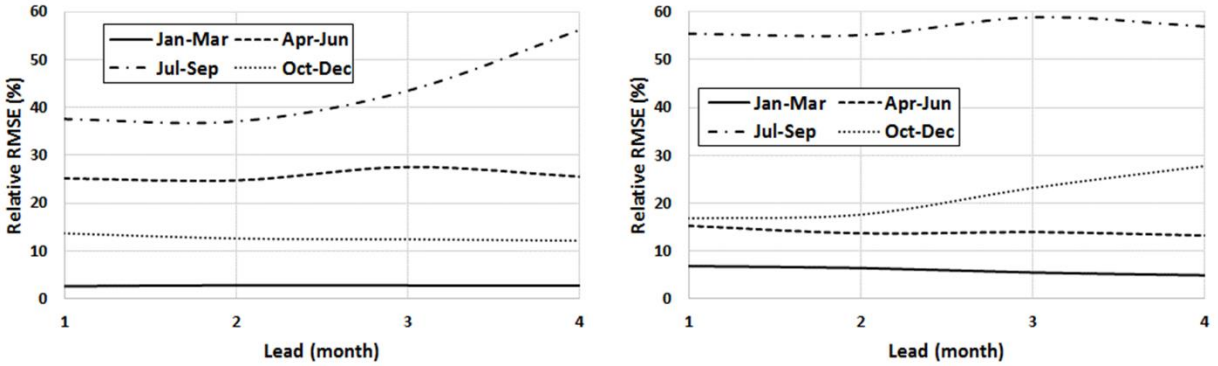


Figure 2.11. Relative RMSE of the streamflow from NMME average (normalized by the streamflow from SGF) at seasonal time scales for different seasons (1982–2012): (left) Bahadurabad in the Brahmaputra River and (right) Hardinge Bridge in the Ganges River.

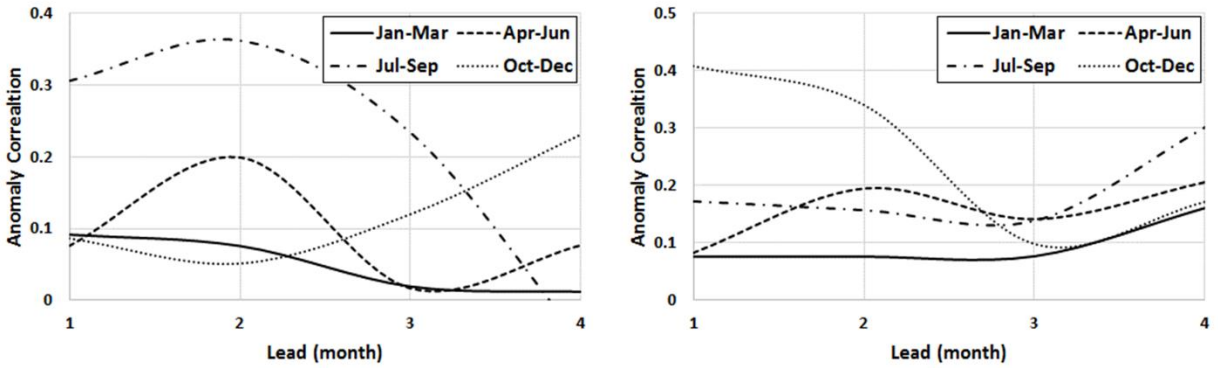


Figure 2.12. ACC of NMME forecast with streamflow from SGF at seasonal time scales for different seasons (1982–2012; 30 seasons): (left) Bahadurabad in the Brahmaputra River and (right) Hardinge Bridge in the Ganges River.

# Chapter 3. ASSESSMENT OF THE WEATHER RESEARCH AND FORECASTING MODEL GENERALIZED PARAMETERIZATION SCHEMES FOR ADVANCEMENT OF PRECIPITATION FORECASTING IN MONSOON-DRIVEN RIVER BASINS

Note: This chapter has been published in its current form as an article in *Journal of Advances in Modeling Earth Systems* [*Sikder and Hossain,* 2016]; the main differences are in section numbering and some reference information. It is used here by permission of John Wiley and Sons.

**Abstract:** Some of the world's largest and flood-prone river basins experience a seasonal flood regime driven by the monsoon weather system. Highly populated river basins with extensive rain-fed agricultural productivity such as the Ganges, Indus, Brahmaputra, Irrawaddy, and Mekong are examples of monsoon-driven river basins. It is therefore appropriate to investigate how precipitation forecasts from numerical models can advance flood forecasting in these basins. In this study, the Weather Research and Forecasting model was used to evaluate downscaling of coarse-resolution global precipitation forecasts from a numerical weather prediction model. Sensitivity studies were conducted using the TOPSIS analysis to identify the likely best set of microphysics and cumulus parameterization schemes, and spatial resolution from a total set of 15 combinations. This identified best set can pinpoint specific parameterizations needing further development to advance flood forecasting in monsoon-dominated regimes. It was found that the Betts-Miller-Janjic cumulus parameterization scheme with WRF Single-Moment 5-class, WRF Single-Moment 6-class, and Thompson microphysics schemes exhibited the most skill in the Ganges-Brahmaputra-Meghna basins. Finer spatial resolution (3 km) without cumulus

parameterization schemes did not yield significant improvements. The short-listed set of the likely best microphysics-cumulus parameterization configurations was found to also hold true for the Indus basin. The lesson learned from this study is that a common set of model parameterization and spatial resolution exists for monsoon-driven seasonal flood regimes at least in South Asian river basins.

## 3.1 INTRODUCTION

Perhaps the most challenging part of flood forecasting is the lack of meteorological observations, particularly precipitation [*Liu et al.,* 2012]. The problem is critical in the transboundary or international river basins where it is almost impossible to obtain reliable precipitation data from the upstream regions in near real-time due to hydropolitical issues [*Hopson and Webster,* 2010; *Hossain et al.,* 2007; *Hossain and Katiyar,* 2006]. A report by *UN-Water* [2008] shows that 40% of the global population resides in the 263 transboundary or International River basins. Moreover, if the real-time (i.e., nowcast) observed data (e.g., rain gauge data, satellite-observed precipitation) are available, these allow forecasting of floods limited by the time taken for runoff once generated in the river, to flow from the most upstream location to the downstream sink of an ocean or lake. In order to extend this forecast lead time beyond the maximum bounded by a basin's time of concentration, precipitation forecasts are needed. Thus, the use of model-based precipitation forecasts in flood forecasting has recently become a trend among many flood forecasting agencies and flood management communities [e.g., *Liu et al.,* 2015; *Liguori et al.,* 2012; *Verbunt et al.,* 2006; *Jasper et al.,* 2002]. For example, the Flood Forecasting and Warning Center of Bangladesh now takes advantage of 5 day precipitation forecasts in the Ganges-

Brahmaputra basins to improve skill of its 5 day river level forecast product during the monsoon season [*FFWC,* 2014].

Precipitation forecasts using Numerical Weather Prediction (NWP) models still face difficulties at scales relevant for flood forecasting [e.g., *Yucel et al.,* 2015; *Nam et al.,* 2014; *Ebert*, 2001]. For example, for convective precipitation processes, this is more challenging due to the lack of better representation of convective processes through appropriate parameterizations [*Yucel and Onen,* 2014; *Lowrey and Yang,* 2008]. Therefore, investigations are required to understand the physical properties of small scale meteorological processes. Assessment of the small-scale meteorological processes (e.g., thunderstorm) can be performed by finer scale NWP models. Many studies suggest that higher spatial resolution models perform better when the precipitation is intense [e.g., *Jang and Hong,* 2014; *Givati et al.,* 2012; *Roberts et al.,* 2009]. Due to the computational limitations of global modeling, most global NWP model-based precipitation forecasts are available at large spatial scales. For example, the Global Forecast System (GFS) of the National Oceanic and Atmospheric Administration (NOAA) produces nowcast and 10 day forecasts of meteorological conditions and precipitation at 0.258 resolution every 6 h. Naturally, there is therefore a need to explore downscaling options available with finer resolution numerical models such as the Weather, Research and Forecasting (WRF) model [*Skamarock et al.,* 2008]. A recent study by *Kumar et al.* [2016] showed that the quality of global NWP model-forecasted precipitation over the Indian continent can be improved by downscaling using the WRF.

In many cases, it is not computationally feasible to operate a regional numerical weather prediction model (e.g., WRF) routinely using a very fine resolution grid over a large domain for flood forecasting operations. For such issues, subgrid-scale parameterization schemes, nesting, and data assimilation techniques have been introduced in numerical models to improve

downscaled output. Thus, the simulated precipitation can be sensitive to spatial resolution, parameterization schemes, nesting ratios, and domain size of the model. Many studies evaluated the sensitivity of these features. *Liu et al.* [2012] studied the downscaling ratio between the nests in the modeling domain. They showed that the performance of the model to predict precipitation decreased with high downscaling ratios (e.g., 1:10). In addition, they noted that model performance is also sensitive to domain size. Model parameterization schemes are likely the most studied feature to optimize model performance. For example, *Efstathiou et al.* [2013] evaluated WRF model performance for a heavy precipitation event in northern Greece using different planetary boundary layer options and microphysics schemes. *Mannan et al.* [2013] tested the WRF model using different microphysics for an intense rainfall event in Bangladesh. *Rao et al.* [2007] assessed the model for several Indian heavy precipitation events using different microphysics and cumulus parameterization schemes. *Pennelly et al.* [2014] evaluated five different cumulus parameterization schemes for heavy rainfall in Alberta with different grid spacing and reported that at 6 km resolution or higher, the model performance is independent of cumulus physics parameterization schemes.

Another critical issue of downscaling forecasted precipitation from global NWP models is the skill dependence on forecast lead time. Usually, precipitation forecast deteriorates with increasing lead time [*Georgakakos et al.,* 2014]. Accuracy of the forecasted precipitation also depends on the model parameterization and spatial resolution. Therefore, evaluation of different sets of parameterization schemes and spatial resolution as a function of precipitation estimation accuracy and forecast lead time is important for advancing numerical model-based downscaling of global NWP forecasts for operational flood forecasting. Such an evaluation can pinpoint a

more manageable set of parameterizations that may need further refinement through atmospheric field studies before operationalization in flood forecasting applications.

In this study, we investigate the performance of the WRF model to predict (nowcast and forecast) precipitation for monsoon-affected flood-prone river basins. We apply a numerical model (e.g., WRF) for spatial downscaling of global NWP model output on precipitation for flood forecasting applications. The definition of monsoon weather systems and its spatial domain as outlined by *Ramage* [1971] was used and is shown in Figure 3.1. This monsoon boundary covers almost 20% of the world's surface, and incorporates some of the largest and most populous transboundary river basins (e.g., Ganges, Brahmaputra, Indus, Mekong, Salween, Upper Nile). The prevalence of transboundary flooding in such monsoon regions is critical as it negatively impacts downstream nations due to the lack of shared hydrometeorological observations in near real-time [*Hossain and Katiyar,* 2006].

This study explores the sensitivity of WRF physics parameterizations and spatial scale to identify a more optimal configuration for downscaling global NWP forecasts that is more likely to ''work'' in monsoon-dominated regions. The goal is to derive a configuration that is computationally efficient and yet skillful enough for a large international river basin for eventual use in operational applications. The question we try to answer in this study is as follows: Is it possible to identify the likely best set of parameterization schemes for cloud and cumulus processes and spatial resolution for WRF downscaling of global NWP forecasts that will hold true for most monsoon-affected river basins? As mentioned earlier, such a set can make further refinement of model parameterizations (or proposal of new ones) through targeted field campaigns practically feasible due to a smaller working sample.

## 3.2 NUMERICAL MODELS FOR PRECIPITATION FORECASTING

The GFS is a global-scale NWP model developed by the NOAA. The model is run four times per day by the US National Weather Service to generate detailed and global output of atmospheric variables. At each run, the model generates a forecast up to 16 days. The model simulation is divided into two steps. In the first step, the GFS generates forecast every 3 h from 000 to 240 h (i.e., 10 days). In the next step, the model generates forecast every 12 h from 240 to 384 h (i.e., next 6 days). The model resolution is different in both steps. However, the 16 day forecast data are available at 0.25˚, 0.5˚, 1˚, and 2.5˚ resolution through the National Center for Environmental Prediction (NCEP). NCEP uses the same GFS model to run with more observational data and generate a more accurate daily output. The product is known as NCEP final analysis. The NCEP final analysis (FNL from GFS) data are available at 1˚ resolution every 6 h.

In this study, we used the WRF-ARW V3.7.1 to dynamically downscale the global NWP model outputs. The WRF is a new generation numerical weather prediction model with advanced dynamics, physics, and numerical schemes, and was developed from its predecessor, the MM5 model. It is a mesoscale meteorological model that uses fully compressible, nonhydrostatic Euler equations. For horizontal discretization, it uses Arakawa-C grid staggering and a third-order Runge-Kutta integration scheme for time separation. The model is capable of dealing with both one-way and two-way nesting. Details of the dynamics and physics of the WRF model are described in *Skamarock et al.* [2008].

In a numerical model like WRF, the Microphysics (MP) and Cumulus Parameterization (CP) schemes are mainly responsible for precipitation generation. Water vapor, cloud, and precipitation process are explicitly resolved by the microphysics. The subgrid-scale convective process and shallow clouds are managed by the cumulus parameterization. The Indian summer

monsoon rainfall prediction using the WRF model has been found to be sensitive to the choice of convective parameterization scheme [*Srinivas et al.,* 2015]. Many studies on the Indian summer monsoon rainfall reported that the Betts-Miller-Janjic CP scheme performs better in that region [e.g., *Srinivas et al.,* 2013; *Kumar et al.,* 2010; *Mukhopadhyay et al.,* 2010; *Vaidya,* 2006].

The cloud microphysics scheme is mainly responsible for nonconductive rainfall in the coarse resolution (>10 km) WRF model. *Rajeevan et al.* [2010] conducted a sensitivity test of four different WRF microphysics schemes on a severe thunderstorm over southeast India. They found that the Thompson scheme performed well out of the four microphysics options, although the Morrison scheme was the most sophisticated among them. At high spatial resolution (less than 5 km), numerical models are expected to capture the convective processes and therefore the use of a convective scheme is optional [*Hsiao et al.,* 2013]. Thus, the sensitivity of different microphysics schemes over the Indian monsoon rainfall needs to be evaluated, particularly for very high-resolution models (<10 km). More recently, *Zheng et al.* [2016] identified that cloud microphysics alone was not sufficient to resolve convective processes at higher resolution in the WRF model. They compared high-resolution model simulations (grid increments of 9 km and 3 km) over the U.S. southern Great Plains with no convective scheme runs, and reported that the updated Kain–Fritsch schemes showed better result in both resolutions.

Precipitation is also sensitive to the planetary boundary layer (PBL). *Ulate et al.* [2014] studied the sensitivity of CP-PBL parameterization schemes for the Indian Ocean and Maritime Continent water cycle, and reported that the water cycle was more sensitive to the PBL than CP. However, a dry bias was found with the Mellor-Yamada-Janjic PBL scheme, while the Yonsei University Scheme performed relatively better. A similar observation was reported by *Efstathiou et al.* [2013] for the heavy rain rate over the eastern Chalkidiki peninsula in northern Greece.

Therefore, the Yonsei University PBL scheme was used in this study. Table 3.1 provides the list of microphysics and cumulus parameterization schemes along with other parameterization schemes used in this study.

## 3.3 Study Approach and Methodology

The main objective of this study is to identify the likely best set of parameterization schemes and spatial resolution that can hold true for most river basins in monsoon-driven flood-prone regions. Due to the computationally prohibitive nature of running WRF, a 1-month period during the monsoon season was selected. This period had short dry spells that allowed for assessment of false rain simulation. We selected the monsoon-driven Ganges-Brahmaputra-Meghna (GBM) basins as the test river basin to explore the various combinations of parameterization and scale (Figure 3.2). GBM basins have the characteristic of incorporating three river basins of contrasting size, precipitation intensity, times of concentration, and flood regime [*Mirza et al.,* 1998]. Here, Meghna is the smallest in size and response time while Ganges is the largest. Brahmaputra has steep terrain with high flow rate flood regime, often exceeding 70,000 $m^3/s$ during the Monsoon season.

We set up the WRF model for the entire GBM river basin system (Figure 3.2). The model setup consisted of three one-way nested domains, where the smallest-scale domain was divided further into two subdomains (D03 and D04) for computational efficiency (Figure 3.2). The smallest domains span different climatic regions of the GBM basin, where there is strong variability in precipitation climatology. Domain 3 covers the heavy rainy region which is a mainly humid subtropical zone and Domain 4 covers the semiarid area (less rainy) of Western India. The outermost domain (D01) has 27 km grid resolution and covers the entire Indian

subcontinent, northern Indian Ocean, southern part of central Asia, northern part of Southeast Asia, and a part of China (spanning 54˚E-106˚E and 2˚N-40˚N). The smallest domains (i.e., D03 and D04) have grids with 3 km resolution. Domains 3 and 4 were configured without any CP parameterization, assuming that the MP is capable of explicitly solving the convective process in 3 km resolution. The second domain (D02) is the child of the outermost domain (D01) and parent of the smallest domains (D03 and D04). The default two-way nesting in WRF updates the parent domain using the results of the child domain. Here, we used one-way nesting to keep the parent domain output ‘‘as is’’ for further analysis. A 1-month time period of the Indian summer monsoon from 5 August 2015 to 4 September 2015 was chosen as the simulation period. During this period several heavy rainfall events occurred in the region. The simulation time step of the outer domain (i.e., D01) was selected as 90 s. Model outputs were saved every 3 h, although output of every 24 h interval was used.

To test if the likely best configuration of parameterizations identified for GBM basins is applicable to other regions, a similar WRF setup was prepared for the Indus river basin (Figure 3.3) with two one-way nested domains. The outermost domain (D01) has 27 km resolution and innermost domain (D02) has 9 km resolution. The analysis extent (Figure 3.3) covers almost entire Indus river basin. The outer domain covers nearly the same area as domain 1 of the GBM basin (47˚N-99˚N and 2˚N-42˚N). Given limitations of CPU resources, a one-week time period (25–31 July 2010) was selected for testing the efficacy of GBM-derived configuration. We consider this an appropriate period as it includes a severe flood event with basin-wide precipitation peaking on 29 July 2010 and leading to large-scale floods in most parts of Pakistan. All other parameters and model configurations remained the same.

As seen from Table 3.1, five MP schemes and three CP schemes were chosen at three different spatial resolutions (27, 9, and 3 km) to evaluate the sensitivity to precipitation simulations. Parameterization schemes beyond CP and MP were selected based on compatibility with the monsoon-driven climate [e.g., *Ahasan and Khan,* 2013; *Kumar et al.,* 2012; *Rao et al.,* 2007] and are also shown in Table 3.1. However, these parameterizations were not part of the sensitivity study. A total of 15 MP-CP combinations (5 MP 3 3 CP) were evaluated in GBM basins over a one-month time period to identify the existence of the likely best MP-CP combination and spatial scale. Each combination is denoted hereafter by their MP-CP abbreviation shown in Table 3.1. For example, WSM5-KF means the combination of the WRF Single Moment 5 class microphysics and Kain-Fritch cumulus parameterization. The 6 hourly 1˚ resolution NCEP GFS final analysis data were used as the boundary data and initial condition for a continuous 1 month simulation of the GBM basins. From the sensitivity study, the three best MP-CP combinations and spatial scales were chosen according to their performance in simulating precipitation in nowcast mode. Thereafter, we applied these MP-CP combinations and spatial resolution to the Indus river basin. The initial and boundary data source remained the same as in the GBM nowcast mode for the Indus river basin. For assessment of the MP-CP combination in the forecast mode, two storm events in the GBM basin were selected and simulated using the GFS forecast data as the model boundary up to 10 days lead time. To generate the forecast for 10 different lead times of a storm event, a total of 10 simulations were carried out for a particular MP-CP combination, starting 10 days before the storm event followed by 9 days, 8 days and so on. The 3 hourly 0.5˚ resolution GFS forecast data were used as the boundary condition for the forecast simulation, while the initial condition of each simulation was taken from the previous day's model output. For example, initial conditions for the 9 day lead

simulation (i.e., starting 9 days before the storm event) were taken from the 1st date output of the 10 day lead simulation thereby minimizing the effect of the model spin-up time error to generate more accurate output at smaller lead times.

## 3.4 DATA

In our parameterization and spatial resolution sensitivity experiments, the 6 hourly 1˚ X 1˚ resolution NCEP GFS final analyses data were used as the boundary in the WRF model [e.g., *Rao et al.,* 2007]. These boundary data were available through the University Cooperation for Atmospheric Research-Research Data Archive (http://rda.ucar.edu/datasets/ds083.2/). Data from the same source were used as the boundary to evaluate the performance of the likely best MP-CP combinations over the Indus basin for the July 2010 storm event. To evaluate the performance of the MP-CP schemes in forecast mode with different lead times, forecasted boundary data were used. In the case of a forecasted boundary, we used 3 hourly 0.5˚ X 0.5˚ resolution archived GFS forecast up to 10 days (http://www.nco.ncep.noaa.gov/pmb/products/gfs/).

Simulated precipitation was compared against satellite-estimated precipitation from the Global Precipitation Measurement (GPM)-Integrated Multi-satellitE Retrievals for GPM (IMERG) final run data (30 min precipitation with 0.1˚ resolution). This global precipitation data set was prepared using satellite-estimated precipitation (from microwave and microwave-calibrated infrared), precipitation gauges analysis [*Huffman et al.,* 2015]. GPM is the core satellite of this data set. WRF-simulated precipitation over the Indus basin precipitation is compared against the daily 0.25˚ X 0.25˚ Climate Hazards Group InfraRed Precipitation with Station data-CHIRPS [*Funk et al.,* 2015], as GPM-IMERG data record begins from 2014. This historical data set (since 1981) was prepared using satellite imagery and gauged station data. The

mean daily precipitation of CHIRPS data shows consistency with GPM-IMERG over the GBM basin for peak one month of the 2015 monsoon (Figure 3.4). Therefore, the comparison between the simulated precipitation performance of GBM basin (with respect to GPM-IMERG) and Indus basin (with respect to CHIRPS) is fair. Finally, the amount of predicted precipitation (areal-averaged precipitation) was evaluated against in situ ground station data available from the World Meteorological Organization though NCDC (National Climatic Data Center) GSOD (Global Surface Summary of the Day). The heavy rainy area of the GBM basin (D03) covers 43 GSOD stations while the less rainy area of the GBM basin (D04) covers 13. Sixty GSOD stations located in the Indus basin were used and the point precipitation values were converted to areal averages using the Thiessen polygon method (see Figures 3.2 and 3.3).

## 3.5 Performance Criteria

We used error metrics proposed by *Liu et al.* [2012] to evaluate model output performance with respect to observed data. Four categorical metrics were used. These included probability of detection (POD), the frequency bias index (FBI), the false alarm ratio (FAR), and critical success index (CSI). The POD indicates the probability of detection of rainfall, while FAR is the probability of the false rain (alarm) produced by the simulation. The CSI also indicates the probability of the detection, but with respect to the total rainfall predicted by model and observation. The FBI evaluates the tendency to over or underestimate simulated rainfall with respect to observed data. The ideal scores for POD, FBI, FAR, and CSI are 1, 1, 0, and 1, respectively. Three continuous metrics, including the root mean square error (RMSE), the mean bias error (MBE), and the standard deviation (SD) were used in this study. Both RMSE and SD

indicate the amount of error in predicted precipitation without showing the bias. The MBE shows the bias of the simulated precipitation with respect to the observed.

The categorical metrics were calculated with respect to the gridded satellite final (gauge-calibrated) products (i.e., GPM-IMERG for GBM and CHIRPS for Indus), while the other three error metrics were calculated with respect to the areal-averaged observed precipitation determined from NCDC-GSOD station data. Here, each error metric represents different characteristics of the performance of simulated precipitation. It is difficult to choose the best options based on these seven different error metrics. Therefore, a multicriteria decision analysis was carried out to find the likely best MP-CP combination over the GBM basin. Furthermore, two unified performance scores were used to compare the results from different model configurations. The description of the multicriteria decision analysis technique and the unified performance scores are given in the next sections.

### 3.5.1 *Multicriteria Decision Analysis*

We used a multicriteria decision analysis technique named TOPSIS (Technique for Order of Preference by Similarity to Ideal Solution) to find the likely best MP-CP combinations. TOPSIS was first developed by *Hwang and Yoon* [1981] and later modified and used in numerous studies [e.g., *Upadhyaya and Ramsankaran,* 2014; *Milani et al.,* 2005]. This multicriteria decision analysis technique determines the best alternative using the shortest and longest geometric distance from the positive and negative ideal solution, respectively [*Assari et al.,* 2012].

TOPSIS consists of six steps, starting with a decision matrix with different alternatives and criteria. In this study, we used 15 different MP-CP combinations to find the likely best combination for monsoon-driven weather. These 15 MP-CP combinations along with three different spatial resolutions provided 45 different alternatives in this case. Therefore, the decision

matrix in this study had 45 alternatives and 7 criteria (i.e., 4 categorical and 3 continuous error metrics). The value of each criterion indicates the performance of different alternatives. In TOPSIS, each criterion should have the evaluation as ‘‘more is better’’ or ‘‘less is better.’’ To meet the requirements, the FBI and MBE were rescaled. Both rescaled metrics were ranging from 0 to 1, where 0 is the perfect score. Therefore, the POD and CSI are ‘‘more is better’’ and FAR, rescaled FBI, RMSE, SD, and rescaled MBE are ‘‘less is better’’ criteria in this study. We used equal weight for all criteria. Finally, the relative closeness to the ideal solution was computed. Hereafter, this computed value is denoted as TOPSIS RCV (Relative Closeness Value). The higher TOPSIS RCV means closer to the observed data or more accurate alternative.

### 3.5.2 *Unified Performance Scores*

The TOPSIS RCV is a relative value to identify the best alternative based on the given criteria. Which means that the value is not absolute and may change with different sets of alternatives. Therefore, two unified performance scores were used to compare overall model performance across different configurations, where the score of each alternative is not relative to others. At first, the values of all error metrics were rescaled to calculate the performance scores.

Table 3.2 shows the relationship between the original error metric and rescaled metric (where subscript ‘‘r’’ denotes ‘‘rescaled’’). Here, the thresholds were selected based on the highest and lowest metric values. All rescaled values range from 0 to 1, where 0 represents the worst case and 1 is for an ideal case. Thereafter, a unified score was calculated by assigning equal weights to all rescaled error metrics (i.e., by averaging all rescaled values). The point of deriving a unified score was to allow a convenient and multidimensional assessment of precipitation simulation quality for various WRF configurations. Here, a higher unified score means better model performance or closer to the observed data.

$$Unified\ Score = \left(\frac{POD_r+FBI_r+FBI_r+CSI_r+MBE_r+RMSE_r+SD_r}{7}\right) \quad (3.1)$$

Another performance score was calculated to evaluate model performance in forecast mode using only the rescaled categorical metrics denoted here as the spatial extent score. Like the unified score, the spatial extent score ranges from 0 to 1 with 1 being the ideal value. This score shows the overall model performance in terms of spatial distribution of precipitation.

$$Spatial\ Extent\ Score = \left(\frac{POD_r+FBI_r+FBI_r+CSI_r}{4}\right) \quad (3.2)$$

## 3.6 Results and Discussion

### 3.6.1 *Identifying the Likely Best Set of MP-CP Configurations*

The model was simulated for 31 days over the GBM domain in nowcast mode to identify the likely best MPCP combinations. Figure 3.4 shows a sample comparison between the mean daily precipitations of the study area from two MP-CP combinations with 9 km resolution (i.e., domain 2) and GPM-IMERG. The black boxes in Figure 3.4 are the analysis extent for heavy rainy areas and less rainy areas, and are equivalent to the area of Domains 3 and 4 of the GBM setup (Figure 3.2), respectively.

Figure 5 shows a sample comparison between the areal-averaged precipitation from two MP-CP combinations with 9 km resolution and NCDC-GSOD. For the combined case, both heavy rainy areas and less rainy areas were considered.

The spatial distribution of simulated precipitation was assessed using categorical metrics (i.e., POD, FBI, FAR, and CSI), which were calculated against the GPM-IMERG data for the heavy rainy area, less rainy area, and for the combined area. Figure 3.6 shows the comparison

between the performance of WRF-modeled nowcast precipitation against GPM-IMERG for different MP-CP combinations and spatial resolutions according to different categorical metrics.

In the heavy rainy area, the POD of the simulated precipitation is relatively better with the BMJ and GF CP schemes. The performance of the GF-CP scheme is marginally better than BMJ in the humid subtropical zone (Figure 3.6a). In the less rainy or semiarid zone, performance of the BMJ scheme is significantly superior to the other two CP schemes (Figure 3.6b). In the combined case (Figure 3.6c), the performance of the BMJ and GF are almost similar, except for a few cases where the GF shows better performance (e.g., WSM3-GF). Across all conditions, the KF CP scheme shows poor performance. An almost similar pattern is visible in CSI (Figures 3.6d–3.6f). Both POD and CSI indicate that the BMJ and GF are adequate to detect rainfall. However, the GF exhibits better rain detection performance over wet regions (Figures 3.6a and 3.6d), while BMJ appears acceptable across all climatic conditions (Figures 3.6a, 3.6b, 3.6d, and 3.6e). The FBI indicates that the BMJ and GF parameterization schemes have a tendency to overestimate precipitation, particularly when the resolution is coarse (Figures 3.6g–3.6i). In general, the KF scheme shows better performance (closer to 1) in coarse resolution (Figure 3.6i). The overall performance of the BMJ scheme is slightly better than the GF scheme in terms of FBI. One of the reasons of selecting continuous 1-month period in the monsoon including few dry spell was evaluating the false alarm of the simulated precipitation. However, the FAR in the heavy rainy area do not appear sensitive to a specific MP-CP combination (Figure 3.6j). This may be due to the fact that the wet region experiences rainfall almost every day and thus there is no opportunity for the WRF model to produce a false rain simulation. In the dry area, the performance of the GF scheme is noticeably poor in terms of FAR, while the KF scheme shows better results (Figure 3.6k). From Figure 3.6k, it is clear that the performance of the MDM MP

scheme is worse than others and ultimately, it reduces the overall performance of the MDM MP scheme in combined conditions (Figure 3.6l). The above analysis of FAR reveals that the selection of the analysis area and period have an impact on the evaluation of model simulated precipitation performance. Similarly POD and CSI are not sensitive in case of dry period, when less or no rain occurs. Therefore, selection of multiple area with different characteristics and longer time period is necessary to correctly evaluate the performance of simulated precipitation. From the analysis of the categorical metrics, we can see that the accuracy of simulating the spatial distribution of precipitation is quite sensitive to the CP schemes, and the overall performance of the BMJ scheme is better than the other two studied.

Daily areal-averaged precipitation for both simulated and observed data were calculated to evaluate the metrics of MBE, RMSE, and SD. The NCDC-GSOD station data were used as reference Figure 3.7 depicts comparisons of the continuous error metrics or RMSE, SD, and MBE. From the MBE plot, it is clear that the WSM3 MP scheme has a tendency to yield negative bias (underestimation), while the GFCP scheme has an opposite tendency of positive bias in all conditions (Figures 3.7a–3.7c). Patterns of the RMSE and SD are almost similar and show sensitivity of the CP schemes to the accuracy of the precipitation amount (Figures 3.7d–3.7i). The performance of the KF-CP scheme is worse for most cases of the wet climate region (Figures 3.7d and 3.7g). In dry conditions, the performance of the GF-CP scheme is relatively inferior to others (Figures 3.7e and 3.7h). In general, the BMJ scheme is better in all conditions in terms of areal-averaged precipitation.

Finally, the calculated TOPSIS RCV indicated that in wet area the BMJ and GF CP schemes perform relatively better than KF (Figure 3.8a). In the dry area, the BMJ is clearly superior (Figure 3.8b). Overall, performance of the BMJ is better in all conditions (Figure 3.8c). Similar

results were found by other studies for the same region [e.g., *Srinivas et al.,* 2013; *Kumar et al.,* 2010; *Mukhopadhyay et al.,* 2010]. The MP schemes are not as sensitive as the CP schemes. The combination of the WSM3, WSM5, and WSM6 microphysics schemes with the BMJ cumulus parameterization scheme shows promising results in the GBM basins. The WSM3-GF with 27 and 9 km resolution and TF-GF, MDM-BMJ, MDM-GF with 3 km resolution also provide favorable results in combined cases. Considering the relatively poor performance of the GF-CP and MDM-MP scheme in the less rainy (semiarid) region and the difference between the TOPSIS RCV at different resolutions with the WSM3-GF, TF-GF, MDM-BMJ, MDM-GF combinations, we discarded combinations in further investigations (over Indus basin). Based on the sensitivity analyses shown in Figures 3.6–3.8, the likely best set of configurations selected for further investigation were: WSM5-BMJ, WSM6-BMJ, and TS-BMJ.

### 3.6.2 *The Likely Ideal Spatial Resolution*

In this study, we also evaluated the performance of three different spatial resolutions of the WRF model over the GBM basin domain. From the POD and CSI (Figures 3.6a–3.6f), it is clear that the probability of detecting precipitation is lower at finer resolutions (i.e., 3 km). Moreover, in most cases, the finer resolution model underestimates precipitation (Figures 3.6g–3.6i). In terms of FAR, the difference between the model resolutions is insignificant. For the semiarid region, the finer resolution model shows slightly better performance in FAR (Figure 3.6k). The 27 km resolution performs better than others in terms of POD and CSI when the KF CP scheme is used. The 9 km resolution model performs reasonably well with BMJ and GF CP schemes showing a modest improvement over the 27 km resolution.

In terms of MBE, the finer resolution model shows a mostly negative bias, while the coarser resolutions are positive (Figures 3.7a–3.7c). In the heavy rainy area, the performance of the 3 km resolution is better in terms of areal-averaged precipitation according to RMSE and SD metrics (Figures 3.7d and 3.7g). In the less rainy (semiarid) area, the sensitivity to spatial resolution is insignificant in terms of RMSE and SD metrics (Figures 3.7e and 3.7h). In TOPSIS RCV plots (Figure 3.8), the overall performance of the finer resolution model is not significantly higher than with coarser resolution, except for the case of TS and MDM MP schemes in the combined case (Figure 3.8c). The MDM is the most sophisticated MP scheme used in this study with a total of 10 variables [*Rajeevan et al.,* 2010]. The TS is the second most complex MP scheme used here. In general, the higher resolution model demands a complex microphysics scheme (i.e., with more variable) to resolve finer-scale processes explicitly [*Stensrud*, 2007]. This indicates the necessity of a complex MP scheme in high resolution to resolve convective process explicitly when no cumulus physics are used. This may explain why the performance of the 3 km resolution is remarkably better than the coarse resolution model with the TS and MDM MP schemes.

The CP scheme was not used with 3 km resolution in this study. The WSM3-GF combination was chosen to assess the performance of the 3 km resolution model using the CP scheme, as this combination shows good performance for 27 km and 9 km resolutions, but remarkably poor performance at 3 km resolutions (Figure 3.8c). We used the unified score (equation (1)) to compare the results before and after using the CP scheme in the 3 km resolution. The simulation of 3 km resolution with the CP scheme significantly improves model performance in finer resolution in terms of unified score (Figure 3.9). A possible reason could be that the relatively simple WSM3-MP scheme (with only three variables) is unable to capture the convective process in the finer resolution grids. Use of the CP scheme appears to overcome this

limitation. Therefore, additional care may be required for the higher-resolution WRF model simulations, where convective precipitation is common. The higher-resolution model performance can be improved by using the CP scheme with it or by using any sophisticated MP scheme with many variables when no CP scheme is used.

Figure 3.10 shows areal-averaged precipitation for all three likely best MP-CP combinations in conjunction with the observed data (GSOD) at different spatial resolutions for all domains (wet, dry, and combined). In the heavy rainy area, the WRF model is able to capture the 20 and 30 August storm events that took place in GBM (GSOD in Figures 3.10a/3.10d/3.10g). All model combinations are found to overestimate the first storm event and underestimate the second storm event. The 27 km resolution shows relatively better performance in the first storm event using the WSM6 scheme (Figure 3.10a), while the 9 km resolution with WSM5 is best for the second event (Figure 3.10d). In the less rainy (semiarid) area, all model combinations show poor performance and fail to capture the storm events on 11 August, but are able to capture the 17 August storm event (Figure 3.10b, 3.10e, and 3.10h). In general, the use of 3 km resolution does not yield superior skill in terms of areal-averaged precipitation. Finally, the difference between the TOPSIS RCV of the 27 km and 9 km resolutions is less than the difference with the 3 km resolution in the combined case (Figure 3.8c). Therefore, both 27 km and 9 km resolutions can be considered to be part of the likely ideal set of combinations.

### 3.6.3 *Reproducibility Over Indus Basin*

The WRF model was set up over the Indus river basin using a set of three likely ideal MP-CP combinations and two resolutions identified over the GBM domain. The simulation period spanned a week time period when a severe storm event in late July 2010 took place and flooded large parts of Pakistan [*Ahasan and Khan,* 2013]. The peak of the storm occurred on 29 July

2010. Similar to the GBM basin, the accuracy of simulated precipitation was calculated using a similar set of metrics (Figure 3.11). The CHIRPS data set was used as the reference data set to calculate the categorical metrics, as the GPM-IMERG data record only starts in 2014.

From Figure 3.11, it is visible that the difference among the three likely best sets of combinations (derived from GBM) in the Indus basin is marginal. Only the MBE shows that the TS-BMJ combination overestimates precipitation slightly more than the others. The unified score was calculated using equation (1) and compared with the unified score of GBM basins (Figure 3.12). The comparison shows that in both cases, the unified score yielded by the WSM5-BMJ is superior followed by the WSM6-BMJ and TS-BMJ combinations. In both basins, the 27 km resolution with WSM5-BMJ and WSM6-BMJ show slightly improved performance over the 9 km resolution. This indicates that the likely best combination of parameterizations hold true for the Indus basin and the yield skill is consistent to that observed for GBM basins (Figure 3.12).

The areal-averaged precipitation calculated for different likely best MP-CP combinations and resolutions are shown in Figure 3.13 along with the observed data. The storm was captured by all combinations, but appeared to have an offset in the time to peak. WRF estimated the timing when rainfall peaked by about a day. The peak achieved by the TS-BMJ combination was somewhat closer to the observed (Figure 3.13). Performance of the other combinations is similar as reflected in the unified score values (Figure 3.12).

Overall, our sensitivity analyses indicate that the WSM5-BMJ at 27 km resolution shows the ideal performance for both GBM and Indus river basins. This therefore serves as a tremendously useful guide and starting platform for various flood forecasting agencies around the world that deal with monsoon-driven seasonal flooding. The validation and reproducibility of performance on an independent and neighboring basin (Indus) to GBM indicates that findings are

representative of the broader South Asian Monsoon climate. For assessing robustness beyond South Asia, further analyses in farther away Monsoon-affected basins such as the Mekong or Upper Nile are required.

### 3.6.4 *Assessment of Forecast Skill*

The previous analyses used WRF nowcast (or in other words—retrospective simulation based on boundary conditions from the NCEP GFS final analysis). In this section, we show the performance of the likely best set of combinations in forecast mode using GFS forecast boundary condition data (GFS real-time forecast from NCEP). For computational efficiency, two storm events were selected that occurred on 20 and 30 August 2015 in the heavy rainy area of the GBM basins. The areal-averaged precipitation of two storms at lead times up to 10 days along with the observed data (GSOD) are shown in the top plot of Figure 3.14. The comparison shows that the WRF model configuration is able to downscale and maintain skill of the GFS forecast well enough to capture the first storm event (20 August). The 9 km resolution shows better performance than 27 km resolution across all combinations after the 5 day lead time. We believe, the ‘‘rising trend’’ in skill between lead times ranging from 5 to 7 days should not be given too much consideration at this stage given that only two events were studied in a limited manner. Rather, what is more telling from Figure 3.14 is that the 30 August 2015 storm could not be forecast well using any of the WRF combinations. Another point to note is that for the 20 August storm, the WSM6-BMJ combination performs similar to the WSM5-BMJ combination (Figure 3.14 bottom plot).

We should note here that the time period selected, especially for assessment of forecast skill, is quite short (a week) compared to what would have been normally desirable. Our main limitation was CPU resources because running WRF in 45 different configurations and scales for

an extended period was a logistic challenge. Nevertheless, readers should note the 1-week assessment as a potential limitation to making broad-based conclusions for the global Monsoon system. For example, we were not able to study how forecasting performs during El Nino or La Nina years or other types of oscillations with such a short period. Rather, the findings should be considered strictly limited to an ‘‘average’’ South Asian monsoon wherein the precipitation characteristics are assumed to be relatively steady in time during the months of July–October.

## 3.7 CONCLUSIONS

In this study, we explored the likely ideal set of WRF physics combination for simulating (downscaling) precipitation from a global NWP model over the monsoon-dominated region of the Ganges-Brahmaputra-Meghna river basins. The likely ideal combination was validated in a neighboring basin. Such an evaluation helped pinpoint a more manageable set of parameterizations for atmospheric modelers that may need further refinement through field campaigns for operational readiness in flood forecasting operations.

It was found that the Indian monsoon rainfall regime is more sensitive to the cumulus physics scheme than the cloud microphysics scheme. Our study showed that the performance of the MP and CP scheme in dry and wet areas of the GBM basins are considerably different. Model sensitivity to the CP scheme was different in both areas, but overall the Betts-Miller-Janjic scheme performed better. The performance of the most complex MP scheme of our study was better in the heavy rainy areas, while the same scheme showed poor results in the less rainy areas of the region. We also found that the finest resolution without using any cumulus physics option underestimated precipitation when a simple cloud microphysics scheme was used with far less variables. On the other hand, a more complex microphysics scheme with more variables

yielded better performance at the finest resolution without the use of cumulus physics parameterization. From a set of 15 combinations of WRF parameterizations and three spatial resolutions, the sensitivity study converged to a set of three likely best MP-CP combinations and two spatial resolutions. Using a multi-criteria decision analysis, it was found that the WRF Single Moment 3 Class, WRF Single Moment 6 Class, and Thompson microphysics schemes with Betts-Miller-Janjic cumulus parameterization scheme works well with 27 and 9 km spatial resolution for all conditions in the GBM basin.

The study found that the likely ideal configurations derived using the GBM domain also held true for the Indus domain. In both regions, the WSM5-BMJ yielded the best result, followed by WSM6-BMJ and TS-BMJ combinations. The difference in performance between 27 and 9 km was marginal, indicating that computational efficiency could be achieved at 27 km without compromising accuracy. Additionally, the study tested the WRF precipitation simulation in forecast mode using GFS forecast boundary data for two storm events in the GBM basin. The results of this skill assessment yielded a mixed bag of results, where skill was found to be storm event sensitive. Although good forecast skill was achieved for a storm event on 20 August 2015, our study points to the need for more investigation in the forecast mode as a function of storm physics characteristics and quality of boundary condition data.

There is no doubt that flood forecasting with longer lead times along with sufficient accuracy can reduce the flood hazard in flood-prone countries. The only way to increase the lead time of a flood forecasting system beyond the hydrologic time of concentration is to produce accurate precipitation forecasts. We believe the freely available global NWP products and regional NWP model packages (like WRF) are the best tools to forecast precipitation in ungauged river basins by flood management agencies constrained by limited financial resources.

Therefore, further development of modeling systems that downscale NWP model forecast should be explored for eventual use by operational flood forecasting agencies. Additional numerical models should also be considered, such as Regional Atmospheric Modeling System (RAMS) [e.g., *Freitas et al.*, 2017]. Use of additional numerical models allows a more robust assessment of forecast skill through multi-model ensembles. Future studies should include the following topics: (1) exploring further refinements to our proposed likely best set of parameterization configurations; (2) evaluation of model performance using forecasted boundary data from NWP models other than NOAA models; (3) exploration of multiple storm events of contrasting characteristics in different regions; (4) assimilation of satellite observations of the atmosphere to improve skill in precipitation forecasts; and (5) exploration of multi-model ensembles.

Based on the recommendations of this chapter, the identified optimized MP-CP combinations were tested for several storm events in the next chapter using GFS forecast data. The chapter 4 also includes the WRF model performance with different model initialization technique and comparing the results with its parent GFS model.

## 3.8 TABLES

Table 3.1. Selected MP-CP Parameterization Schemes for Evaluation Along With Other Parameterization Schemes.

| Physics Options | Parameterization Schemes |
|---|---|
| Microphysics (MP) | WRF Single Moment 3 Class Scheme (WSM3) [Hong et al., 2004] |
| | WRF Single Moment 5 Class Scheme (WSM5) [Hong et al., 2004] |
| | WRF Single Moment 6 Class Scheme (WSM6) [Hong and Lim, 2006] |
| | Thompson Scheme (TS) [Thompson et al., 2008] |
| | Morrison 2-Moment Scheme (MDM) [Morrison and Thompson, 2009] |
| Cumulus Parameterization (CP) | Kain-Fritsch Scheme (KF) [Kain, 2004] |
| | Betts-Miller-Janjic Scheme (BMJ) [Janjic, 1994] |
| | Grell-Freitas Ensemble Scheme (GF) [Grell and Freitas, 2014] |
| Planetary Boundary Layer (PBL) | Yonsei University Scheme (YSU) [Hong et al., 2006] |
| Radiation-Shortwave (Ra-SW) | Dudhia Shortwave Scheme [Dudhia, 1989] |
| Radiation-Longwave (Ra-LW) | RRTM Longwave Scheme [Mlawer et al., 1997] |
| Land Surface (SF_SURFACE) | Unified Noah Land Surface Model [Tewari et al., 2004] |
| Surface Layer (SF_SFCLAY) | MM5 Similarity Scheme [Zhang and Anthes, 1982] |

Table 3.2. Relationship Between Original and Rescaled Error Metrics[a] Rescaled Error Metrics.

| Rescaled Error Metrics | Threshold Value |
|---|---|
| $POD_r$ = POD | N/A |
| If FBI>1: $FBI_r$ = (2-FBI) | +2 max |
| If FBI<=1: $FBI_r$ = FBI | |
| $FAR_r$ = 1-FAR | N/A |
| $CSI_r$ = CSI | N/A |
| If MBE>0: $MBE_r$ = 1+MBE/6 | -6 to +6 |
| If MBE<0: $MBE_r$ = 1-MBE/-6 | |
| $RMSE_r$ = (1-RMSE/12) | +12 max |
| $SD_r$ = (1-SD/12) | +12 max |

[a]Values of the rescaled error metrics range from 0 to 1, and were used to calculate the ‘‘Unified Score’’ and ‘‘Spatial Extent Score".

## 3.9 FIGURES

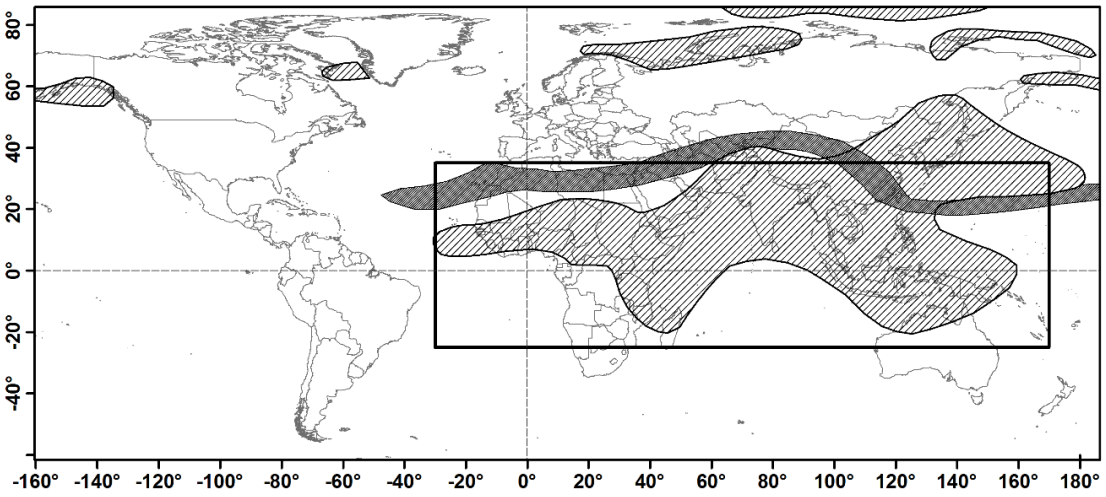


Figure 3.1. The area inside the box is the Monsoon climate regime, according to *Ramage* [1971]. The monsoonal areas defined by *Khromov* [1957] are shown by the hatched polygon [after *Ramage*, 1971].

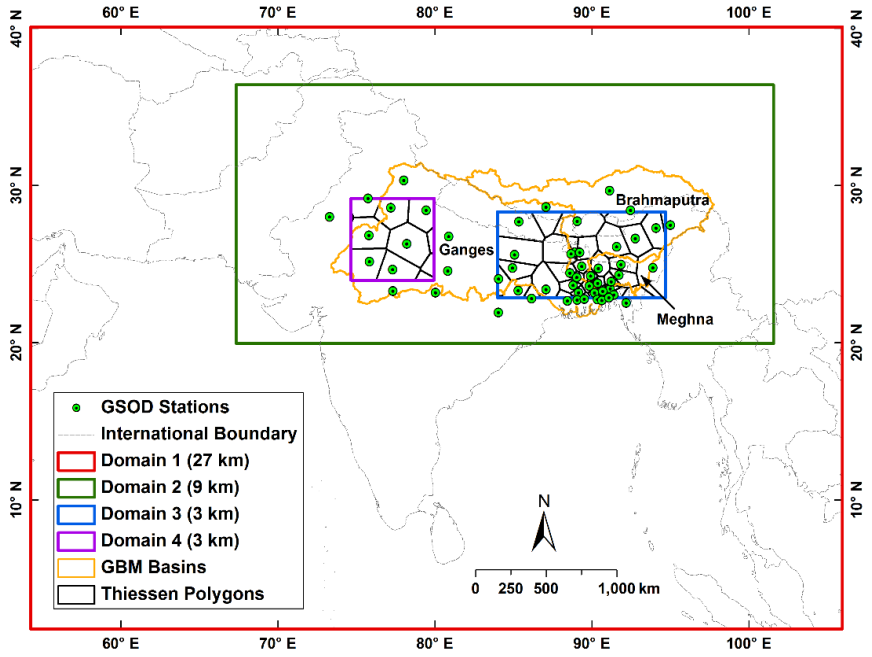


Figure 3.2. WRF model domains for the GBM basin. Here, Domain 3 and 4 are for the heavy rainy and less rainy areas, respectively. The weather stations (obtained from NCDC Global Summary of the Day-GSOD) are shown along with the Thiessen polygons inside the 3 km domains. Data from these stations were used to calculate the areal-averaged observed precipitation.

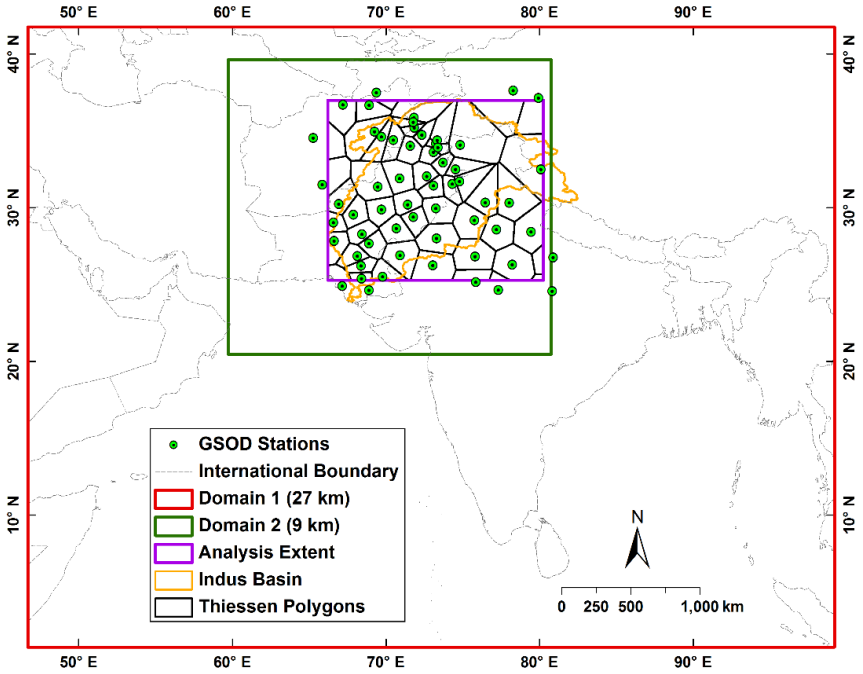


Figure 3.3. Same as Figure 3.2 but for the Indus basin to test if the likely best configuration identified using GBM basins hold true for Indus. Here, the GSOD stations and their respective Thiessen polygons are shown over the entire domain of analysis.

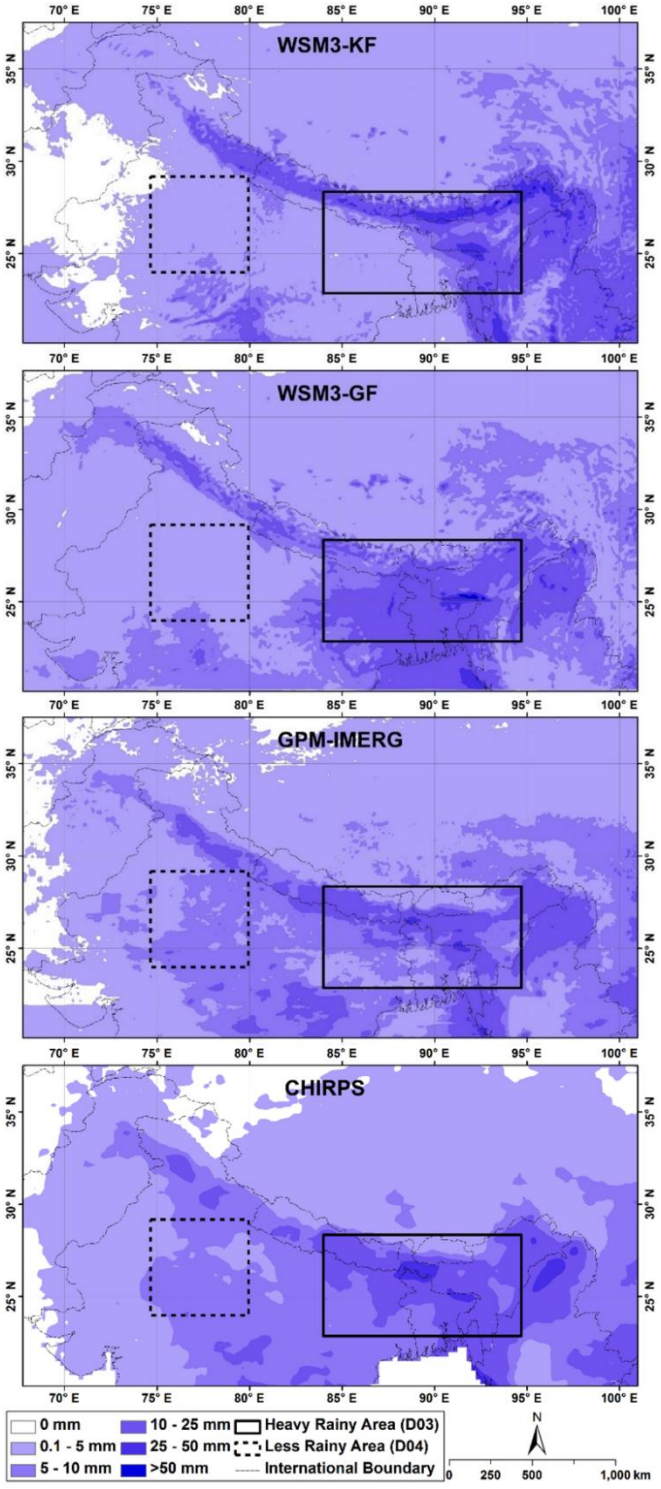


Figure 3.4. Mean daily precipitation (mm/day) from the WSM3-KF– 9 km simulation, WSM3-GF– 9 km simulation, GPM-IMERG (0.18 resolution), and CHIRPS (0.258 resolution) of the GBM basins for peak 1 month of the 2015 monsoon season. The boxes show the analysis extent of the heavy rainy area (same as Domain 3) and less rainy area (same as Domain 4).

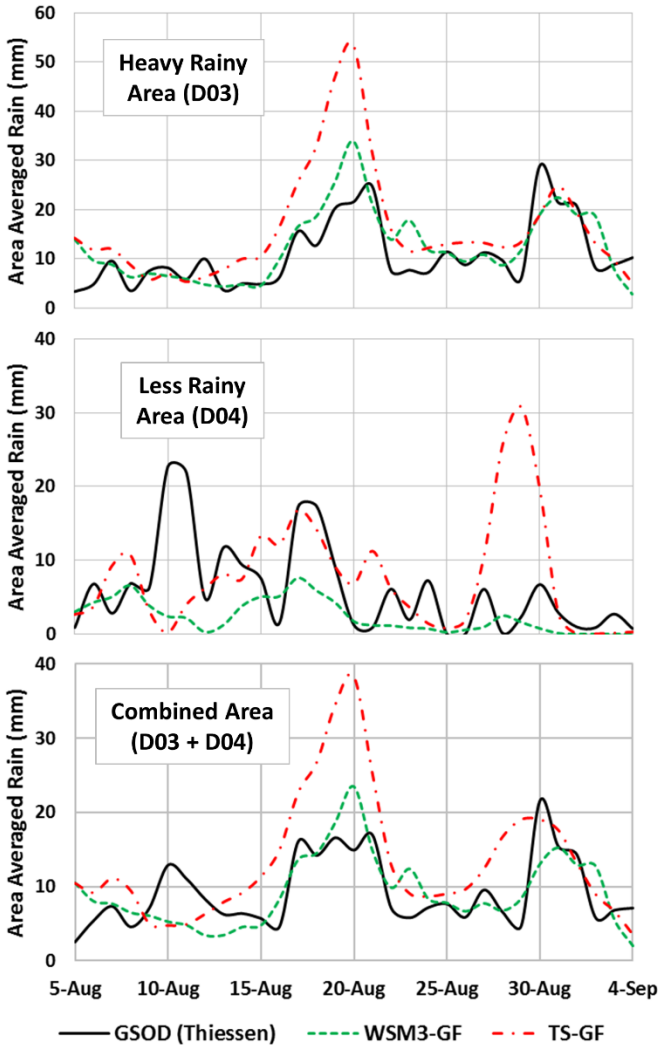


Figure 3.5. Areal-averaged precipitation from WSM3-GF– 9 km simulation, TS-GF– 9 km simulation, and GSOD station data (i.e., using the Thiessen polygon method). The areas covered in the analysis (i.e., D03, D04) are shown in Figure 3.4.

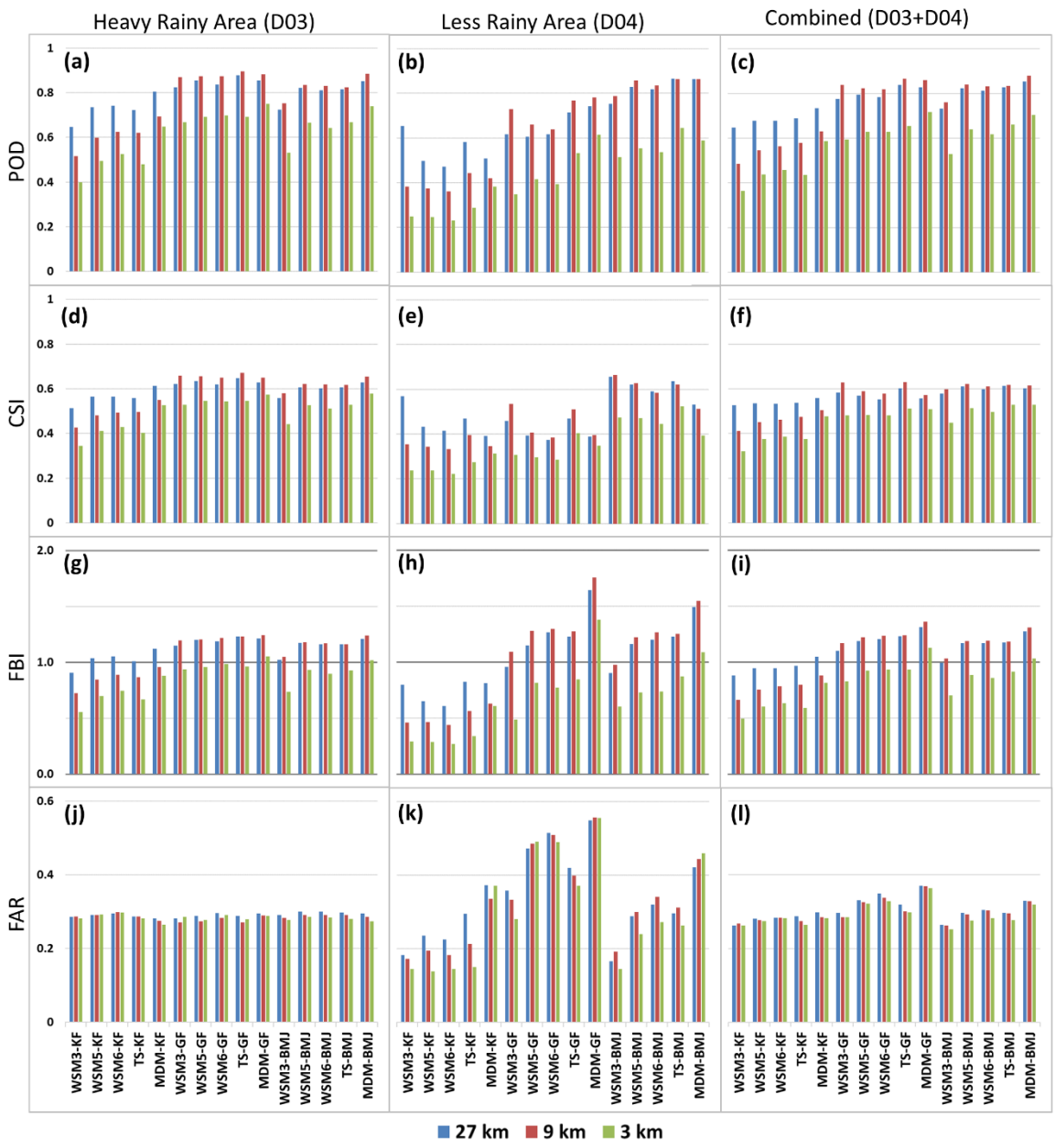


Figure 3.6. Comparison between different combinations of parameterizations (MP-CP and spatial resolution) in terms of spatial distribution accuracy in GBM basins for the 2015 monsoon season. Different spatial resolutions are represented by different lines in each subplot. In the case of POD, CSI, and FBI, the combination closer to 1 is more accurate, while for FAR, the value closer to 0 is better with respect to the GMP-IMERG.

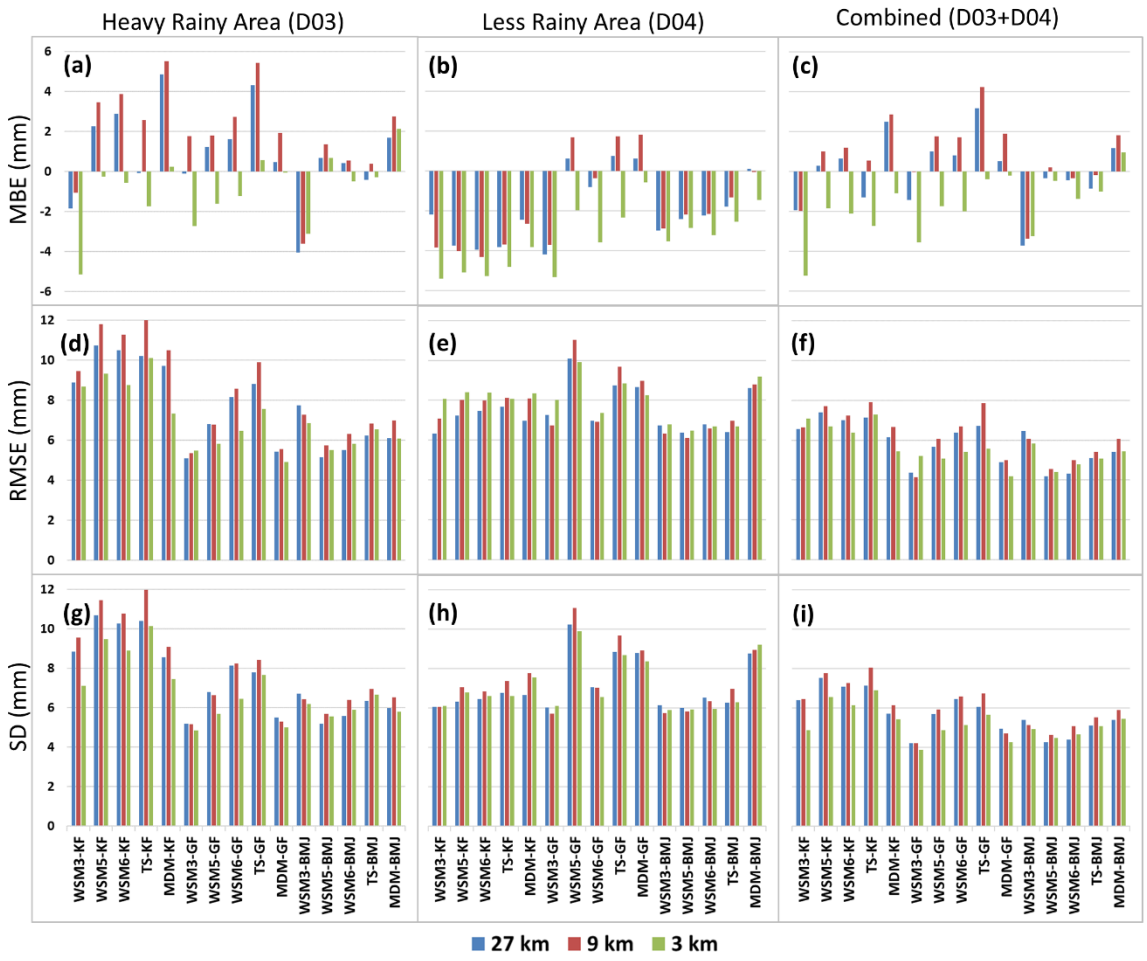


Figure 3.7. Same as Figure 3.6 but in terms of accuracy in areal-averaged precipitation with respect to the NCDC-GSOD data.

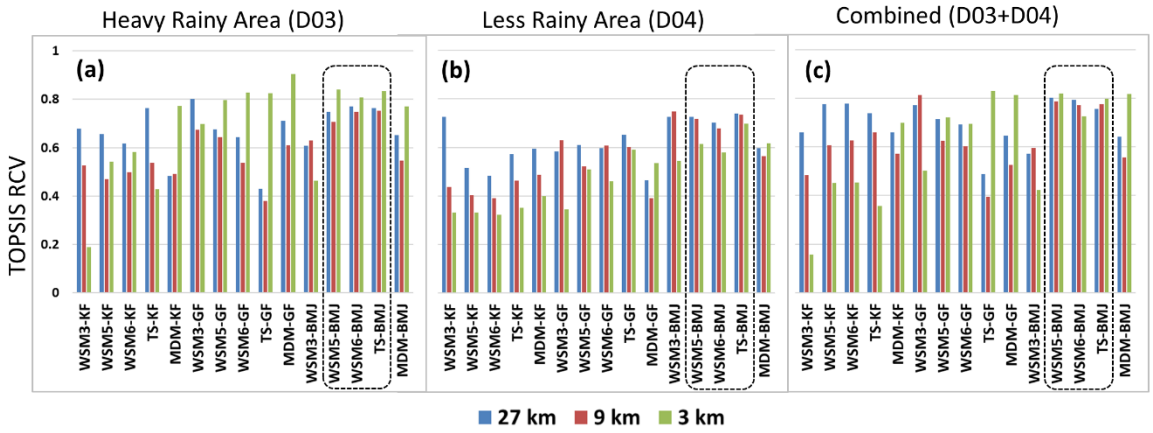


Figure 3.8. TOPSIS RCV of different combinations (MP-CP and spatial resolution) in GBM basins for the 2015 monsoon season. Higher TOPSIS RCV means it is more optimal. The selected combinations (i.e., with better and consistent performance) are shown by dashed border.

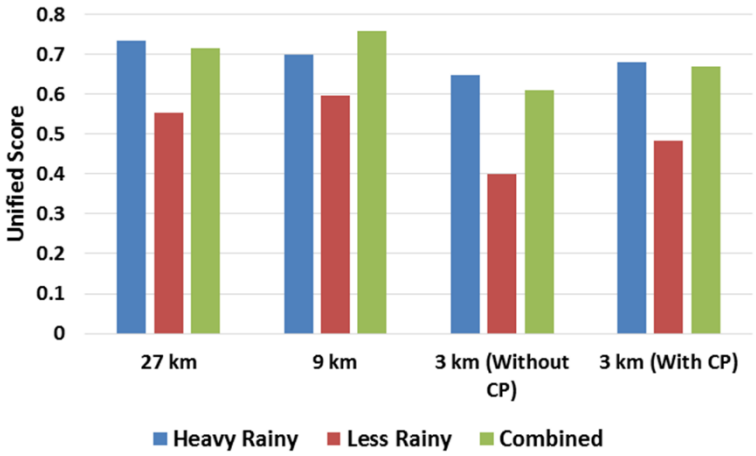


Figure 3.9. Comparison between the unified scores of the WSM3-GF combination in higher resolution (3 km) using CP and without CP in GBM basins for the 2015 monsoon season.

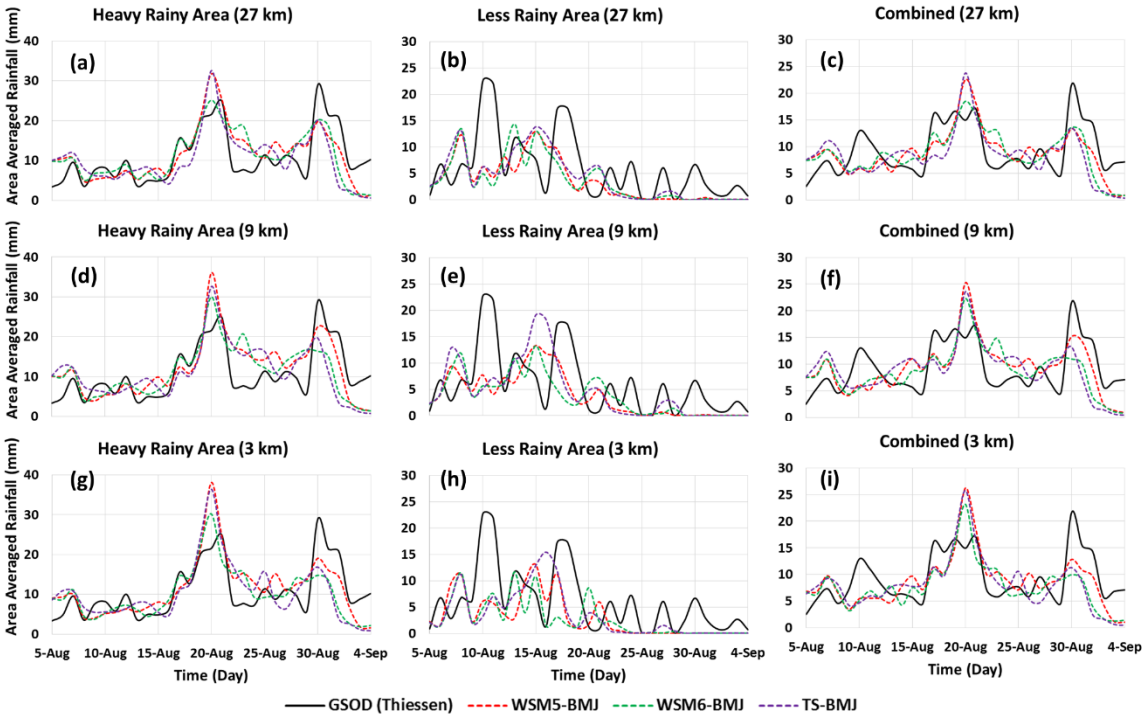


Figure 3.10. Comparison between areal-averaged precipitation for the three likely best MP-CP combinations and observed precipitation (GSOD) in GBM basins for the 2015 monsoon season. The extent of the heavy rainy areas and less rainy areas are shown in Figure 3.5. Combined areas consider both heavy and less rainy areas.

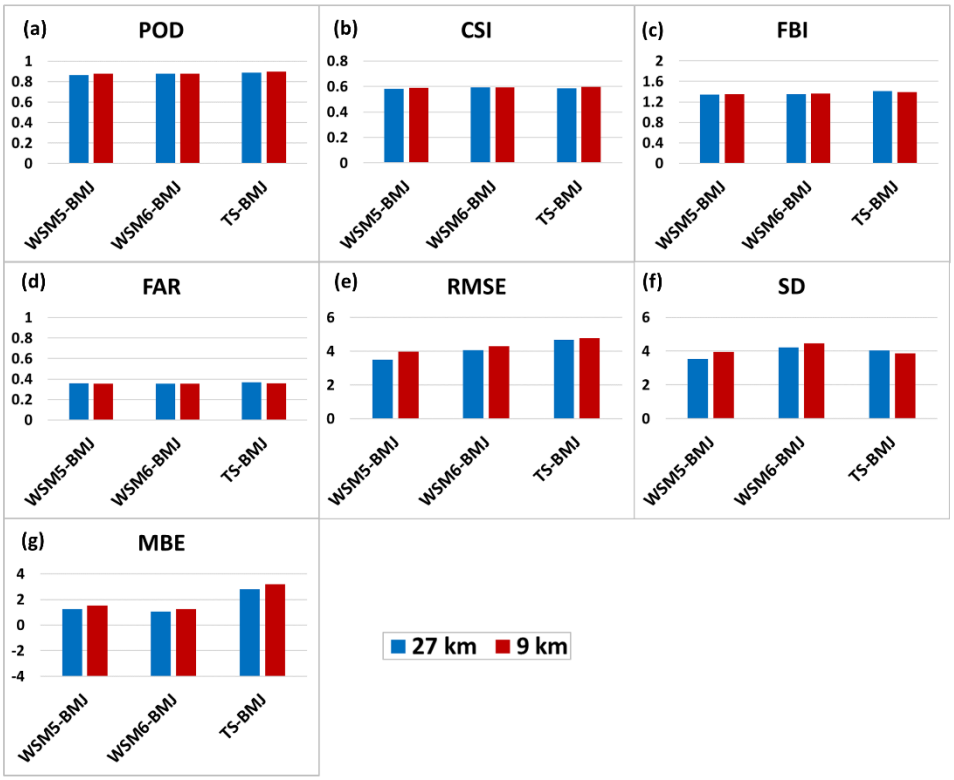


Figure 3.11. Comparison between the performance of the likely best MP-CP and spatial resolution combinations in the Indus basin for a one week time period for the late July 2010 storm event. The most optimized value for POD, CSI, and FBI is 1 and is 0 for FAR, RMSE, SD, and MBE.

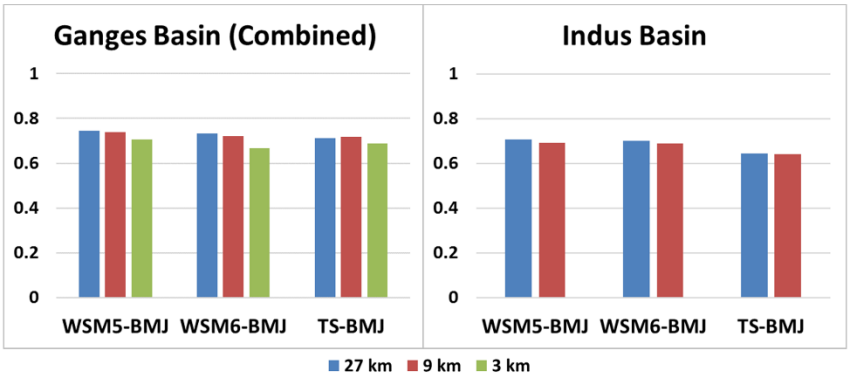


Figure 3.12. Comparison between the performances of the likely best MP-CP combinations in GBM basins for the 2015 monsoon season (one month) and Indus basin for the storm event of late July 2010 (1 week) in terms of unified score.

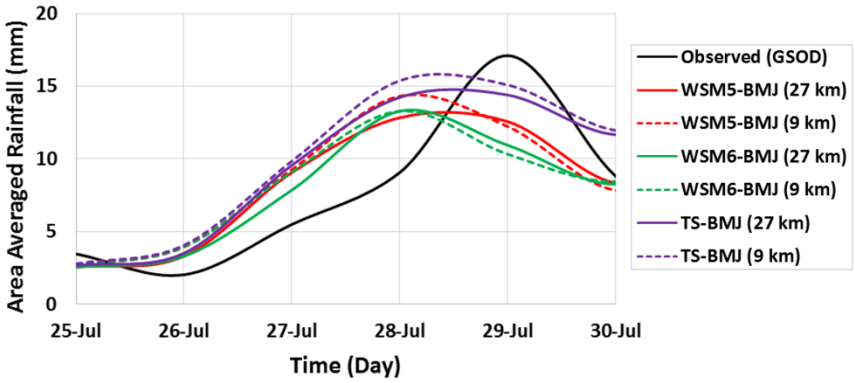


Figure 3.13. Same as Figure 3.10 but in the Indus basin domain for the storm event of late July 2010.

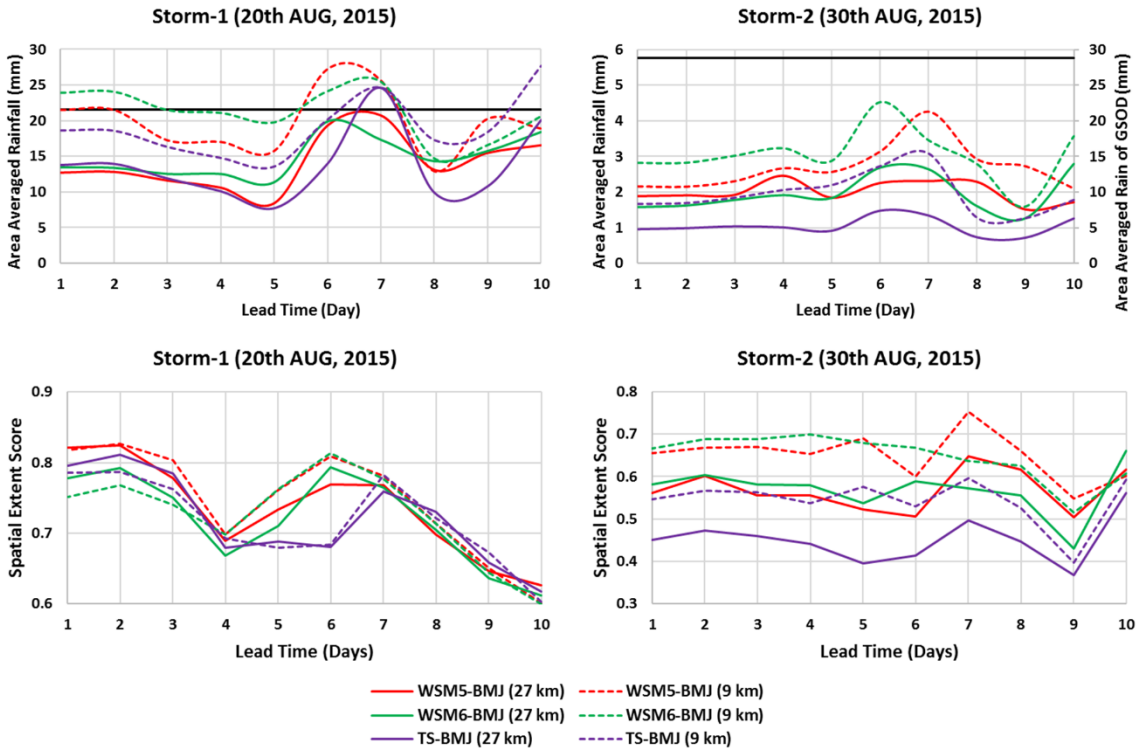


Figure 3.14. (top) Comparison of areal-averaged precipitation in forecast mode using the likely best MP-CP combinations along with the observed (GSOD in black line) as a function of lead times. (bottom) The skill of forecasted precipitation in terms of spatial distribution.

# Chapter 4. SENSITIVITY OF INITIAL CONDITION AND CLOUD MICROPHYSICS TO FORECASTING OF MONSOON RAINFALL IN SOUTH ASIA

Note: This chapter has been provisionally accepted in the *Meteorological Applications* and currently in revision.

**Abstract:** The main objective of this study is to assess the impact of using different initialization techniques and cloud microphysics of a numerical atmospheric model to improve forecasting of Indian Summer Monsoon Rainfall (ISMR). A total of six intense precipitation events over Ganges-Brahmaputra- Meghna (GBM) and Indus river basins were tested to identify the most suitable combination of parameterization and initialization technique. The Global Forecast System (GFS) based numerical weather prediction (NWP) forecast fields were dynamically downscaled by the mesoscale model of Weather Research and Forecasting (WRF). Performance of four types of initial conditions with three cloud microphysics was assessed using the model resolution up to 9 km. A main conclusion is that the more complex initial condition techniques involves more uncertainty through process and cannot exceed the performance of simple initialization techniques. The study findings provide evidence that the finer resolution initial condition is promising in higher resolution models. In case of cloud microphysics, the performance of WSM5 was sufficient for South Asian monsoon systems within this scale of the model resolution. The study findings provide a general guideline for flood forecasters for WRF model setup for forecasting ISMR from publicly available GFS-based NWP forecast fields.

## 4.1 INTRODUCTION

The economies of South Asia are pre-dominantly agrarian with a significant dependence on monsoon rainfall [*Molden,* 2007]. The high population density in most of the South Asian river basins (e.g., Ganges, Brahmaputra, Indus) make the situation more complex [*Kale,* 2012]. Flooding in such river basins causes substantial damage to lives and properties. For example, A widespread flood in the Ganges basin caused by monsoon rainfall in 2007 killed over 2000 and displaced about 20 million people [*Dulal,* 2014]. Therefore, understanding and prediction of monsoon rainfall are very important for this region.

Predicting monsoon rainfall is complicated for the irregular characteristics of monsoon in the tropical cycle [*Dwivedi et al.,* 2006]. Numerous studies have been conducted to better understand the monsoon system. Such studies have explored how to predict ahead of time (hereafter referred to as 'forecasting') the timing and intensity of Indian Summer Monsoon Rainfall (ISMR). Many of these studies typically use a global Numerical Weather Prediction (NWP) model as the primary tool [e.g., *Srinivas et al.,* 2013; *Medina et al.,* 2010; *Bhaskaran et al.,* 1996]. Such NWP is perhaps the only plausible option for forecasting rainfall by piecing together the fundamental building blocks of weather prediction variables that lead to precipitation, i.e., humidity (mass), pressure/wind speed (momentum) and temperature (energy).

Quantitative Precipitation Forecast (QPF) using NWP models have not yet reached the required accuracy at the regional scale [*Nam et al.,* 2014; *Cuo et al.,* 2011; *Kalnay,* 2003]. QPF is challenging due to inadequate observational data, as well as the improper physical representation of precipitation (hereafter used interchangeably with 'rainfall') process in models due to lack of knowledge [*Yucel and Onen,* 2014; *Vaidya,* 2006; *Ebert,* 2001]. The uncertainty in the NWP model derived precipitation can be introduced from a number of sources. These are:

model physical parameterization, initial condition or computational precision [*Rakesh et al.,* 2009a]. The simulation uncertainty can be reduced by advancing the physical parameterization, applying better numerical techniques and improving state estimation of initial condition via data assimilation [*Jang and Hong,* 2014]. QPF is also sensitive to the model resolution [*Roberts et al.,* 2009], model domain size [*Bray et al.,* 2011], model downscaling ratio [*Liu et al.,* 2012], initial and boundary data [*Kumar et al.,* 2015]. Moreover, the suitable model parameterization, resolution, and boundary can vary by region, season and storm type, and often needs to be fine-tuned separately [*Sikka and Rao,* 2008].

Model parameterization is the most studied feature of NWP models. Many studies have conducted sensitivity tests of different model parameterizations on real storm events [e.g., *Alam,* 2014; *Rakesh et al.,* 2007; *Ratnam and Cox,* 2006]. Past studies have shown that the cloud microphysics and cumulus parameterization of high resolution NWP models are directly related to QPF [*Sikder and Hossain,* 2016]. The microphysics (MP) explicitly resolves water vapor, cloud and precipitation process in the model. In simple words, MP scheme is responsible for cloud and ice formation, their evolution and eventual fallout as precipitation. The cumulus parameterization (CP) is used in coarse resolution NWP models (>10 km), when the MP scheme is unable to capture the fine scale convective events explicitly [*Hsiao et al.,* 2013; *Roberts and Lean,* 2008]. The CP scheme is responsible for sub-grid scale convective precipitation in NWP models. Numerous studies reported that the ISMR is sensitive to the choice of CP scheme [e.g., *Sikder and Hossain,* 2016; *Srinivas et al.,* 2015]. Many of these studies found that the Betts-Miller-Janjic (BMJ) CP scheme [*Janjic,* 1994] performs reasonably well in case of ISMR [e.g., *Kumar et al.,* 2010; *Mukhopadhyay et al.,* 2010].

Besides the physical parameterization, QPF also depends on the accuracy of initial conditions [*Bei and Zhang,* 2007]. The errors in representing initial condition are eventually amplified by the chaotic nature of the primitive equations of weather models. Therefore, several approaches can be introduced into NWP models to reduce the uncertainty in representing initial condition (IC for shot). One of the theses approaches is the use of ensembles [e.g., *Georgakakos et al.,* 2014; *Durai and Bhardwaj,* 2013]. In the ensemble approach, the model is initialized with multiple perturbations of IC to reduce sensitivity to a single realization of the initial condition. Data assimilation is another approach [*Kalnay,* 2003]. This approach has been used frequently to improve ISMR forecasts [e.g., *Raju et al.,* 2015; *Sowjanya et al.,* 2012; *Routray et al.,* 2010; *Rakesh et al.,* 2009b].

If one had to prioritize key issues, then the short term rainfall forecast can be considered most sensitive primarily to model parameterization and initial condition. In this study, sensitivity of both of these NWP factors to ISMR forecast was investigated. The motivation of such a study is two-fold. From a societal stand point, any improvement in QPF translates directly to greater benefits in flood forecasting or water supply management at short lead times (days to weeks). From a computational standpoint for the weather modeler, exploring the impact of initial condition demands revisiting the chaotic nature of the weather system vis a vis its physical modeling complexity.

This study is particularly skewed towards the latter motivation of exploring initial condition. The natural intuition is to expect any improvement in initial condition representation to translate directly as improved skill in forecast of rainfall. However, given the chaotic nature of weather and the further computational complexities of today's NWP models, how consistent is the impact of initial condition on forecast accuracy? To the best of this author's knowledge, such a question

has not been answered before for the monsoon driven climate regime. In order to elucidate the weather-scale features of a storm system, dynamic downscaling of coarse resolution NWP output through higher-resolution cloud resolving model is the common strategy that is employed in this study. In scientific terminology first defined by *Castro et al.* [2005], the study focuses on Type 1 downscaling that is tailored for short-term weather prediction and involves the representation of initial condition.

The main objective of this study is therefore to assess the impact of using different model initialization techniques (for IC) and cloud microphysics to improve rainfall forecasting of ISMR and guide the flood forecaster. In addition to the previous question, an overarching question that is asked here is- *Is it possible to improve the precipitation forecast over South Asian river basins affected by the monsoon using the appropriate model initialization techniques and cloud microphysics?*

## 4.2 WRF MODEL AND BOUNDARY DATA

The Weather Research and Forecasting (WRF) model V3.7.1 was used for dynamic downscaling (type 1) of coarse resolution global NWP weather forecast and generate high resolution precipitation forecast over South Asia. See the previous chapter (Section 3.2) for more details about the WRF model.

The WRF model can be initialized with the boundary from various global NWP models like GFS (Global Forecast System), CFS (Coupled Forecast System) and regional NWP models like NAM (North American Mesoscale Model). These large scale NWP model forecast output data are used to generate the initial and lateral boundary condition for the WRF model. In this study, the GFS (see Section 3.2 for details about GFS) outputs were used as WRF initial and boundary

condition. As a publicly available service for the world, GFS is ideal for short-term weather prediction applications, particularly in South Asia where economic resources are constrained. Historical data of this model are available in 0.5˚ resolution since October 2006. Lead time of the historical data varies with time. The 0.5˚ GFS model outputs were used to run the WRF in this study.

Another set of GFS product is generated by NCEP (National Centers for Environmental Prediction) known as NCEP final analysis, often termed as GFS-FNL. This final analysis usually contains 10% more observed data in the representation of the initial condition than standard 'quick-view' GFS forecast. These data are not technically weather forecast, but are near-real time GFS model outputs and available at 1˚ and 6 hour resolution. Recently, NCEP start to distribute more finer analysis data from Global Data Assimilation System (GDAS) called GDAS final analysis (GDAS-FNL). These GDAS-FNL data are available in 0.25˚ resolution. The GDAS-FNL product is the output of the model, which initiated at every 6 hours with 10-15% more observed data than GFS forecast. Therefore, expected to be more accurate than normal GFS forecast. Unlike GFS-FNL, the GDAS-FNL provides forecast up to 9 hours lead time (3 hourly forecast). Thus, for monsoonal flood forecasting operations for lead times up to a week, there is no reason why the GFS-FNL and GDAS-FNL cannot be used in a real-world environment.

## 4.3 STUDY REGION AND METHODOLOGY

The Indian Summer Monsoon (ISM) covers most of the Indian subcontinent. The Ganges-Brahmaputra-Meghan (GBM) river basin system of this region, which drains out through Bangladesh to Bay of Bengal was selected for this study. This system covers about 1.7 million

km2 where at least 750 million people reside [*FAO*, 2011]. Another selected large river basin within the ISM regime was the Indus basin. The area of this river basin is 1.12 million km2 where about 200 million. In total, about 1 billion people live in the river basins of GBM and Indus and are directly or indirectly affected by the ISMR.

The earlier model setups of GBM and Indus basin used by *Sikder and Hossain* [2016] were used as a starting point in this study. Setups for both basins have two modeling domains. The outer domain (D01) covers almost the same area of the Indian subcontinent and India ocean in both setups (Figure 4.1). The inner domain (D02) covers a slightly larger area than the river basin extent. In both model setups, the resolution of D01 and D02 are 27 km and 9 km, respectively. More details about the extent of these domains are available in the previous chapter (Section 3.3). Furthermore, an analysis extent within the D02 was selected to evaluate precipitation forecast accuracy. The analysis extent within the GBM basin was divided into two segments due to strong gradients of precipitation within this large basin system. The heavy rainy area within the GBM basin covers the humid subtropical region of eastern Indian subcontinent (Figure 4.1a). The less rainy area covers mainly the semi-arid region of mid-western Indian subcontinent. For Indus basin, the analysis extent covers almost the entire basin area (Figure 4.1b).

*Sikder and Hossain* [2016] had already identified three appropriate MP-CP combinations for the monsoon climate regime of South Asia. They reported that three different MP schemes work well with the BMJ CP scheme in both GBM and Indus basins. These MP schemes are WRF Single Moment 5 Class (WSM5) [*Hong et al.,* 2004], WRF Single Moment 6 Class (WSM6) [*Hong and Lim,* 2006], and Thompson Scheme (TS) [*Thompson et al.,* 2008]. In this study, the

sensitivity of these three likely best MP schemes was assessed in terms of forecasted precipitation. Other model parameterizations remain same as the previous chapter (Table 3.1).

Besides the sensitivity test of MP schemes in WRF forecast, performance of four different WRF model initialization techniques was tested in this study. In the first experiment case, the traditional "cold start" technique was used to initiate the WRF model using GFS forecast [e.g., *Givati et al.,* 2012]. The initial condition of the WRF model was directly taken from the GFS forecast in this case. The second case was also a "cold start" setup, but the first hour GFS forecast data were replaced by the GFS-FNL data that are expected to represent more accurate initial condition given the higher number of assimilated observations. Thus, the initial condition of the model is derived from GFS-FNL and simulation continued using the GFS forecast data as the model boundary. The first 6 hour simulation is excluded from the results in case of "cold start" setup to eliminate the "spin up" time error. Although, the first two cases involved "cold start" initialization, the spin up effect was not considered in this study to evaluate the advantages of other initialization techniques.

The next two cases were based on "warm start" (often called "hot start") approach [e.g., *Jankov et al.,* 2007]. The output of one day pre-simulated WRF model was used to initiate the WRF forecast model in these cases. In this way, the uncertainty related to model instability during the so called "spin up time" is expected to be reduced. The GFS-FNL data were used as the initial and boundary condition for this one day pre-simulation. Thereafter, the WRF forecast model was initiated with the output of this pre-simulated model, and continued with GFS forecast data as the boundary condition in the third experiment case. The last experimental case was almost similar to the third experimental case. The only difference was the first hour GFS forecast data were replaced by the GFS-FNL data in WRF forecast simulation. Therefore, the last

case is the fusion of the second and third experimental cases. These four experiment cases are denoted here with IC and a serial number denoting the experimental case. Hereafter, the IC1 means the first experiment case to initiate the WRF model. Similarly, the IC2, IC3, and IC4 mean second, third and fourth experimental cases, respectively.

The IC might have effect on forecasted temperature and wind speed, which directly influence the precipitation and other forecasted variables. Thus, the sensitivity of different IC approaches in forecasted daily average wind speed at 10 m height, maximum and minimum temperature at 2 m height was assessed in this study. Furthermore, the sensitivity of spatial resolution of IC data was tested to better understand the IC approaches used in this study. To do that the IC2, IC3 and IC4 test cases were simulated again, but using the GDAS-FNL instead of GFS-FNL data.

Six different events associated with heavy rainy day over the GBM and Indus basin during the monsoon period were selected (Table 4.1). Thus, twelve different combinations (3MP X 4IC) were run for each of these six events. Each event was simulated for at least 7 days lead time. In other words, the total number of simulations required would be 504 (= 12 MP-IC X 6 events X 7 days). Because it is computationally challenging to simulate all of these six events using all twelve combinations, the events were simulated for a sample of MP-IC combinations. Only the Indus 2007 event was simulated for all of these 12 MP-IC combinations. The selected combinations are listed in Table 4.1.

## 4.4 HISTORY AND BACKGROUND OF SELECTED PRECIPITATION EVENTS

### 4.4.1 *GBM 2007 Event*

The year 2007 was a widespread flood year in South Asia. Several countries, including Bangladesh, Bhutan, India, Nepal were affected severely from this flood event. The event has been one of the major five flood events in Bangladesh within a 20 year return period (last recorded similar event was in 1987) [*Mirza,* 2011]. The precipitation amount over the Brahmaputra and Meghna river basins on July 2007 was higher than any other month of previous two years [*Islam et al.,* 2010]. In this study, a particular day of the event was selected in July month (26th July of 2007), when the 24 hour accumulated areal-averaged precipitation (from NCDC-GSOD) exceeded 26 mm within the heavy rainy area of the GBM basin (Figure 4.2a).

### 4.4.2 *GBM 2015 Event*

The year 2015 was also a substantial flood year for the GBM basin. Two events were selected when the 24 hour accumulated - areal average precipitation (from NCDC-GSOD) within the heavy rainy domain exceeded 20 mm. The first event was on 20th August and the second was on 30th August of that year (Figure 4.2c, and 4.2e). The first and the second events of the year 2015 are denoted here as GBM 2015.1 and GBM 2015.2, respectively.

### 4.4.3 *Indus 2007 Event*

Pakistan was also severely affected by the 2007 South Asian floods in 2007. The coastal area of the country was affected by a cyclone in late June, followed by heavy monsoon precipitation in July-August. The cyclone disappeared on 26th June 2007. Immediately after the cyclone, heavy rainfall event affected the North-West Frontier and Punjab [*World Bank,* 2007]. The peak was

observed within the Indus basin on 28th June 2007 (Figure 4.2b), when the 24-hour accumulated basin average rainfall was over 10 mm (from NCDC GSOD).

### 4.4.4 *Indus 2010 Event*

The 2010 flood event in the Indus basin was one of the most severe in the recent history of Pakistan [*Paulikas and Rahman,* 2015]. The flood was caused by heavy monsoon precipitation in late July. Unusual wind and pressure anomaly on that day conveyed moisture into the northwestern part of the country and caused heavy rainfall [*Houze et al.,* 2011]. *Wang et al.* [2011] claimed that the anomalies observed during the 2010 event was not intermittent, and this abnormal circulation was a part of long-term trend of the monsoon. However, precipitation of this event intensified on 28th July (Figure 4.2d). The 24 hour accumulated basin average precipitation was over 17 mm on that day (from NCDC-GSOD).

### 4.4.5 *Indus 2012 Event*

During the year of 2012, monsoon precipitation within the Indus basin was moderate until the August. Rainfall rapidly intensified during the first half of September and caused severe flooding in Pakistan. The precipitation peaked during September 6 to September 11 in Punjab and Sindh province of Pakistan [*Memon et al.,* 2015]. The maximum 24 hour accumulated areal-averaged precipitation within the basin area was on 9th September (Figure 4.2f), and exceeded 11 mm (from NCDC-GSOD).

## 4.5 Reference Data and Analysis Technique

Two sets of reference data were used in this study to evaluate the performance of WRF forecasted precipitation. A gridded reference data set was used to determine the ability of the model to capture precipitation in the spatial direction. The TRMM (Tropical Rainfall Measuring Mission) product 3B42V7 was used as the gridded reference data source. This daily data are available in 0.25˚ resolution. Details of this product are described by *Huffman* [2013]. Another data set was used to evaluate the accuracy of the model to estimate precipitation amount. The GSOD (Global Summary of the Day) data set provided by the NCDC (National Climatic Data Center) was used for this purpose. This in-situ station-based data set is available through WMO (World Meteorological Organization). The Thiessen polygon approach was applied to determine the areal average precipitation within the analysis extents of GBM and Indus basins. Figure 4.2 shown the locations of the available stations within the study areas and their associated Thiessen polygons in GBM and Indus basin, respectively. The same data source (i.e., NCDC-GSOD) was used for the performance evaluation of simulated daily maximum temperature, minimum temperature and average wind speed. Based on the data availability, total 9 and 10 stations were used for the GBM and Indus basin, respectively. The stations were selected carefully to cover the entire basin as well as different climate regime. The locations of these stations are shown in Figure 4.1.

The model performance metrics in this study were divided into two parts like *Liu et al.* [2012]. Four categorical metrics were used to understand the model accuracy to determine rainfall in the spatial direction. These metrics are POD (Probability of Detection), FBI (Frequency Bias Index), FAR (False Alarm Ratio), and CSI (Critical Success Index). These four

metrics were calculated with respect to the gridded reference data (i.e., TRMM). The categorical metrics were calculated based on the contingency table of precipitation (Table 4.2).

The equations for calculating the average categorical metrics are;

$$POD = \frac{1}{n}\sum_{i=1}^{n}\frac{RR_i}{RR_i+NR_i} \quad (4.1)$$

$$CSI = \frac{1}{n}\sum_{i=1}^{n}\frac{RR_i}{RR_i+RN_i+NR_i} \quad (4.2)$$

$$FAR = \frac{1}{n}\sum_{i=1}^{n}\frac{RN_i}{RR_i+RN_i} \quad (4.3)$$

$$FBI = \frac{1}{n}\sum_{i=1}^{n}\frac{RR_i+RN_i}{RR_i+NR_i} \quad (4.4)$$

Here, n is the number of time steps multiplied by the number of grid cells. The POD is the probability of success to detect rainfall with respect to all observed rainfall. The CSI, often termed as “Theta Score” is also represents the same characteristics as POD, but with respect to all observed rainfall as well as the unwanted rainfall generated by the simulation. Both these metrics are ranging from 0 to 1, where 1 is for the ideal case. The FAR indicates the probability of false rainfall generated by the simulation with respect to all rainfall generated by the model. The perfect score of the FAR is 0. All of these metrics (POD, CSI, FAR) do not consider the bias of forecasted rainfall. The FBI was used here to detect the trend (i.e., underestimation or overestimation) of the simulated precipitation with respect to the observed data. The value of the FBI is ranging from 0 to infinity, where 1 is the ideal score. Any value smaller than 1 or greater than 1 indicates that the simulation is underestimating or overestimating the event, respectively.

Similarly, two continuous metrics were used here to evaluate the ability of the model to estimate the amount of precipitation. These continuous metrics are RMSE (Root Mean Squared Error) and MBE (Mean Bias Error). All of these continuous metrics were evaluated with respect to the areal averaged in situ measured rainfall data (i.e., NCDC-GSOD).

The equations of the continuous metrics are;

$$RMSE = \sqrt{\frac{1}{n}\sum_{i=1}^{n}(R_{sim} - R_{obs})^2} \quad (4.5)$$

$$MBE = \frac{1}{n}\sum_{i=1}^{n}(R_{sim} - R_{obs}) \quad (4.6)$$

$$SD = \sqrt{\frac{1}{n-1}\sum_{i=1}^{n}(R_{sim} - R_{obs} - MBE)^2} \quad (4.7)$$

Here, n is the number of time steps. Rsim and Robs are simulated and observed areal averaged precipitation within the analysis extent, respectively. The RMSE and SD represent the amount of error but not the direction of the error with respect to the observes. The MBE indicates the cumulative error as well as the direction of the simulated rainfall bias. The value of MBE can be any real number. The negative or positive value of MBE indicates that the model is underestimating or overestimating the amount of precipitation, respectively.

Evaluating the performance of simulated rainfall derived from different sets of combinations is difficult using seven different metrics. Therefore, a single skill score that can combine the characteristics of these seven metrics is useful. Two skill scores, called “Unified Score” and “Spatial Extent Score” defined in earlier chapter were used here (see Section 3.5.2). However, the threshold values of the MBE, RMSE, and SD were ±15, 15, and 15 respectively, which were set based on the maximum and minimum values of these metrics found in this study (see Table 3.2).

Performance of the simulated daily maximum temperature, minimum temperature, and average wind speed were evaluated using average MBE and RMSE of all stations within the basins.

## 4.6 RESULTS AND DISCUSSION

In GBM basin, the analysis was carried out in two different locations to observe the WRF precipitation forecast performance in different climate regimes. The selected intense precipitation events were located within the heavy rainy area of the GBM basin. Thus, the outputs of the heavy rainy area revealed the forecast performance during the instance of rainfall event at that region. On the other hand, the results over the less rainy area provides the performance criteria when the precipitation is sparse or negligible. In case of Indus basin, almost the entire basin was considered for the analysis.

At first, the sensitivity of three different cloud microphysics on the forecasted precipitation was tested. In the next step, the sensitivity of four different IC test cases on the WRF forecasted precipitation was evaluated. The main objective is to identify the suitable test cases in all conditions of the monsoon driven South Asian river basins. These analyses were carried out for a few day time period (3-6 day, depending on the available 5-day simulated forecast, Table 4.1), and results are shown up to 5 days lead. For example, the GBM 2007 storm event was simulated from 20-26 July 2016. Results up to 5 day lead time were available from 24-26 July 2016 for this event. Therefore, these three consecutive days were considered for the IC-MP sensitivity analysis. Likewise, the performance of simulated daily average wind speed, maximum and minimum temperature were evaluated with respect to different IC approach, up to 5 day lead time. The impact of using finer resolution data (i.e., GDAS) as model IC then evaluated for GBM 2015.1 event with respect to different MP schemes and IC approaches. Finally, the ability of the model to capture the intense precipitation events was evaluated. To do this, only the rainiest day of each event was considered. Thus, this analysis was carried out only for one day of each event.

To carry out the IC and MP sensitivity tests, the categorical and continuous metrics were used. The rescaled error metrics then calculated using the equations from Table 4.2. These rescaled metrics are ranging from 0 to 1, and 1 is the ideal value in all cases. Finally, the unified score was calculated using Equation (8) to evaluate the overall performance of each combination. In GBM basin, all three MP schemes were simulated using only the IC4 test case (Table 4.1). Thus, only the IC4 test case (i.e., warm start) was considered for MP scheme sensitivity analysis. On the other hand, all four IC test cases were simulated with WSM5 MP scheme in GBM 2007, and with TS MP scheme in GBM 2015.1 event. Therefore, the IC sensitivity analysis was carried out only for these two events. It should be noted here, 3 days were considered from GBM 2007 event for this analysis, while 6 days in case of GBM 2015.1 (Table 4.1). Thus, the IC sensitivity analysis in GBM basin is biased to the performance of GBM 2015.1 event as well as TS MP scheme. In contrast with the analysis of GBM basin, the Indus basin is more uniform. The number of warm start and cold start simulation is equal in this basin (Table 4.1). All the simulations were considered for MP scheme sensitivity test. The simulations of Indus 2010 event were used for IC sensitivity test, as all the IC test cases were simulated for this event. Overall, the result of Indus analysis is partially and fully biased by the performance of Indus 2010 event in case of MP and IC sensitivity test, respectively.

Figures 4.3 shows the IC-MP sensitivity results. Each line of these radar charts represents a lead time, while each spoke (i.e., radii) represents an alternative (e.g., IC or MP). The results for both 27 km and 9 km domains are shown here to evaluate the sensitivity of these variables under different model resolution. Here, the higher score (i.e., unified score) means a better match with the observation. Thus, the line closer to the circumference of these radar chart means more accurate result, and less accurate results are closer to the center.

The selected MP schemes (Figure 4.3a) are not much sensitive as the IC approaches (Figure 4.3b) in the heavy rainy area of the GBM basin. Within this area, the WRF forecasted precipitation with all MP scheme shows relatively poor performance than GFS in higher lead time (Figure 4.3a). The reason is, only IC4 was considered for MP scheme sensitivity analysis in GBM basin. The sensitivity analysis of IC approaches (Figure 4.3b) suggested that the cold start options (i.e., IC1 and IC2) are better than warm start within the wet area of GBM basin. This explains why the GFS shows relatively better result in MP scheme sensitivity test. The same figure also shows that the 27 km domain simulate the precipitation with greater accuracy. Though, individual analysis of events (not shown here) indicates that the simulated precipitation is not much sensitive to resolution in this scale, except GBM 2015.1 event (explained later). Here, the IC sensitivity test is dominated by the GBM 2015.1, and showing the 27 km slightly better. The WRF shows relatively better result than GFS in all lead time within the less rainy area of the basin (Figure 4.3c), yet using only IC4 test case. However, the performance of forecasted precipitation is not much sensitive to MP scheme (Figure 4.3c) or IC approach (Figure 4.3d) within less area of GBM basin. The results of the heavy rainy area are dominating in the combined case, as the analysis extent of the heavy rainy area is larger than the less rainy area (Figure 4.3e and 4.3f). The Indus basin shows almost a similar response to different MP schemes (Figure 4.3g) and IC approaches (Figure 4.3h). The WRF forecasted precipitation is not notably sensitive to the selected MP schemes as well as spatial resolution in this scale. The optimized MP schemes and resolutions identified by *Sikder and Hossain* [2016] for monsoon weather remains true for forecasting mode. The WRF model shows sensitivity to the IC test cases in the heavy rainy area of the GBM basin. Here, the cold start IC approaches showing promising result than warm start.

Precipitation is a derived variable in NWP models. Temperature and wind vectors are directly calculated by the primitive equations of NWP models. Therefore, the performance analysis of the WRF simulated daily average wind speed, maximum and minimum temperature was conducted to better understand the sensitivity of IC approaches. The MBE and RMSE of daily temperature and wind speed up to 5 day lead are shown in Figure 4.4. The MBE in GBM basin (Figure 4.4a) indicates that the daily maximum temperature (Tmax) is overestimated by the WRF model. The Tmax is more overestimated by the warm start approaches (i.e., IC3 and IC4). On the other hand, the estimated Tmax is more sensitive to the model resolution than IC approaches in the Indus basin (Figure 4.4b). The RMSE of Tmax (Figure 4.4c and 4.4d) shows that in this scale of model resolution, the WRF forecasted Tmax cannot exceed the accuracy of its model boundary (i.e., GFS). However, the finer resolution model shows slightly and significantly better result in GBM and Indus basin, respectively. Almost a similar performance was found for daily minimum temperature (not shown here) and daily average wind speed (Figure 4.4e and 4.4f). Like precipitation, the rather counterintuitive finding of insignificant improvement in forecast using IC3 and IC4 (supposedly a better representation of initial condition with assimilated observations) can attributed to the spatial scale issue. The GFS-FNL is actually available at 1 degree resolution, while the cold start IC fields are at 0.5 degree. It is therefore likely that the coarser scale in the observation-assimilated IC scenarios provide no significant benefit to improving forecast accuracy. This finding regarding the impact of spatial scale in dynamic downscaling is somewhat consistent with *Xiaodong and Hossain* [2016]. Therefore, the results of GBM 2015.1 initiated with GDAS-FNL (0.25 degree) was compared with the same model initiated with GFS-FNL in the next step.

The impact of using fine resolution IC within the heavy rainy area is shown with respect to different MP schemes (Figure 4.5a), and different IC approaches (Figure 4.5b). The analysis of 9 km domain is reported here, as the impact of finer IC in 27 km domain is not significant. This indicates that the use of finer resolution IC is only suitable in higher resolution models. The use of GDAS-FNL does not have any positive impact in case of WSM5 and WSM5 MP schemes (Figure 4.5a). Though, the difference between GDAS-FNL and GFS-FNL initiated model is less in 9 km domain than the 27 km domain (not reported here). A slight improvement with TS MP scheme is visible in lower lead time. It should be noted here that only IC4 test case was considered for this analysis. In case of different IC approaches (Figure 4.5b), the impact of using finer resolution IC is clearly visible, as only the TS scheme was considered here. However, the figure reveals that the cold stat approach (here, IC2) significantly improves the result with GDAS-FNL from 1 day lead time. In case of warm starts (i.e., IC3 and IC4), a late improvement is noticeable. Here, the cold start approach IC2 directly got the IC form GDAS-FNL without any further degradation of quality. The warm starts in this study used a one day pre-simulation using the available analysis data, seems not reducing the spin-up time error. Instead of reducing any error, the process adds some further uncertainty in the IC through simulation. Therefore, the warm start approaches used in this study are not worthy for heavy precipitation forecasting in monsoon weather.

Furthermore, each of the precipitation events was evaluated separately to see the performance of the WRF model to detect the rainiest day of the events. The performance of different combinations was calculated in term of accuracy in spatial distribution using Equation (9), as well as the areal average amount of precipitation. Only the heavy rainy area of the GBM basin was considered for this analysis, while the full basin was considered in case of Indus.

Model performance on 26 July 2007 shows that the cold start case IC1 exhibit better performance in terms of spatial extent as well as in precipitation amount (Figures 4.6a, 4.6b) within the heavy rainy area of the GBM basin. The IC4 test case with TS MP scheme shows slightly better performance in spatial extent score. The accuracy of different combinations in terms of spatial distribution is not varying significantly on 20 August 2015 (Figure 4.6c). However, in areal average precipitation, the accuracy of the 27 km domain is significantly better than 9 km domain (Figure 4.6d). The 20 August 2015 is the only intense event among the selected six days, where WRF simulated precipitation is significantly overestimated. Only the IC4 was tested on August 30, 2015 with different MP schemes, where the variation in terms of spatial extent (Figure 4.6e) and amount of precipitation (Figure 4.6f) is not significant. In general, the performance of the WSM5 and WSM6 MP schemes is almost similar and they perform well, particularly with cold start approaches.

In Indus basin, the 28 June 2007 event was only tested for IC1 test case with different MP schemes. The TS scheme shows slightly better performance at higher lead time (after 4 day lead time) both in terms of spatial extent and precipitation amount (Figure 4.7a, 4.7b). The 28 July 2010 is the only event where all the MP-IC combinations were tested. However, only WSM5 with all IC approaches are reported here (Figure 4.7c, 4.7d). The IC1 and IC2 perform better here. On 9 September 2012, only the IC4 experiment case was tested, and the TS shows relatively better performance (Figure 4.7e, 4.7f). Overall, the cold start approaches perform relatively better in Indus basin like GBM. However, the TS performs slightly better in Indus basin in case of heavy rainy day.

The WSM5 and WSM6 relatively simple MP scheme, which were designed to work with less complex and commonly used data and other physical parameterization schemes. The TS is the most complex MP scheme used in this study, with double moment capability in case of cloud ice and rain [*Lim and Hong,* 2010]. This is the reason of the difference in performance of WSM schemes with TS. However, all three MP schemes produced almost similar result within the range of 9 km to 27 km domains. Thus, the impact of using any sophisticated MP scheme seems not suitable due to computational time within this scale of model resolution (i.e., 9-27 km). Furthermore, using a MP scheme with graupel (e.g., WSM6, TS) is worthy only when the model resolution is below 10 km. Therefore, using the WSM5 scheme up to 9 km domain is sufficient to generate precipitation forecast in monsoon weather. In case of finer models (< 9 km), the complex schemes may provide better forecast.

## 4.7 CONCLUSIONS

The major goal of this study was the assessment of the sensitivity of different model initializing techniques (IC) and cloud microphysics (MP) on the accuracy of the WRF forecasted precipitation of South Asia. A total of six events including intense rainy day in GBM and Indus river basin were tested to identify the most suitable MP-IC combination for the flood forecaster. From the results of this study, the authors have attempted to present a general guideline to predict rainfall more accurately using the WRF model in the monsoon driven climate regime. Such a guideline can be helpful for the flood forecasting agencies of the South Asian countries where the ISMR is the governing reason of floods.

The primary conclusion is that the warm start options designed for this study are unable to significantly outperform the cold start options. In most cases, the cold start shows better performance than warm start options. From the comparison of GDAS-FNL and GFS-FNL initiated models, it seems that the one day pre-simulation of warm start options does not remove the spin-up time error. Rather, this pre-simulation process adds further uncertainty in the model IC. The same comparison analysis reveals that the use of higher resolution IC with simple cold start option may improve the forecast performance. A similar finding has been reported about the model boundary resolution for the Indian subcontinent by *Kumar et al.* [2016].

In case of cloud microphysics, the performance of WSM5 and WSM6 MP schemes is mostly similar. These two MP schemes perform well with cold start options. The WSM schemes showing their consistency in case of the heavy rainy days within the GBM basin. On the other hand, the TS MP scheme seems works well in the heavy rainy days of Indus basin, no matter what is the IC case. Though, the difference between the WSM schemes and TS scheme in not much significant in this scale. Thus, considering the computational requirement of complex microphysics, it can be concluded that the WSM5 is the recommended option with the cold start IC approach in this scale. The sensitivity of the MP schemes from this study shows consistency with the findings of *Sikder and Hossain* [2016].

Meteorological data from the WRF model using the suitable configurations for monsoon climate (identified in the last two chapters), were applied in a hydrological model to generate the forecasted flow. The next chapter exploring the performance of this forecasted flow and compare it with the flow derived from the GFS forecast to identify the best operational technique for flow forecasting.

## 4.8 TABLES

Table 4.1. Selected events and lead time along with simulated MP-IC combinations.

| Basin | Event | Simulation Period (Peak Rainy Day) | Sim. Lead Time (Day) | Simulated 5-day Forecast Available | IC | MP | | | Number of Simulations |
|---|---|---|---|---|---|---|---|---|---|
| | | | | | | WSM5 | WSM6 | TS | |
| GBM | GBM 2007 | 20-26 July 2007 (26 July 2007) | 7 | 24-26 July 2007 | IC1 | X | | | 7 |
| | | | | | IC2 | X | | | 7 |
| | | | | | IC3 | X | | | 7 |
| | | | | | IC4 | X | X | X | 21 |
| | GBM 2015.1 | 11-20 August 2015 (20 August 2015) | 10 | 16-20 August 2015 | IC1 | | | X | 10 |
| | | | | | IC2 | | | X | 10 |
| | | | | | IC3 | | | X | 10 |
| | | | | | IC4 | X | X | X | 30 |
| | GBM 2015.2 | 21-30 August 2015 (30 August 2015) | 10 | 26-30 August 2015 | IC4 | X | X | X | 30 |
| Indus | Indus 2007 | 22-28 June 2007 (28 June 2007) | 7 | 26-28 June 2007 | IC1 | X | X | X | 21 |
| | Indus 2010 | 22-29 July 2010 (28 July 2010) | 7 | 26-29 July 2010 | IC1 | X | X | X | 24 |
| | | | | | IC2 | X | X | X | 24 |
| | | | | | IC3 | X | X | X | 24 |
| | | | | | IC4 | X | X | X | 24 |
| | Indus 2012 | 1-9 September 2012 (9 September 2012) | 8 | 5-9 September 2012 | IC4 | X | X | X | 27 |

Note: Cross marks are indicator of selected IC-MP combination.

Table 4.2. Contingency table for precipitation analysis.

| Simulated/Observed | $Rain_{observed}$ | No $Rain_{observed}$ |
|---|---|---|
| $Rain_{simulated}$ | RR (Hit) | RN (False Rain) |
| No $Rain_{simulated}$ | NR (Miss) | NN (Correct Negative) |

## 4.1 FIGURES

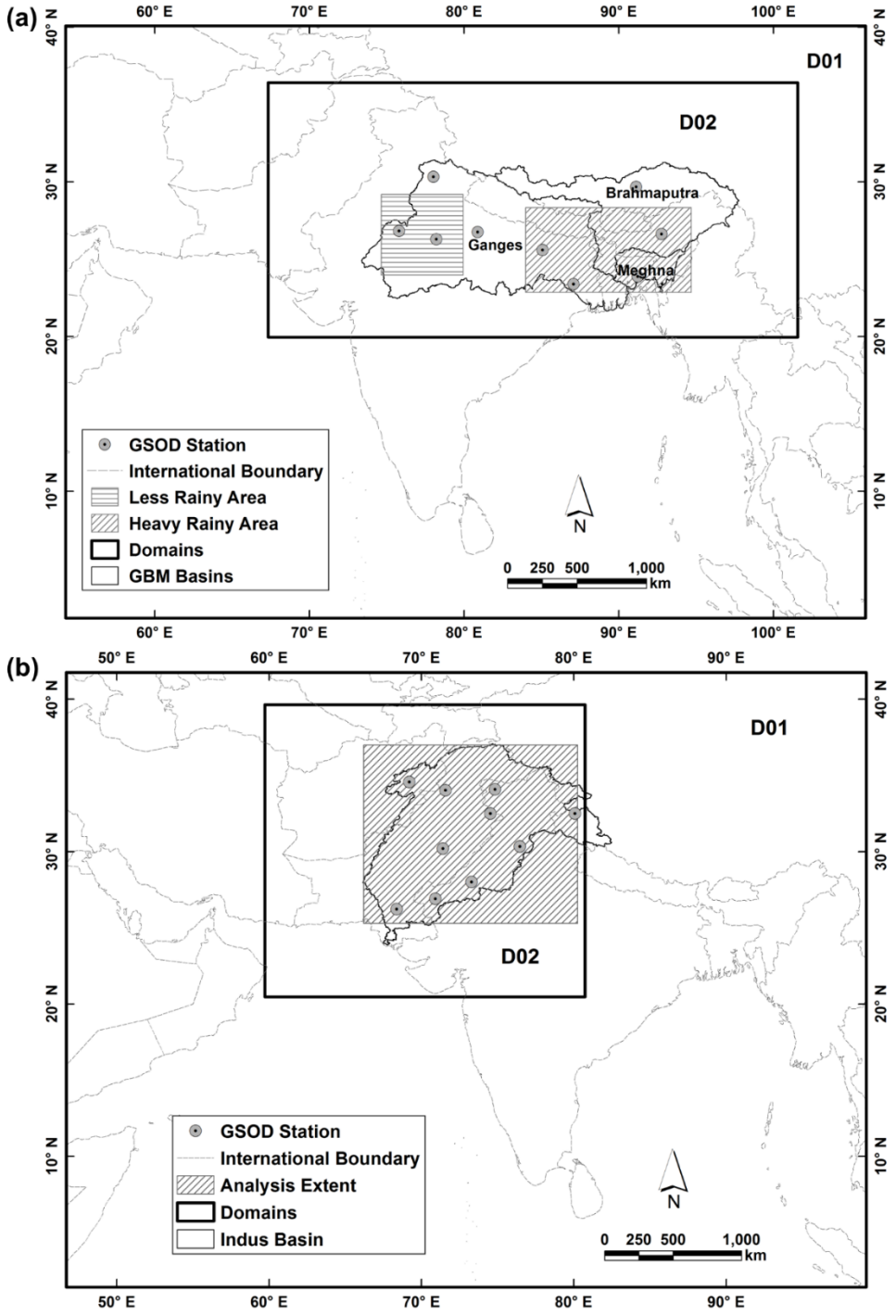


Figure 4.1. WRF model domains and analysis extents of a) GBM, and b) Indus basin along with the selected NCDC-GSOD stations, used for the performance evaluation of simulated temperature and wind speed.

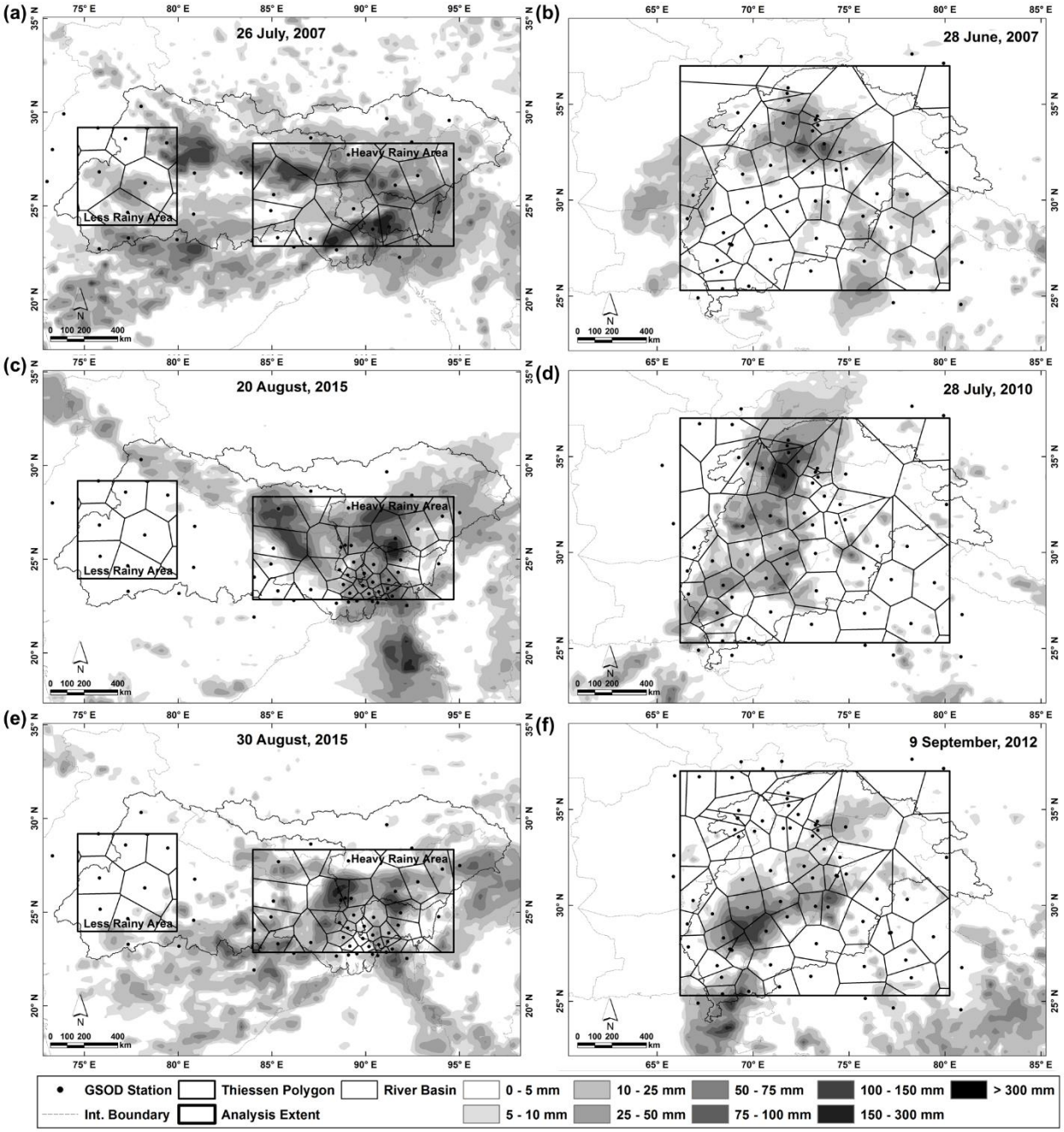


Figure 4.2. Selected intense precipitation events (TRMM 3B42V7) in the GBM (left panel), and Indus basin (right panel) along with available NCGC-GSOD station within the analysis extents and their associated Thiessen polygons.

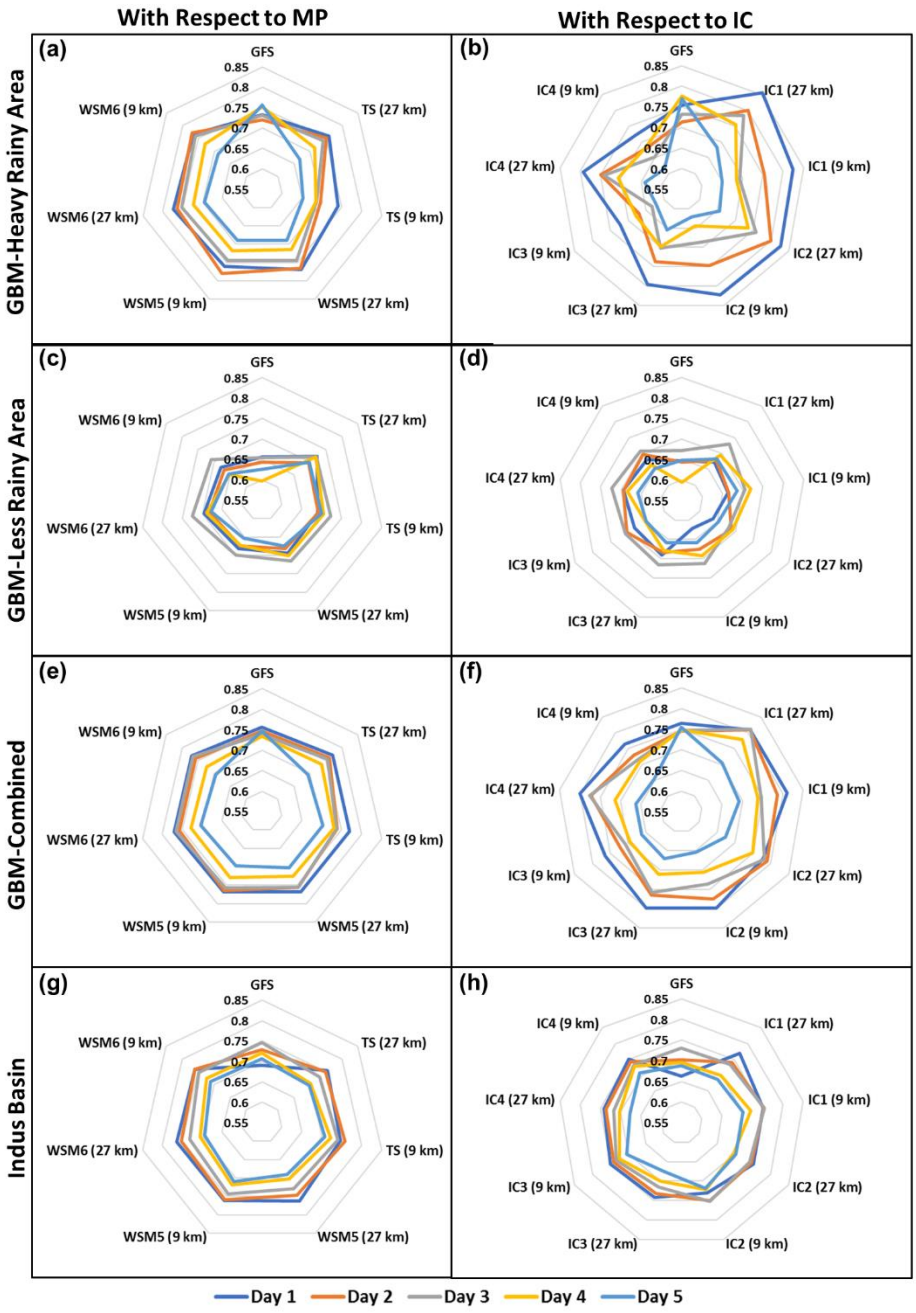


Figure 4.3. Performance (unified score) of the WRF forecasted precipitation at different lead time with respect to different microphysics (MP) schemes (left panel), and initial condition (IC) experiment cases (right panel). Performance of the QPF within the heavy rainy area, less rainy area, combined area of GBM basin, and within the analysis extent of Indus basin are shown in upper, upper-middle, lower-middle, and lower panel, respectively. Here, each line represents a lead time. The alternatives (e.g., WSM6, IC3) with higher scores (i.e., closer to the circumference) are more accurate.

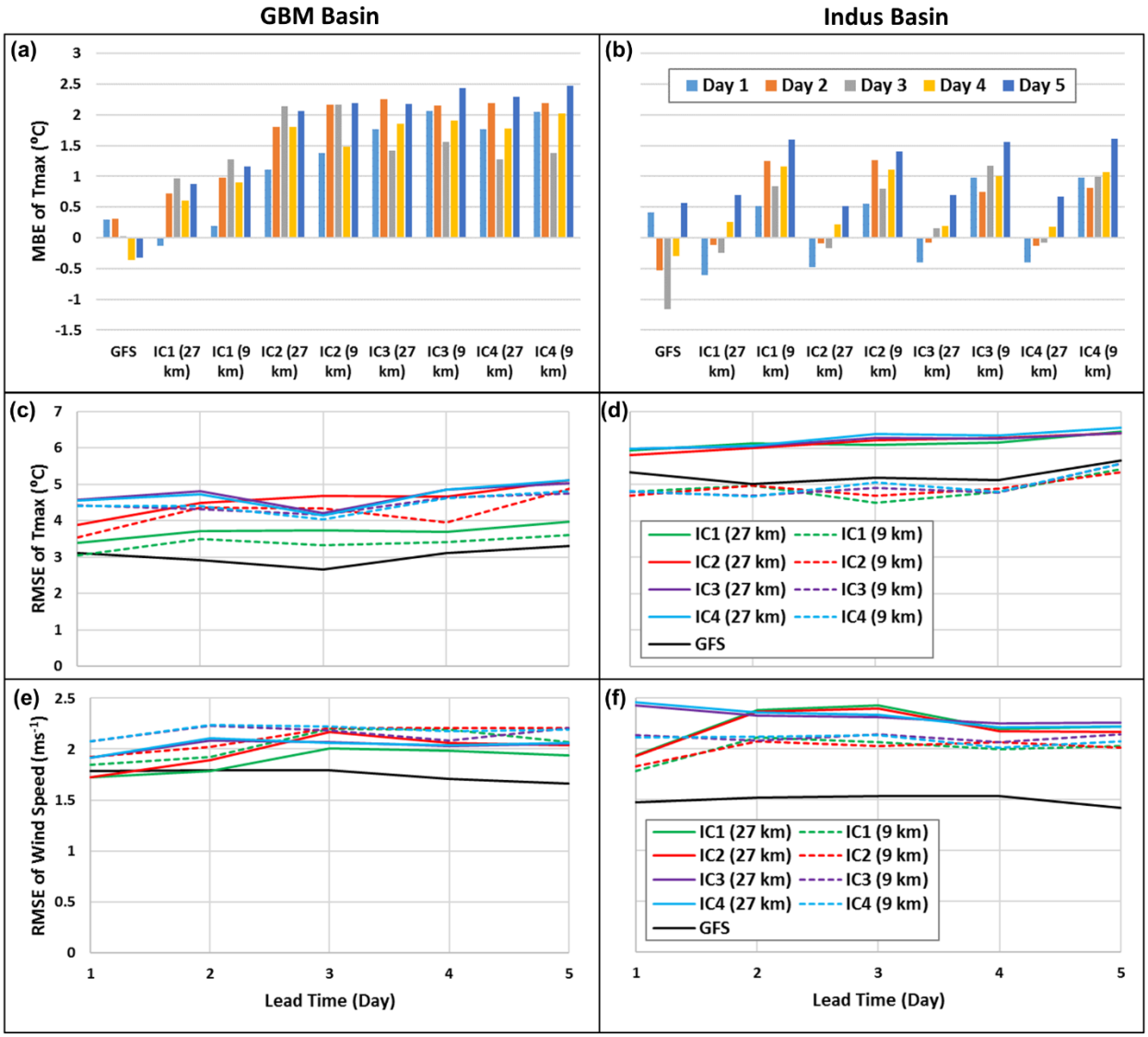


Figure 4.4. Upper panel: MBE of the daily maximum temperature (Tmax); Middle panel: RMSE of the daily maximum temperature (Tmax); Lower panel: RMSE of the daily average wind speed with respect to different IC approaches in GBM (left panel), and Indus basin (right panel).

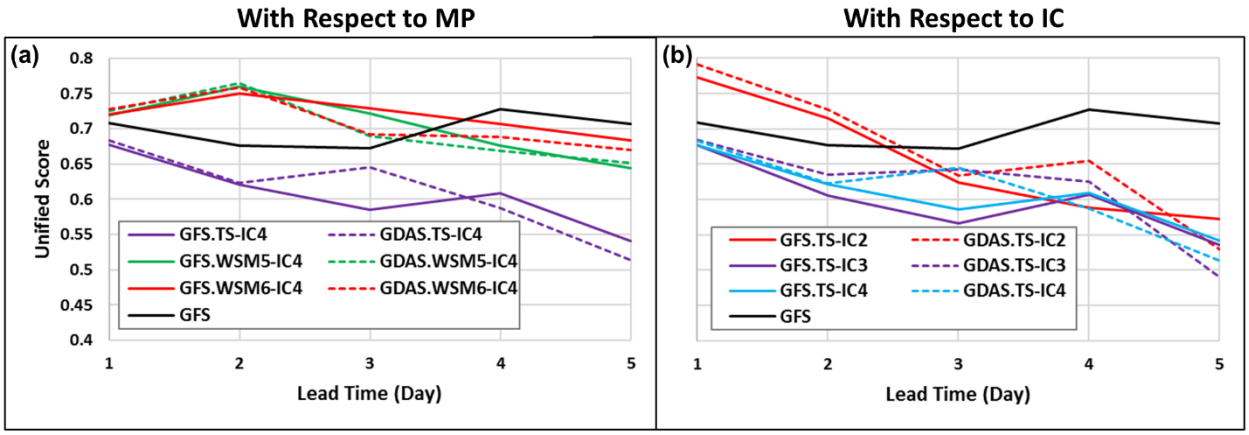


Figure 4.5. Comparison between the GFS-FNL and GDAS-FNL initiated model results with respect to different MP schemes (left panel), and IC approaches (right panel). Analyses are shown here for the 9 km domain of the heavy rainy area of the GBM basin.

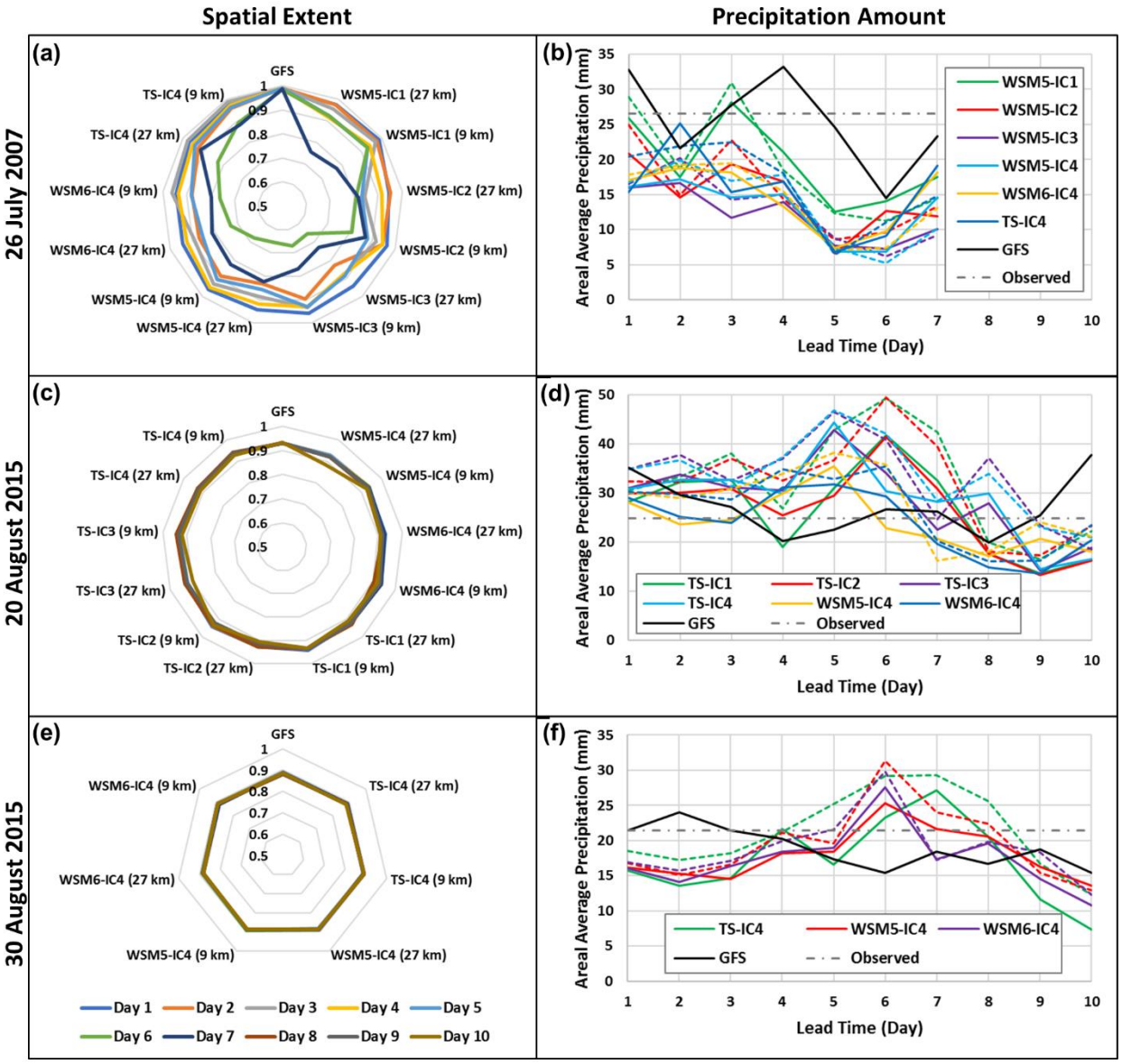


Figure 4.6. Assessment of forecast accuracy within the heavy rainy area of the GBM basin in terms of spatial extent score and as a function of lead time (left panel), and in terms of precipitation amount (right panel). In left panel, the firm and dashed lines are for results from 27 km and 9 km domains, respectively.

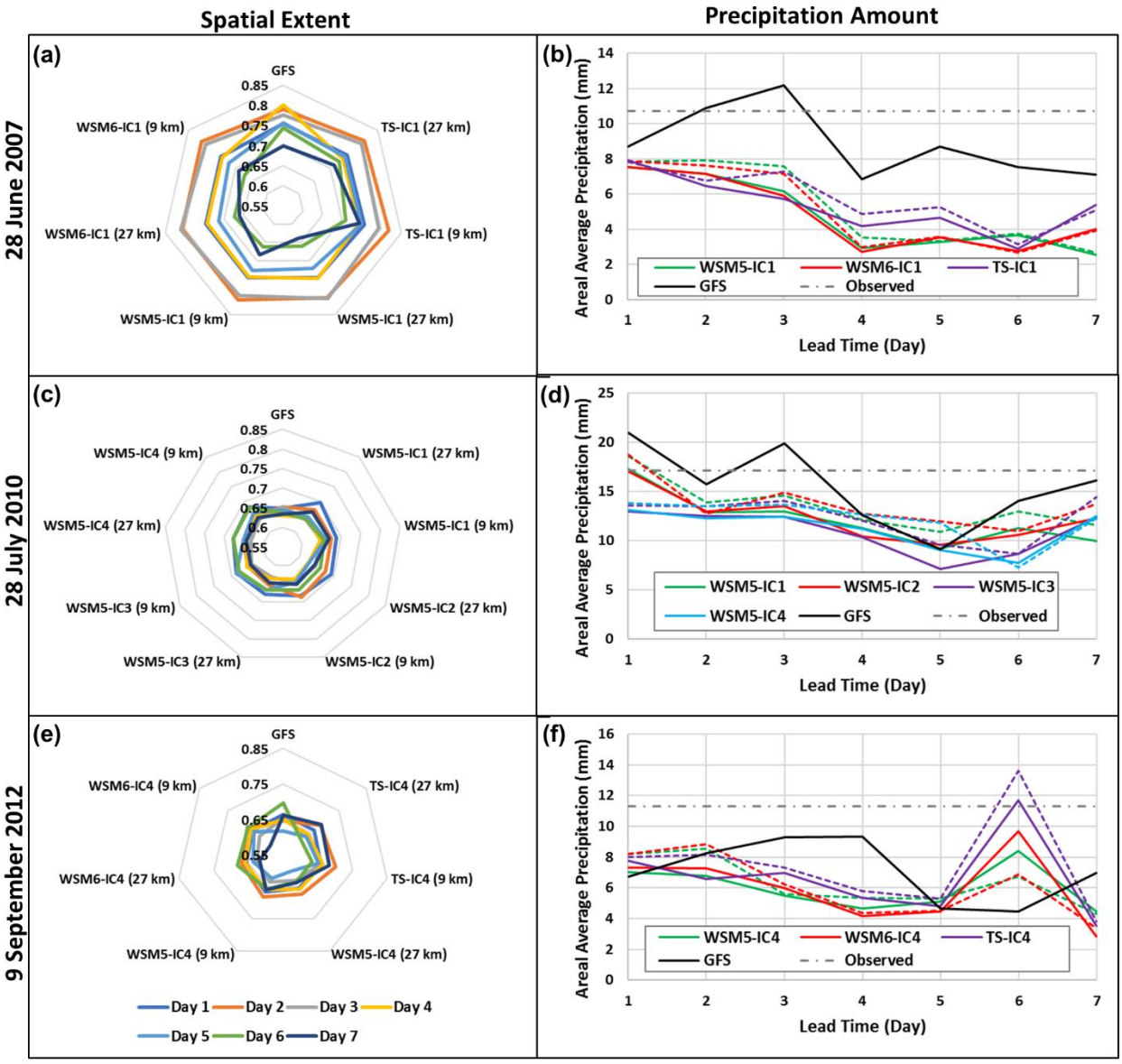


Figure 4.7. Same as Figure 4.6, but for Indus basin.

# Chapter 5. IMPROVING OPERATIONAL FLOOD FORECASTING IN MONSOON CLIMATES WITH BIAS-CORRECTED QUANTITATIVE FORECASTING OF PRECIPITATION

Note: This chapter is currently under review in the *International Journal of River Basin Management*.

**Abstract:** For flood prone countries subject to large scale and seasonal flooding, precipitation forecasting is the single most important factor for improving skill of flood forecasting for such large river basins dominated by the monsoon. Several flood forecasting agencies in South and Southeast Asia, where monsoon floods dominate (e.g., Bangladesh; Pakistan; India, Thailand and Vietnam), are currently using quantitative precipitation forecast (QPF) from numerical weather prediction (NWP) models. Although there are numerous studies reported in literature to evaluate QPF precipitation performance, there appears to be lack of studies about the impact on the flood forecasting skill. In this study, we demonstrate tangible improvements in flood forecasting based on NWP precipitation forecast using an approach that is operationally feasible in resource limited settings of many flood agencies. Our improvement is based on a proposed bias correction methodology for enhancing the skill of QPF using observed and QPF climatology and anomalies. The proposed approach can be applied to any type of QPF dataset such as those dynamically downscaled from regional NWP. We demonstrate clear and consistent improvement in enhancement of flood forecasting skill at longer lead times of up to 7 days in three river basins of Ganges, Brahmaputra and Mekong by about 50% (reduction in RMSE) or 25% improvement in correlation when compared to the forecasts obtained from uncorrected QPF. Furthermore, our proposed bias correction methodology yields significantly higher skill improvement in flood

forecast for global (non-downscaled) QPF than those dynamically downscaled QPFs for the macroscale hydrologic model used for predicting stream flows. The simplicity of the QPF bias correction methodology along with the numerical efficiency can be of tremendous appeal to operational flood forecasting agencies of the developing world faced with large-scale monsoonal flooding and limited computational resources.

## 5.1 INTRODUCTION

In large river basins located in the monsoon dominated climates of Asia and Africa, such as the Ganges, Brahmaputra, Indus, Mekong, Niger, Nile, the most flood-prone country is often located downstream [*Katiyar and Hossain*, 2007]. Such countries receive the lion share of flooding as seasonal and transboundary flow [*Sood and Mathukumalli*, 2011]. In general, the forecasting of such flooding can be performed in many different ways by operational flood management agencies. Examples of various approaches are: persistence techniques based on auto-regression [*Hirpa et al.,* 2013], statistical-dynamical technique [*Cane et al.,* 2013], use of hydrologic-hydrodynamic models [*Maswood and Hossain*, 2015], or assimilation of weather forecast and satellite data [*Biancamaria et al.*, 2011].

For flood prone countries, precipitation forecasting is the most critical factor for improving skill of flood forecasting for such large river basins dominated by the monsoon [*Coe,* 2000]. Forecasting of precipitation is needed to increase the lead time of a flood forecast beyond the time of concentration of the river basin. Hereafter, we shall use flood forecast with flow forecast to imply the same physical phenomenon. If we assume that nowcast estimated precipitation (such as satellite multi-sensor precipitation products) provides the most reliable source of precipitation for large river basins, the lead time will remain limited by the hydrologic time of concentration

of flow. Thus, one of the most common practices to increasing the flood forecasting lead time beyond the time of concentration is to use Numerical Weather Prediction (NWP) models [*Yucel et al.,* 2015; *Nam et al.,* 2014; *Cloke and Pappenberger,* 2009]. NWP models can quantitatively forecast precipitation and their use are becoming widespread among operational flood agencies as data on meteorological forcings and computational resources are more widely available [e.g. *Liu et al.,* 2015; *Liguori et al.,* 2012; *Jasper et al.,* 2002]. In this study, NWP forecast precipitation is considered synonymous with Quantitative Precipitation Forecast (QPF).

Many studies have been conducted for real time flood forecasting using NWP precipitation along with hydrologic and hydrodynamic models [*Liguori et al.,* 2012; *Roberts et al.,* 2009; *Verbunt et al.,* 2006]. However, such studies have shown that the precipitation forecasting using the NWP remains challenging [*Yucel el al.,* 2015; *Ebert,* 2001]. The high uncertainty of NWP precipitation at longer lead times propagates through the hydrologic transformation of flooding to often results in low skill in forecast of flood level [*Nam et al.,* 2014; *Bartholmes and Todini,* 2005].

Recent studies also show that the use of more regionally constrained NWP models (such as the Weather Research and Forecast-WRF - model) can improve the QPF estimates in monsoon climates [*Kumar et al.,* 2016]. Regional NWPs allow one to physically and dynamically predict the mesoscale phenomena comprising convective, cumulus and various cloud processes by taking advantage of features of terrain and land use afforded by a higher resolution model [*Sikder and Hossain,* 2016; *Ahasan and Khan,* 2013; *Hsiao et al.,* 2013; *Hong and Lee,* 2009; *Rao et al.,* 2007].

Several flood forecasting agencies in South and Southeast Asia where monsoon floods dominate (e.g., Bangladesh; Pakistan; India, Thailand and Vietnam), are currently using WRF as the regional NWP model as a source for higher resolution QPF [*Shrestha et al.* 2015]. The Department of Hydrology and Meteorology-Nepal and Department of Hydro-meteorological Services-Bhutan have also begun introducing dynamically downscaled QPF precipitation for flood forecasting [*World Bank,* 2016].

Although there are numerous studies reported in literature to evaluate global QPF or the dynamically downscaled QPF precipitation performance, there appears to be lack of studies about the impact on the flood or flow forecasting skill. This study is motivated by the current lack of a structured approach to the use of NWP based QPF forecasting for flood forecasting in monsoon dominated flood regimes. In particular, we are motivated by the need to improve the use of global QPFs from NWP in a way that is cognizant of the resource limitations of forecasting agencies of flood prone countries. Our current study is also a natural progression from a series of two previous works carried out to systematically understand impact of NWP parameterizations for cloud microphysics, cumulus physics and initial conditions on QPF skill [*Sikder and Hossain,* 2016; 2017a]. The goal of these two studies was to explore if an optimal set of core parameterizations existed for skillful QPF in monsoonal climates. The key findings from those studies were:

1) An optimal set of core parameterizations and scale exists for South and Southeast Asian regions that can be independently validated [*Sikder and Hossain,* 2016].

2) Betts-Miller-Janjic cumulus parameterization scheme with WRF Single-Moment 5-class, WRF Single-Moment 6-class, and Thompson microphysics schemes exhibited the most skill in South Asian region [*Sikder and Hossain,* 2016].

3) Finer spatial resolution (3 km) regional NWP models without cumulus parameterization schemes do not necessarily yield significant improvements, especially if the cloud microphysics scheme is not sufficiently complex [*Sikder and Hossain*, 2016].

4) The more complex initial condition techniques typically involve more QPF uncertainty and cannot significantly exceed the performance of simple initialization techniques [*Sikder and Hossain*, 2017a].

The natural extension of above two studies is to now explore how well NWP-based QPF precipitation from global or regionally constrained models (i.e., dynamically downscaled by WRF) performs in flow forecasting during the flood season. An issue worth an investigation for operational flood agencies is whether flood forecasting in large river basins truly benefits from regionally constrained and higher resolution NWP models that are computationally prohibitive. We test the idea of publicly available global QPFs being sufficient for capturing flooding in large river basins of monsoon climates.

Although it is not the focus of this study, assessment of flood forecasting performance requires recognition of the compounding issues of uncertainty. The propagation of uncertainty of QPF forecasting from regional or global NWP models in the non-linear and physically complex hydrologic models implies that the same benefits of using optimally parameterized QPF may not translate to flow forecasting. Also, operational-scale dynamic downscaling of QPF through higher resolution NWP models represents a computationally expensive exercise for real-time forecasting in developing nations that are constrained by resources. On the other, if non-downscaled QPF as already available publicly from global NWPs (such as NOAA's Global Forecasting System) is found reasonably acceptable, then the appeal for operationalization of

such publicly available QPFs would far outweigh the cost of operational downscaling in regional NWP models like WRF.

The specific research question we ask in this study is *"How can we improve flood forecasting based on NWP precipitation forecast that is skillful and operationally feasible in resource limited settings of flood agencies of monsoon dominated countries?"*

## 5.2 STUDY REGION

For assessment of operational flood forecasting based on NWP QPF, two of the world's largest river basins that experience large scale and seasonal flooding during the monsoonal season were selected. These are: Ganges Brahmaputra Meghna (GBM) basin and the Mekong river basin (MRB).

The Ganges, Brahmaputra, and Meghna (GBM) river basins comprise land areas from Bangladesh, India, Nepal, Bhutan, and China (Nishat and Rahman 2009, Figure 5.1). With Meghna river basin being a considerably smaller part of GBM, we shall confine our study to Ganges and Brahmaputra river locations. The total drainage area of GBM is about 1.72 million sq. km, with a population of at least 630 million. The downstream most country (i.e., Bangladesh) if the most flood-prone and occupies only 8% of GBM basin area. All of the basin stream flow flows through that country and discharges into the Bay of Bengal [*Nishat and Rahman,* 2009]. For more details about the basin, the reader is referred to *Siddique-E-Akbor et al.* [2011], while historical evolution of the flood forecasting system of Bangladesh may be found in *Webster et al.* [2010], *Hossain et al.* [2014a, 2014b, 2014c].

The Mekong River Basin (MRB) (Figure 5.2) is also a monsoon dominated river basin currently undergoing rapid development due to increasing water and energy demand [*Zarfl et al.,* 2014]. It comprises land areas from China, Myanmar, Thailand, Vietnam, Laos and Cambodia [*Kummu and Sarkula*, 2008]. In addition to development pressures, a changing climate (e.g. a changing Monsoon) and rising sea level are perhaps the biggest threats to livelihood in the MR [*Syvitski et al.,* 2009]. For more details on the MRB, the reader is referred to *Hossain et al.* [2017].

## 5.3 MODELS

### 5.3.1 *Hydrologic Model for QPF based Flood Forecasting*

The Variable Infiltration Capacity (VIC) model, first developed by *Liang et al.* [1994] was used as the macroscale distributed hydrological model for forecasting of riverine flooding in GBM and MRB. The basic structure of the VIC model is described in detail by *Liang et al.* [1994]; followed by many papers that provide various updates to the model [e.g., *Cherkauer et al.* [2003] for cold land process updates, *Andreadis et al.* [2009] for snow model updates, *Bowling and Lettenmaier* [2010] for lakes and wetlands, among others]. The model has been widely applied for purposes such as seasonal hydrological forecasting, climate change impacts studies, and water and energy budget studies among various other applications. VIC's distinguishing hydrologic features are its representation of the role of sub-grid variability as a control on soil water storage and in turn runoff generation, and its parameterization of base flow, which occurs from a lower soil moisture zone as a nonlinear recession [*Dumenil and Todini,* 1992]. The basic model features of VIC were discussed in chapter 2 (Section 2.4).

The VIC model was set up over GBM and MRB at daily time step and 0.1 degree spatial resolution, calibrated and subsequently validated based on quality controlled hydro-meteorological forcing datasets from in-situ and space platforms. Most of these quality controlled forcing are derived from Global Summary of Day (GSOD) archived by National Climatic Data Center (NCDC). Details of the calibration and validation are available in *Siddique-E-Akbor et al.* [2011] for GBM and *Hossain et al.* [2017] for MRB. Currently, this calibrated setup provides routine nowcast of streamflow, soil moisture and runoff at 0.1 degree grids operationally for 4 national agencies. These nowcast hydrologic variables are currently rendered for end users on the South Asian Surface Water Modeling System (SASWMS) portal developed by the research group of the second author and hosted at http://depts.washington.edu/saswe. Figures 5.1 and 5.2 show the skill of the VIC model to capture the flow peaks during the Monsoon season for GBM and Mekong, respectively. Table 5.1 provides performance metrics in terms of RMSE and efficiency of the VIC model calibrated using the quality controlled forcing datasets prepared from GSOD. These metrics indicate that the VIC model acceptable for assessing the propagation of NWP-based QPF precipitation forecasts for assessment of skill in flood forecasting.

### 5.3.2 *NWP model for QPF*

The Global Forecasting System (GFS) developed by the National Oceanic and Atmospheric Administration (NOAA) was used as the key source of global NWP model based QPF. As a publicly available service for the world, GFS is ideal for short-term weather prediction applications, particularly in South Asia where economic resources are constrained. More details about the GFS model is available in chapter 3 (Section 3.2). Historical data of this model are available in 0.5 degree resolution since October 2006. Lead time of the historical data varies with

time. The 0.5 degree GFS based NWP model QPFs were used to run this study for propagation through VIC model with or without dynamic downscaling by WRF.

### 5.3.3 *The Weather Research and Forecasting (WRF) Model*

The Weather Research and Forecasting (WRF) model V3.7.1 was used for dynamic downscaling of coarse resolution global NWP weather forecasts, such as from GFS. Such downscaling generated high resolution precipitation forecast over the GBM and MRB. Details about the WRF model was discussed in chapter 3 (Section 3.2).

The WRF model was recently applied in two previous studies to assess the role of cumulus and cloud microphysics parameterizations with scale [*Sikder and Hossain,* 2016] and initial conditions [*Sikder and Hossain,* 2017a] over GBM and Indus river basins. The *Sikder and Hossain* [2016] study explored the choice of 3 spatial resolutions from 3 to 27 km with 5 cloud microphysics and 3 cumulus parameterizations. A total of 45 combinations of WRF configuration were assessed to identify a set up that was most skillful in predicting precipitation in the monsoon climates of Ganges, Brahmaputra. This optimal set up was later independently verified over Indus [*Sikder and Hossain,* 2016]. In the *Sikder and Hossain* [2017a] study, various combinations of initialization of WRF model (known as hot start and cold start) were investigated with the optimal WRF set up identified in the earlier study. In this study, we have applied most optimal WRF set up (comprising the appropriate parameterization and skill) identified in the previous two studies, over GBM and MRB and for investigation of the impact of dynamic downscaling of QPF on flood forecasting. This set up is: 27 km spatial resolution; WSM5 cloud microphysics scheme and Betts-Miller-Janjic cumulus parameterization with cold start for model initialization.

## 5.4 IMPACT OF NWP BASED QPF ON FLOOD FORECASTING

We first investigated the impact of regional NWP (i.e., WRF) based dynamic downscaling of global QPF on flood forecasting by comparing it with flood forecasts generated from global QPFs only. For both basins, a one month time period was selected during the peak of the monsoon. The selected time range for the basins is: 1 August – 10 September 2015 (41 days) for GBM; and 1 September – 30 September 2011 (30 days) for MRB. These two periods were unusually flood prone (high flow) episodes and therefore ideal for investigation of QPF based flood forecasting.

The available 3 hourly GFS forecast data (global QPF and other relevant forcings) have a lead time up to 10 days and 8 days in case of GBM and Mekong basin, respectively. To generate the continuous 10 days WRF forecast within the study period of GBM basin, the WRF model was initialized 9 days before 1 August 2015 (i.e., 23 June 2015, total 50 days of simulation). In this way, 1-10 day WRF simulated forecasts were generated for 1-9 August. Similarly, the simulation of the MRB was started 7 days before 1 September to generate a complete 8 day forecast for the study period (total 37 days of simulation). For each day of forecast, the VIC model was spun up with the prior 2 years of data to reach equilibrium conditions. Figure 5.3 shows an example of the skill of flood forecast in the MRB at the location of Kampong Cham at a 6 day lead time. The flow forecast pertinent to Julian Day on the x-axis that was predicted 6 days ago is presented for various combinations of QPF (global from GFS or regionally downscaled by WRF) and compared against observed and VIC modelled streamflow.

Figures5. 4a and 5.4b provide a closer look at the performance of flood forecast for various lead times for GBM basin in the context of VIC simulated flow from quality controlled nowcast forcing (shown as ‘GSOD’ in the figure). The various lines represent the forecast as obtained

from global QPF (GFS) and downscaled QPF (GFS downscaled by WRF) for a given optimum spatial resolution (i.e. 27 km). A good quality and skilful forecast is one that closely remembers the line obtained with quality controlled nowcast forcings (i.e., from GSOD in Figures 5.4a and 5.4b). What is clear from these Figures 5.3, 5.4a and 5.4b is that the skill of regionally downscaling global QPF in flood forecasting is comparable to that from using only global QPFs. At times, the global QPF (see GFS-3day in Figure 5.4a for Brahmaputra river basin) seems to outperform modestly the downscaled QPF in flow forecasting. For the Ganges river basin, it appears there is some modest benefit of applying regional NWP for flood forecasting. Overall, due to the very modest gain (or the lack of it) in flood forecasting skill, there is no clear trend that informs an operational flood forecaster that incorporating computationally intensive QPF dynamic downscaling is worthwhile.

There could be many factors at play for this apparent lack of clarity on the flood forecasting benefits of using downscaled QPF as indicated earlier. There may also be potential dependency on the quality of the hindcast meteorological data used in VIC model due to the hydrological system memory or the lack of appropriate hydrologic process complexity to take advantage of higher resolution and dynamically downscaled QPFs. It is however, not the goal of the study to investigate the underlying hydrologic factors, but rather to explore practical and operationally feasible ways where an agency can advance operational flood forecasting using global QPFs that are publicly available (see next section).

## 5.5 TOWARDS AN OPERATIONALLY FEASIBLE APPROACH

Given the apparent lack of overwhelming benefit of dynamically downscaled QPF in flood forecasting for the hydrologic model in question (VIC), our next goal was to develop a practically efficient approach as a correction technique for global QPFs in order to maximize its skill in precipitation. This approach is modular enough that it can be applied to downscaled QPFs from WRF as well. The developed approach is based on climatology of forecasts from NWP and it applies bias correction by taking advantage of anomaly from climatology of observations. The approach does not require any regional NWP for downscaling and is therefore a computationally efficient technique involving only simple numerical adjustments. We applied the approach on both global QPFs and downscaled QPFs to compare the relative performance.

In our proposed bias correction methodology for QPF, the daily gridded precipitation climatology was derived from gridded NCDC-GSOD data that is available in a quality controlled format over a long period. These gridded NCDC-GSOD data were already used for VIC model calibration and validation. This gridded climatology is considered as the true (or observed) climatology of the area or the river basin. Next, the daily gridded climatology was calculated for global NWP QPFs (i.e., GFS) for a given lead time from 1 (L1) to 7 days (L7). The gridded daily anomaly of GFS precipitation for each Julian day of forecasting was then calculated using this global QPF climatology for a given lead time (L1-L7). Finally, this anomaly was added to the true (or observed) gridded climatology from the NCDC GSOD dataset to derive the bias corrected NWP QPF for use in operational forecasting. The bias corrected global QPFs generated for each day was then used to force the VIC model and forecast the consequential flow at river locations. In essence, what the flood forecaster would do every day is extract the global QPF for

the forecasting domain or river basin, then derive the anomaly from QPF climatology pertaining to various lead times and finally add that anomaly to the observed climatology for that day.

In this study, two types of bias correction were carried out. At first, the gridded GFS climatology was calculated using only 1-day lead time precipitation forecast. Herein, GFS and QPF imply the same forecast dataset. This 1-day lead time GFS climatology was considered as the constant or universal GFS climatology for different lead times for the sake of computational efficiency. In the second approach, the gridded daily GFS climatology was calculated for different lead times and not just for lead time 1 day or L1. For example, the 3-day lead time (L3) QPF climatology was calculated using the 3-day lead time QPF. Figure 5.5 demonstrates the concept of our proposed bias correction methodology to daily QPF using QPF climatology and true climatology using over the GBM basin.

The impact of bias correction analysis was carried out for 7 and 6 years for GBM and Mekong basin, respectively. The years were selected based on the rated (observed) discharge availability. Figures 5.6, 5.7 and 5.8 show the impact of applying this bias correction to QPF for flow forecasting for Brahmaputra, Ganges and Mekong river basins, respectively. These figures are showing the flow climatology (6-7 year average flow) of three river basins.

Two clear trends are apparent from these figures. First, the bias correction approach based on QPF climatology yields significant improvement in flood forecasting skill with drastic reduction in flow bias between observed and forecast at all lead times for all three river basins. Second, the use of QPF (GFS) climatology pertaining to the corresponding lead time improves flood forecast skill further compared to the use of computationally simpler 1 day QPF climatology (see the middle and lower panels of Figures 5.6, 5.7 and 5.8).

In the next step, we implemented the same bias correction approach on downscaled QPF (GFS) derived from WRF to identify the potential net benefit of using regional NWP for flood forecasting. Table 5.2 summarizes the forecast performance (skill in terms of correlation and normalized RMSE) for all three river basins. As the performance results for all basins follow mostly a similar trend, we show herein results from the Mekong river basin as an example (Figure 5.9). Two contrasting years were picked for the assessment of bias correction of WRF downscaled QPF – 2010 as the relatively weak flood year and 2011 as a very strong flood year.

What is clear from Figure 5.9 or Table 5.2 is that while at lower lead times, there is no apparent difference between the flood forecasting skill of global QPF or downscaled QPF, the bias correction approach yields higher benefits for global QPF at longer lead times. At longer lead times, the bias correction methodology for WRF downscaled QPF appears to perform modestly worse than the bias corrected global QPF. There are likely many reasons behind this observation, with the critical ones being hydrologic, and stemming from the choice of hydrologic model, model initialization, hindcast, sensitivity to scale etc. These physical features of a hydrologic model are known to interact in a non-linear fashion with higher resolution forcing to often magnify the uncertainty in the simulation of the output (i.e. flow) [*Nam et al.*, 2014]. This also brings up the intriguing issue of commensurate hydrologic model complexity in terms of scale and processes that can take advantage of the dynamically downscaled QPFs with higher spatial resolution. Perhaps a higher resolution and more physically distributed and complex hydrologic model (such as MIKE – SHE) would be able to accentuate the benefits of downscaled QPF in flood forecasting. However, the operational agency has to weigh in the benefit of such models in the context of the significant cost to its daily operations.

It is beyond the scope of this study to investigate the underlying hydrologic causes and this study is motivated by the need for an operationally feasible approach in resource-constrained settings of the developing world. We are therefore of the opinion that for an open-source, macroscale (10kmX10km, daily) hydrologic model like VIC, the use of global QPF with bias correction based on QPF climatology (and without any dynamic downscaling) has tremendous operational appeal to flood forecasters in developing nations. This appeal stems from the fact that the computationally prohibitive WRF need not be applied every day or every time step to update flow forecasts in large and higher order rivers with a lot of hydrologic processes integration. The publicly available global QPFs can be used 'as is' after some efficient bias correction to maximise the flood forecasting skill. In our study, the consistent performance of the computationally efficient bias correction approach for global QPFs is the take home message. We therefore recommend this approach to flood forecasters who routinely use QPF as a practical innovation for improving operational flood forecasting in monsoon dominated flood regimes. We believe such a simple approach has not appeared in flood forecasting literature to the best of our knowledge.

## 5.6 CONCLUSIONS

Our study was motivated by our long association with operational flood forecasting agencies of the developing world that deal with large scale monsoonal flooding and yet have limited resources. The first author had worked extensively in the flood management division of Institute of Water Modeling (Bangladesh) to provide routine support to Flood Forecasting and Warning Center (FFWC) of Bangladesh (www.ffwc.gov.bd), which currently applies regional NWP downscaled QPFs to issue official forecasts for up to 5 day lead times during the monsoon

season. The second author has been involved in capacity building and training of flood forecasting agencies of the developing world in an effort to bring in technological and science-based solutions [*Hossain et al.,* 2014a; 2014b; 2014c]. In our combined experience of having worked closely in real world operational settings, we have realised that the advancement of existing flood forecasting schemes in monsoon-drivel flood regimes require both computational feasibility as well as enhanced skill at longer lead times (> 5 days). The skill requires to be of a nature that allows agencies to issue specific warnings at specific locations with quantitative clarity in advance of the hardship the local inhabitants are likely to face.

In our study, it is quite clear that flood forecasting systems using macroscale hydrologic models like VIC can benefit modestly from the application of regionally downscaled QPFs by WRF. However, the modest benefit does not appear to justify the significant computational burden of dynamic downscaling when compared with the bias corrected approach for global QPFs. We have developed our bias correction methodology for global and publicly available QPFs such that flood forecasting agencies can apply efficiently every day without requiring complex dynamic downscaling. Such a correction approach has been shown to significantly and consistently improve the skill in flood forecast for all three river basins of Ganges, Brahmaputra and Mekong studied here for important flood years. To the best of our knowledge, flood forecasting agencies of the developing world are not yet applying such an efficient approach to take advantage of the global QPFs that are publicly available. Furthermore, the simplicity of the bias correction methodology implies that it can be applied to any other forecast dataset such as WRF downscaled QPF or those that are not publicly available (e.g., from European Center for Medium Range Forecasting). If agencies are already employing computationally intensive techniques routinely (such as dynamic downscaling every time step), the bias correction

methodology will further improve the skill with the choice of an appropriate hydrologic model. It is our belief therefore that such computationally efficient methodology to reduce bias in QPF and enhance the consequential flood forecast skill is the future for most, if not all, flood forecasting agencies that deal with monsoon-driven large-scale flooding in the developing world.

## 5.7 TABLES

Table 5.1. VIC Hydrologic model calibration and validation metrics for Ganges, Brahmaputra and Mekong river basins. Ganges and Brahmaputra basins were assessed at Hardinge Bridge and Bahadurabad, respectively, while Mekong basin was assessed at Kampong Cham (see Figure 5.1).

| Basin | | Period | RMSE ($m^3/s$) | Correlation | Efficiency |
|---|---|---|---|---|---|
| Calibration | Ganges | 2002-05 | 6523 | 0.89 | 0.78 |
| | Brahmaputra | 2002-05 | 7606 | 0.91 | 0.86 |
| | Mekong | 2003-08 | 6390 | 0.93 | 0.84 |
| Validation | Ganges | 2006-10 | 7081 | 0.89 | 0.77 |
| | Brahmaputra | 2006-10 | 10918 | 0.92 | 0.82 |
| | Mekong | 2009-13 | 5615 | 0.92 | 0.85 |

Table 5.2. Performance (correlation and % NRSE in parenthesis) of the bias correction methodology for global QPF (GFS) and WRF downscaled QPF in flow forecast for Ganges, Brahmaputra and Mekong rivers.

| Lead Time (Day) | Ganges | | Brahmaputra | | Mekong | |
|---|---|---|---|---|---|---|
| | GFS | WRF | GFS | WRF | GFS | WRF |
| 1 | 0.63 (81.3) | 0.49 (79.3) | 0.70 (37.5) | 0.71 (33) | 0.91 (24.2) | 0.89 (33.1) |
| 2 | 0.77 (52.2) | 0.72 (45.1) | 0.58 (31.3) | 0.59 (35.9) | 0.87 (32.2) | 0.80 (57.9) |
| 3 | 0.84 (44.2) | 0.71 (45.6) | 0.52 (33) | 0.52 (40.1) | 0.86 (29.6) | 0.82 (64.1) |
| 4 | 0.88 (47.1) | 0.80 (42.4) | 0.42 (37) | 0.6 (37.6) | 0.77 (30.2) | 0.75 (72.7) |
| 5 | 0.82 (78.8) | 0.88 (45.9) | 0.38 (41) | 0.52 (38.3) | 0.72 (33.3) | 0.66 (92.9) |
| 6 | 0.8 (87.1) | 0.80 (63.4) | 0.23 (45.4) | 0.29 (47.1) | 0.72 (29.6) | 0.57 (103.6) |
| 7 | 0.7 (103.2) | 0.65 (87.2) | 0.0 (66.6) | 0.14 (53.9) | 0.66 (30.8) | 0.43 (94.1) |

## 5.8 FIGURES

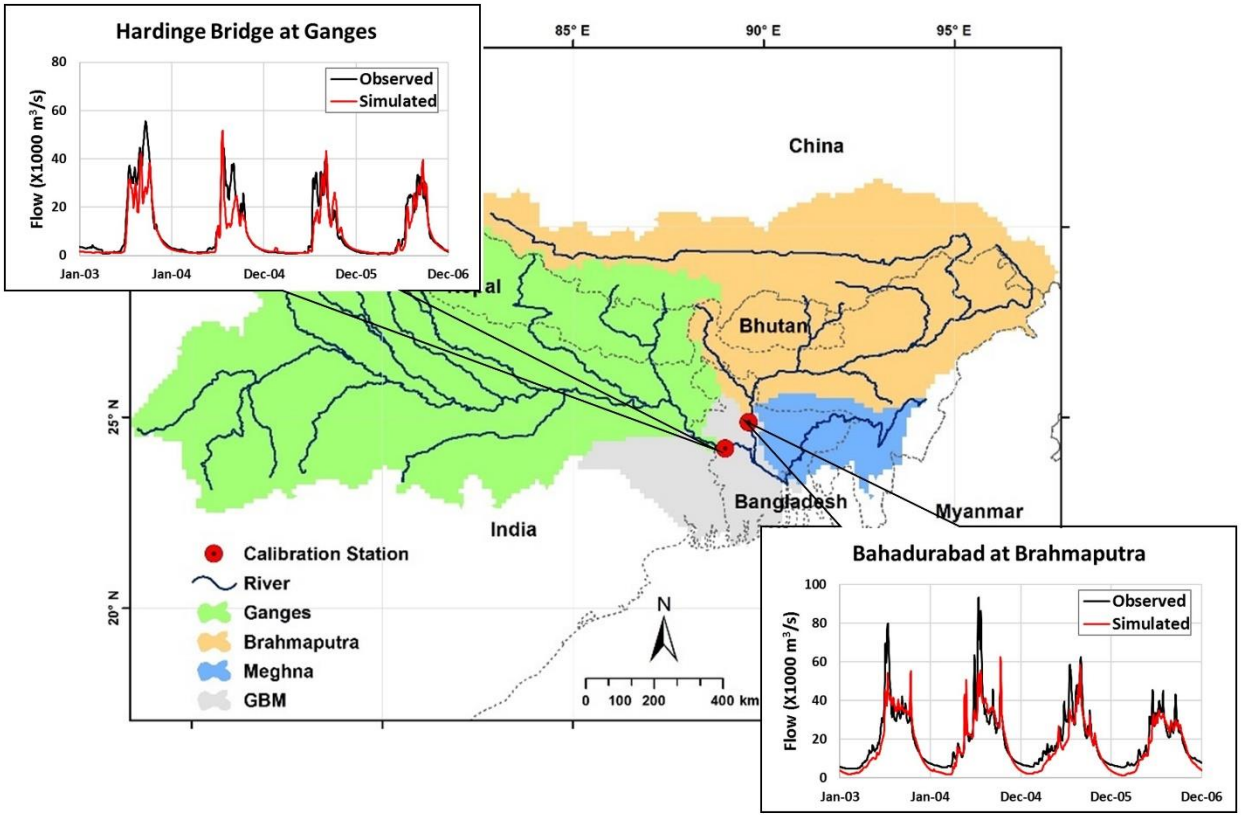


Figure 5.1. GBM Basin as one of the study region along with VIC Model calibration points.

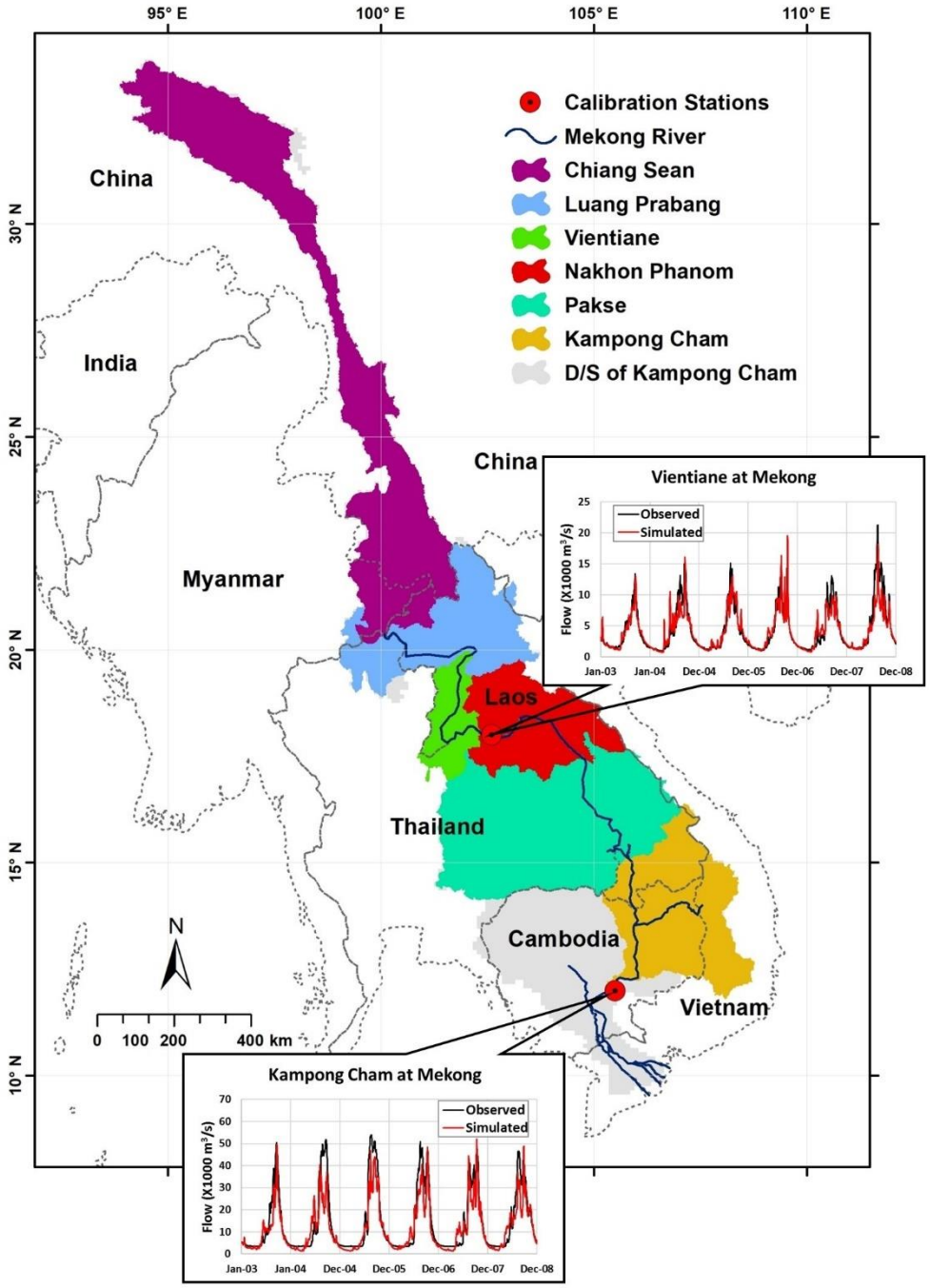


Figure 5.2. Same as Figure 5.1 but for Mekong River Basin.

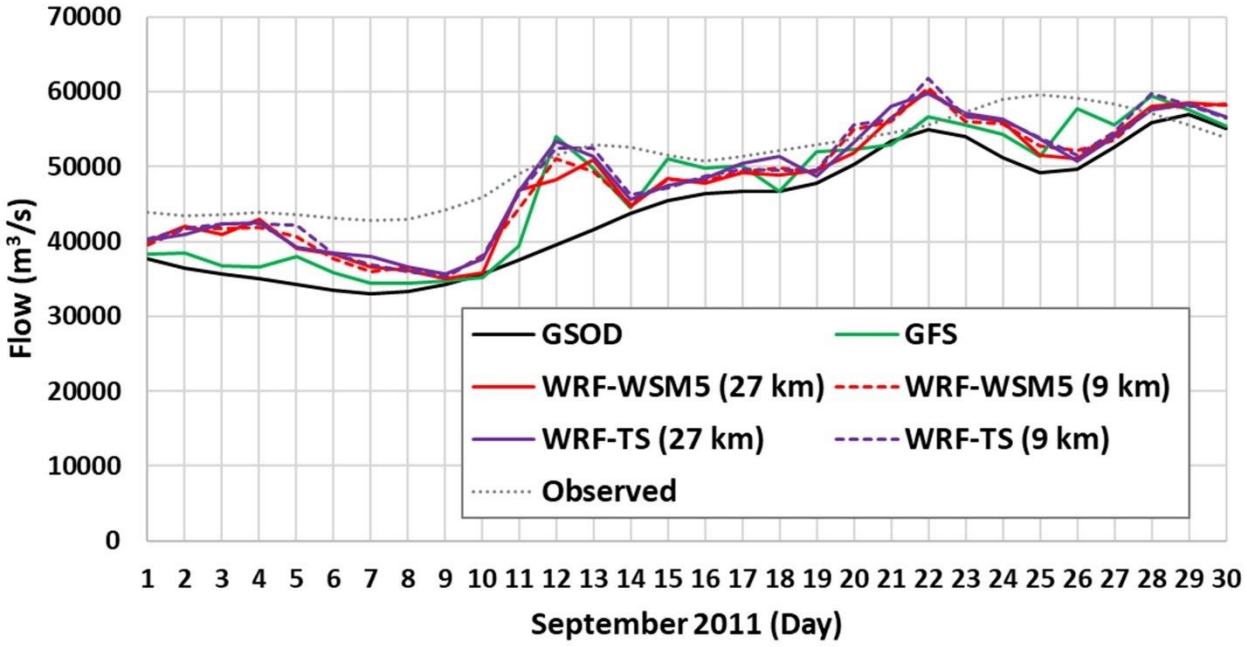


Figure 5.3. Flow forecast obtained from WRF downscaled GFS forecasts and global QPF (as GFS)and compared with GSOD and observed flow at the 6 day lead time. The comparison was conducted at Kampong Cham in Mekong river (see Figure 5.2 for location of Kampong Cham). Here: GSOD is Global Summary of Day archive by National Climatic Data Center (NCDC) and represents the flow simulation by VIC model from quality controlled forcing datasets ; GFS is the flow forecast obtained at 6 day lead using the global QPF in VIC model as is without any dynamic downscaling; All other lines except for "Observed" represent various combinations of dynamically downscaled QPF via WRF. WSM5 – a cloud microphysics (MP) scheme found optimal for monsoon climates; TS – Thomson cumulus scheme found optimal for monsoon climates. Details on the skill of precipitation forecast for TS and WMS5 parameterizations can be found in Sikder and Hossain (2016, 2017a).

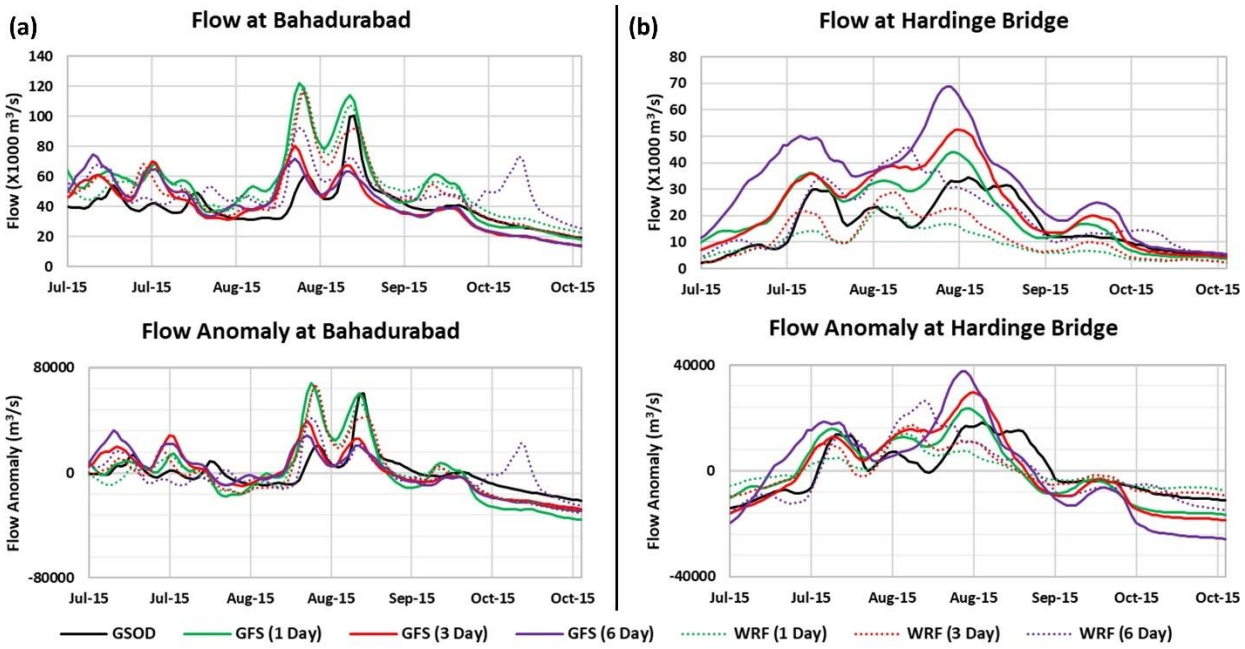


Figure 5.4. (a) Assessment of flood forecasting from NWP QPF (downscaled or global) for various leads times for Brahmaputra river basin at Bahadurabad location inside Bangladesh (see Figure 5.1). GFS represents the global QPF forecast as publicly available without any downscaling, while WRF represents the dynamically downscaled QPF via WRF. The WRF configuration pertains to 27 km resolution and WSM5 and BMJ combination. GSOD represents the VIC modelled flow from quality controlled forcing datasets (nowcast). Upper panel shows actual forecasted flows; Lower panel shows flow anomalies relative to the observed flow climatology. (b) Same as Figure 5.4a but for Ganges river basin assessed at Hardinge Bridge location inside Bangladesh (see Figure 5.1).

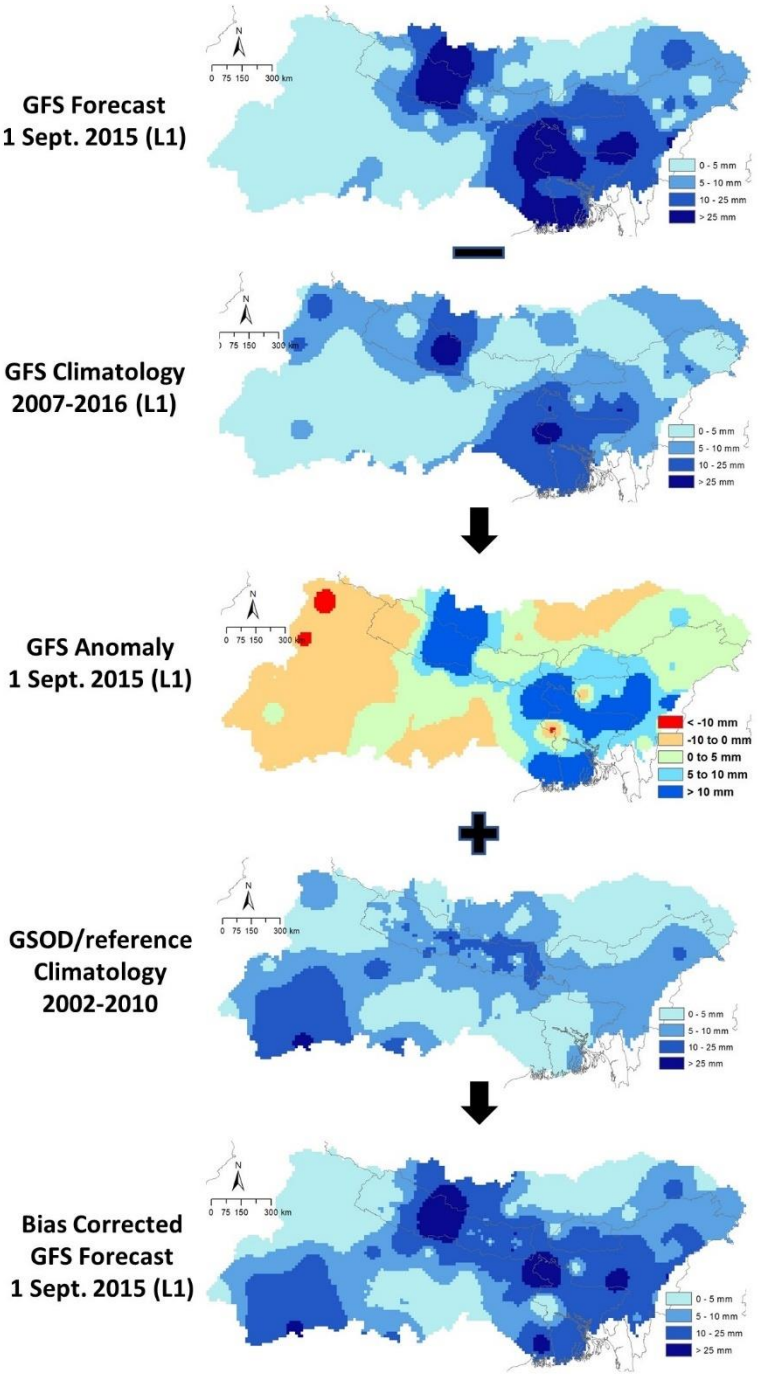


Figure 5.5. A proposed and simple methodology for bias correction of QPF data based on climatology of observation, QPF or downscaled QPF.

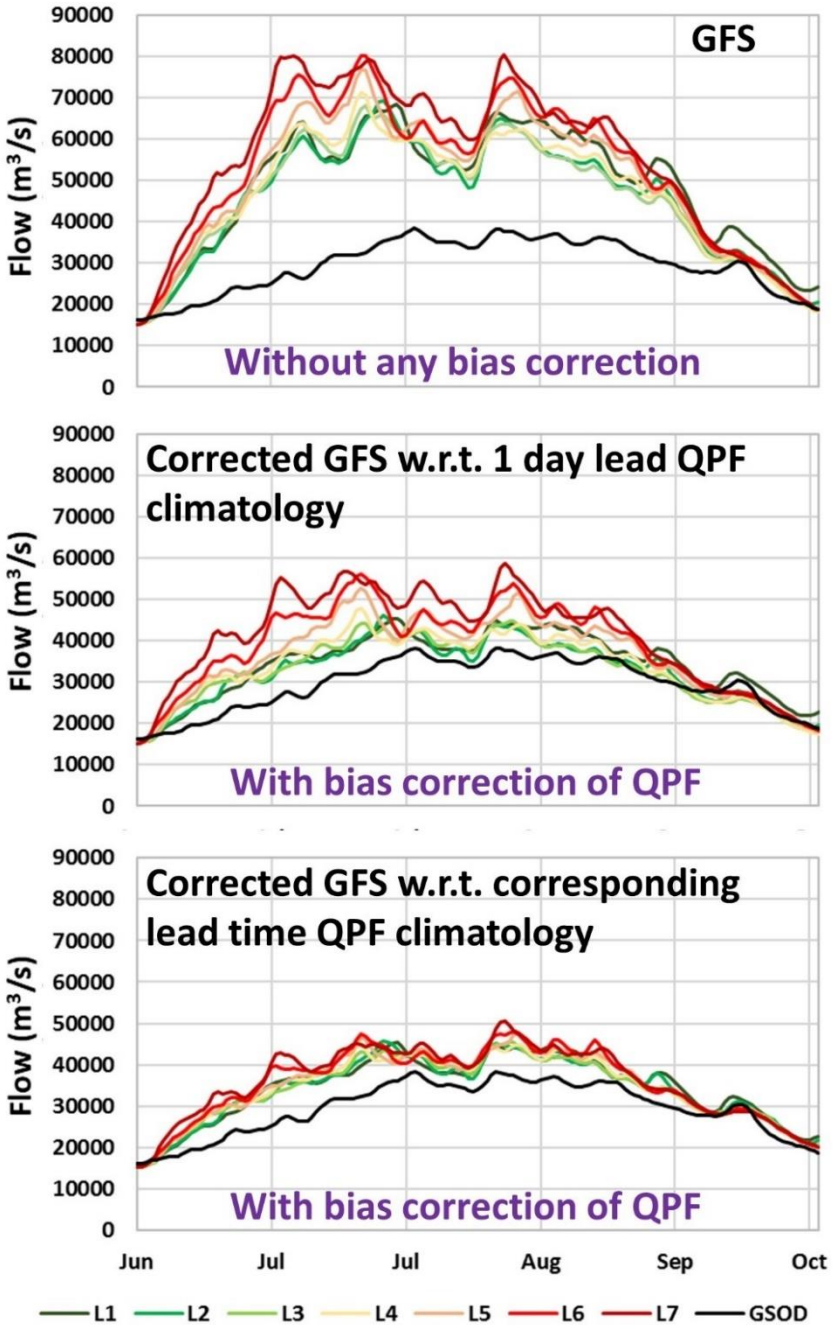


Figure 5.6. Impact of using bias corrected global QPF (from GFS) on flow climatology, with no dynamic downscaling on flood forecasting for Brahmaputra river basin at Bahadurabad station. The lower panel is the flood forecast based on bias corrected QPF using QPF climatology of the corresponding lead time; middle panel is bias corrected QPF using QPF climatology corresponding to lead time 1 day as representative climatology for all lead times. The GSOD line is the simulated VIC flow obtained from quality controlled nowcast forcing. LX stands for lead time at X day.

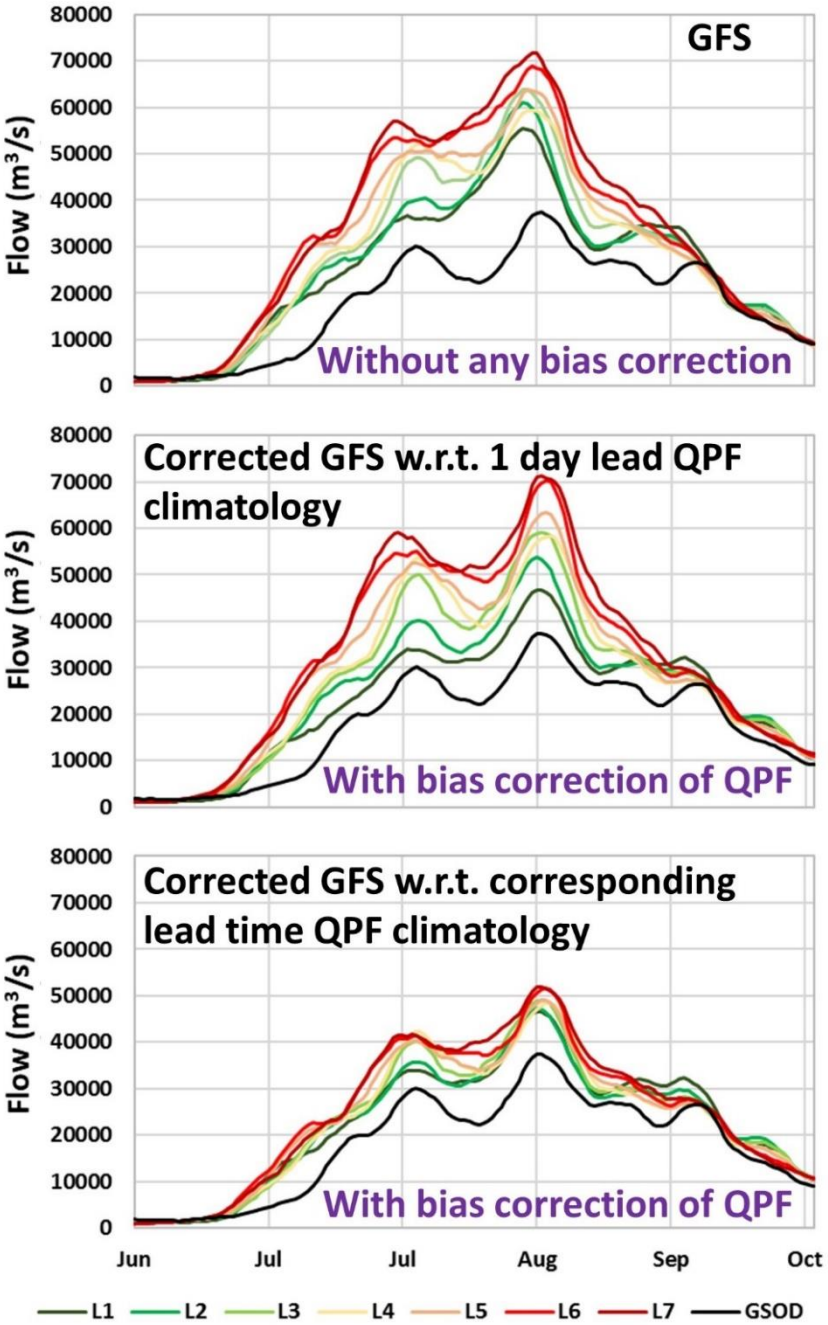


Figure 5.7. Same as Figure 5.6 but for Ganges river basin at Hardinge Bridge station.

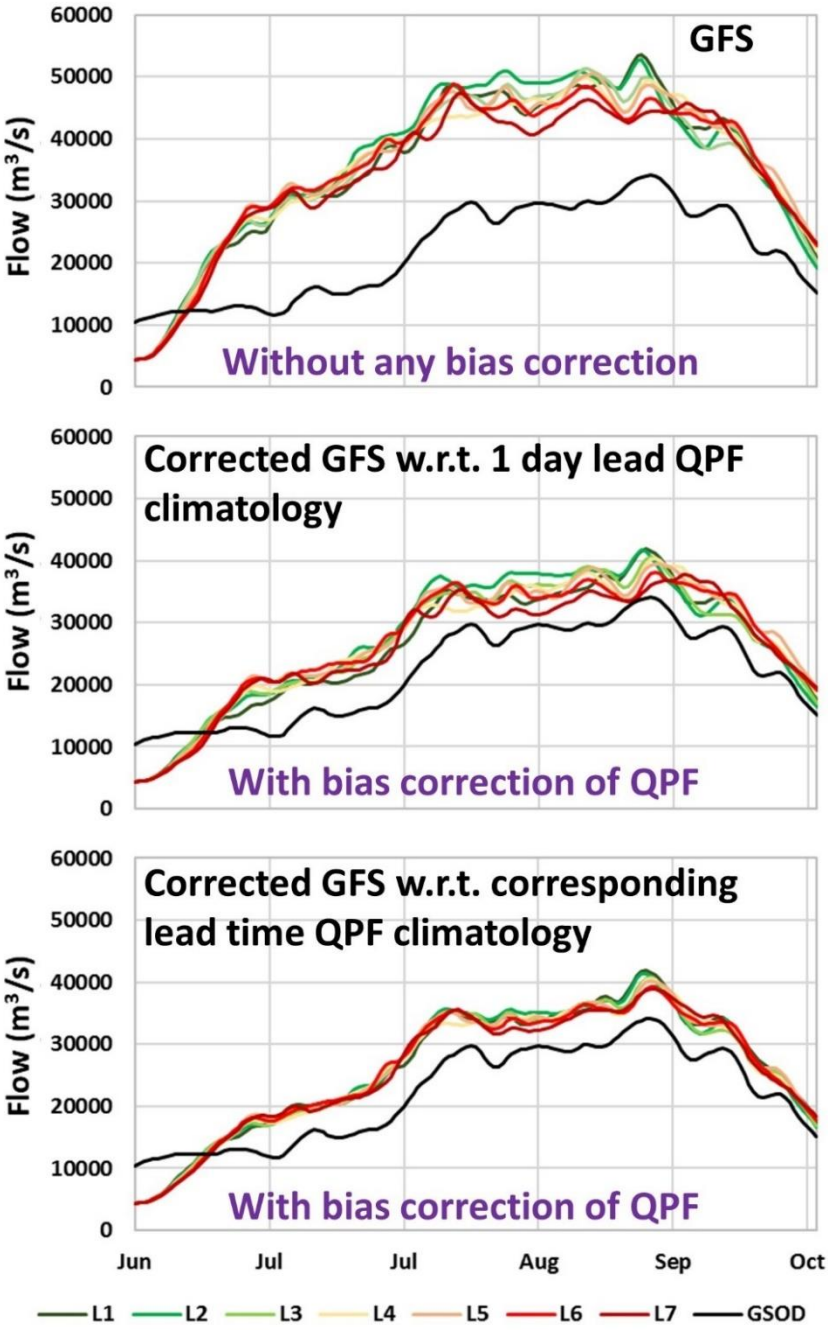


Figure 5.8. Same as Figures 5.6 and 5.7 but for Mekong River basin at Kampong Cham station.

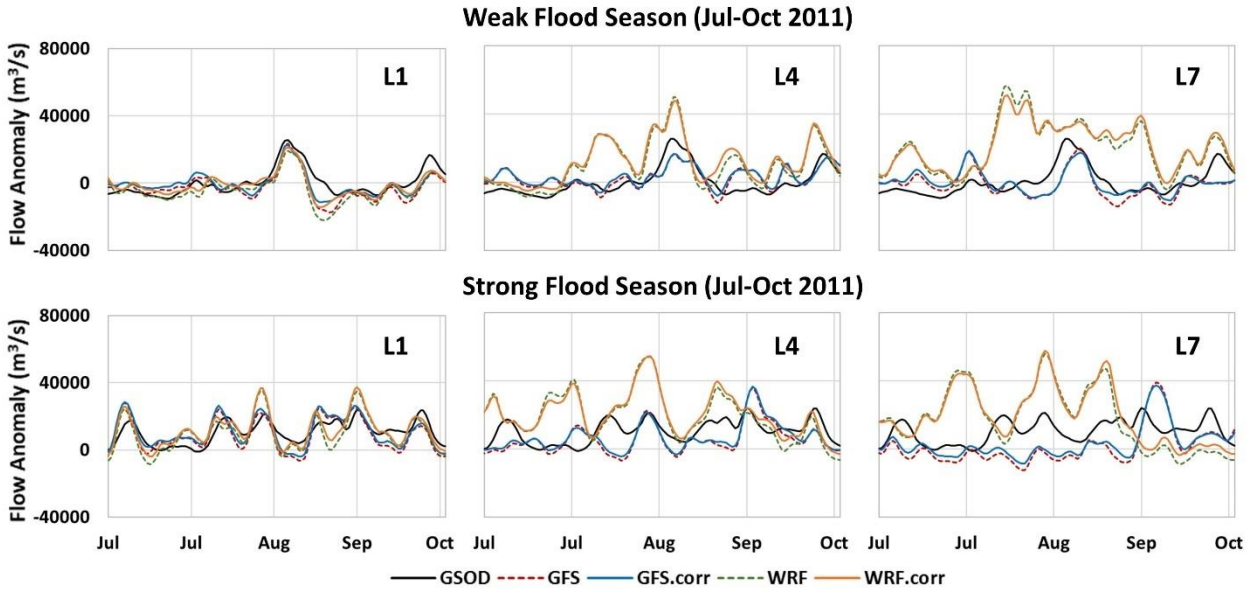


Figure 5.9. Flow anomaly (relative to climatology of observed flow) for various combinations QPF (bias corrected or downscaled) for Mekong river at Kampong Cham. Suffix '.corr' stands for the bias corrected QPF.

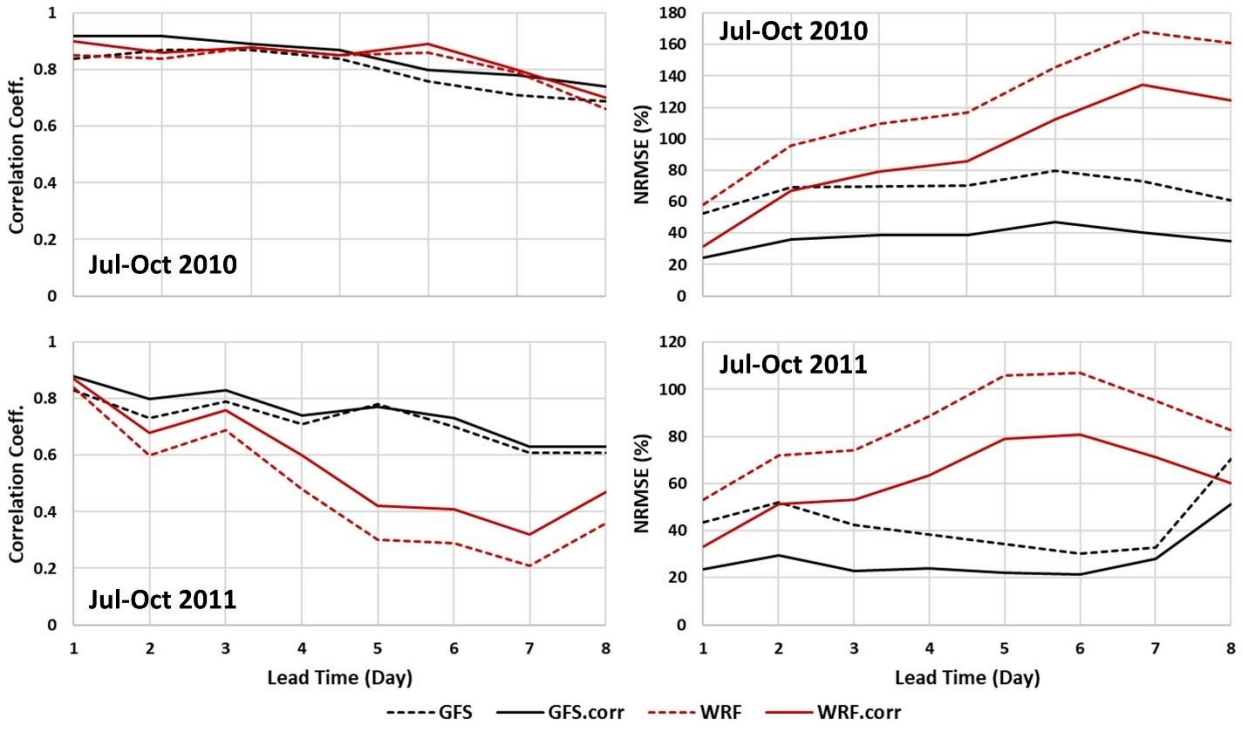


Figure 5.10. Flood forecasting skill in the Mekong river basin at Kampong Cham based on bias corrected and uncorrected QPF data with and without dynamic downscaling. NRMSE refers to RMSE of forecasted flow normalized by observed flow and expressed as a %.

# Chapter 6. CONCLUSIONS AND RECOMMENDATIONS

The focus of the study was to evaluate the performance of forecasted flow using different numerical modeling based approaches during the monsoon to improve current operational flood forecasting. This assessment was carried out by evaluating the flow derived from different numerical model forecasted precipitation and other meteorological data. The study started with the GCM products, and continued with the optimization of a regional NWP model configurations and exploration of initial conditions. In closure, the forecasted flow derived from the optimized regional NWP model and global NWP model was compared to address the research questions posed earlier in this study.

To address the first question, "*Is GCM forecasts skillful enough to use it in the operational flood forecasting system in monsoon climate?*", the calibrated VIC model of GBM basin was forced with the statistically downscaled NMME precipitation, temperature, and wind speed data. The forecasted flow up to 6-month lead at Ganges and Brahmaputra outlet shows the relative RMSE above 35% and 20% in monthly and seasonal case, respectively. While, the anomaly correlation coefficients were below 50% in all cases, which is unsatisfactory for operational propose. The study also indicates that the flow climatology performs better than the NMME based forecast.

In the next step, to answer the second question, "*Is it feasible to derive a generalized dynamic downscaling approach using the WRF model to forecast precipitation in the river basins with monsoon climate?*", the WRF model was optimized for the monsoon climate before use it to dynamically downscale the GFS products. This step was divided into two parts. At first the sensitivity of 15 different combinations model parameterization schemes was evaluated with 3 different spatial resolution was evaluated to identify the optimized combination. For this study,

the combination between fire microphysics (MP) and three cumulus parameterization (CP) schemes were used in GBM basin. Three suitable MP-CP combination was identified and applied in the Indus basin. The similar response in the Indus basin indicates that a generalized approach for dynamic downscaling in monsoon weather is feasible. In the second part of this step, the WRF model was initialized with different model initialization technique, which were classified as warm start (complex) and cold start (simple). The results indicate that the cold start approach is better as the warm start approach introduce more uncertainty into the system through its complex process.

At the last step, the GFS forecasted precipitation was dynamically downscaled by the optimized WRF setup, and named as WRF forecast. The flow was derived from both GFS and WRF forecasted precipitation using the calibrated VIC model of GBM and Mekong river basins. In the flow performance analysis, the WRF forested flow failed to prove any significant improvement form the GFS forecasted flow. Both models show a significant positive bias in flow prediction. To reduce this bias a simple correction technique based on the climatology was applied. This bias correction technique shows significant improvement in the forecasted flow.

It is clear from this study that the GCM is not a feasible option for operational flood forecasting in monsoon weather regimes. The second step of this study indicates that a generalized dynamic downscaling approach exists for the rain-abundant monsoon season. The most important finding of this study is for end users is perhaps the impact of using the WRF model in flow forecasting, which is not significant in large river basins with monsoon climate when compared with non-downscaled forcing from global NWP. Rather, the simple bias corrected GFS precipitation is an operationally more attractive option for the large river basins of Asia where computational resources are limited and time is of the essence in issuing forecasts

every day. However, it must be mentioned that in a finer resolution, the WRF can more effectively introduce the topographic effect into the atmospheric process than the hydrostatic GFS model of the global NWP model. Such a feature of the regional NWP (WRF) can be valuable for small and flash flood prone river basins like Nepal (Koshi River), or the Northeast region of Bangladesh (Upper Meghna river), especially if WRF is run at < 3 km spatial scale.

Recommendations for a future study should therefore investigate the use of regional NWP models for smaller and flashier river systems where forecasts need to be issued far more frequently (hourly) than monsoonal scale large river flooding (daily). Future studies should also explore the choice of hydrologic models, hydrologic processes and scales that this study has assumed as constant. Lastly, this study recommends that findings from this study, particularly the bias corrected scheme of Chapter 5, be comprehensively promoted and presented to operational flood forecasters of Asia and be operationally implemented. Research is meant to be not only use-inspired, but also user-ready and thus it is the view of this study that several user-ready findings have been identified for the operational flood forecasting community.

# REFERENCES

Adler, R. F., G. J. Huffman, A. Chang, R. Ferraro, P. Xie, J. Janowiak, B. Rudolf, U. Schneider, S. Curtis, D. Bolvin, A. Gruber, J. Susskind, and P. Arkin, (2003), The Version 2 Global Precipitation Climatology Project (GPCP) Monthly Precipitation Analysis (1979-Present), *Journal of Hydrometeorology*, 4(6), 1147-1167, doi:10.1175/1525-7541(2003)004<1147:TVGPCP>2.0.CO;2.

Ahasan, M. N. and A. Q. Khan (2013), Simulation of a flood producing rainfall event of 29 July 2010 over north-west Pakistan using WRF-ARW model, *Natural Hazards*, 69(1), 351-363, doi:10.1007/s11069-013-0719-6.

Alam, M. M. (2014), Impact of cloud microphysics and cumulus parameterization on simulation of heavy rainfall event during 7–9 October 2007 over Bangladesh, *Journal of Earth System Science*, 123(2), 259-279, doi:10.1007/s12040-013-0401-0.

Alexander, M. A., I. Bladé, M. Newman, J. R. Lanzante, N. C. Lau, and J. D. Scott (2002), The atmospheric bridge: The influence of ENSO teleconnections on air-sea interaction over the global oceans, *Journal of Climate*, 15(16), 2205-2231, doi:10.1175/1520-0442(2002)015<2205:TABTIO>2.0.CO;2.

Andreadis, K., P. Storck, and D. P. Lettenmaier (2009), Modeling snow accumulation and ablation processes in forested environments, *Water Resources Research*, 45(5), W05429, doi:10.1029/2008WR007042.

Assari, A., T. M. Maheshand, and E. Assari (2012), Role of public participation in sustainability of historical city: usage of TOPSIS method, *Indian Journal of Science and Technology*, 5(3), 2289-2294.

Bakker, M. H. N. (2009), Transboundary river floods: examining countries, international river basins and continents, *Water Policy*, 11(3), 269-288, doi:10.2166/wp.2009.041.

Bartholmes, J., and E. Todini (2005), Coupling meteorological and hydrological models for flood forecasting, *Hydrology and Earth System Science*, 9(4), 333-346, doi:10.5194/hess-9-333-2005.

Becker, E. J., H. van den Dool, and M. Peña (2013), Short-Term Climate Extremes: Prediction Skill and Predictability, *Journal of Climate*, 26(2), 512–531, doi:10.1175/JCLI-D-12-00177.1.

Bei, N., and F. Zhang (2007), Impacts of initial condition errors on mesoscale predictability of heavy precipitation along the Mei-Yu front of China, *Quarterly Journal of the Royal Meteorological Society*, 133(622), 83-99, doi:10.1002/qj.20.

Bhaskaran, B., R. G. Jones, J. M. Murphy, and M. Noguer (1996), Simulations of the Indian summer monsoon using a nested regional climate model, domain size experiments, *Climate Dynamics*, 12(9), 573-587, doi:10.1007/BF00216267.

Biancamaria, S., F. Hossain, and D. P. Lettenmaier (2011), Forecasting transboundary river water elevations from space, *Geophysical Research Letters*, 38(11), L11401(1-5), doi:10.1029/2011GL047290.

Bowling, L. C., and D. P. Lettenmaier (2010), Modeling the effects of lakes and wetlands on the water balance of Arctic Environments, *Journal of Hydrometeorology*, 11(2), 276-295, doi:10.1175/2009JHM1084.1.

Bray, M., D. Han, Y. Xuan, P. Bates, and M. Williams (2011), Rainfall uncertainty for extreme events in NWP downscaling model, *Hydrological Processes*, 25(9), 1397-1406, doi:10.1002/hyp.7905.

Byerlee, D. (1992), Technical change, productivity, and sustainability in irrigated cropping systems of South Asia: Emerging issues in the post-green revolution Era, *Journal of International Development*, 4(5), 477-496, doi:10.1002/jid.3380040502.

Cane, D., S. Ghigo, D. Rabuffetti, and M. Milelli (2013), Real-time flood forecasting coupling different postprocessing techniques of precipitation forecast ensembles with a distributed hydrological model. The case study of May 2008 flood in western Piemonte, Italy, *Natural Hazards and Earth System Sciences*, 13, 211-220, doi:10.5194/nhess-13-211-2013.

Castro, C. L., R. A. Pielke Sr., and G. Leoncini (2005), Dynamical downscaling: Assessment of value retained and added using the Regional Atmospheric Modeling System (RAMS), *Journal of Geophysical Research*, 110, D05108, doi:10.1029/2004JD004721.

CEGIS (2006), Sustainable end-to-end climate/flood forecast application through pilot projects showing measurable improvements, *Center for Geographic and Environmental Information Services (CEGIS) Report*, 78.

Cherkauer, K. A., L. C. Bowling, and D. P. Lettenmaier (2003), Variable infiltration capacity cold land process model updates, *Global and Planetary Change*, 38(1-2), 151-159, doi:10.1016/S0921-8181(03)00025-0.

Chowdhury, M. R. (2000), An Assessment of Flood Forecasting in Bangladesh: The Experience of the 1998 Flood, *Natural Hazards*, 22(2), 139-163, doi:10.1023/A:1008151023157.

Chowdhury, M. R., and N. Ward (2004), Hydro-Meteorological Variability in the Greater Ganges–Brahmaputra–Meghna Basins, *International Journal of Climatology*, 24(12),1495–1508, doi:10.1002/joc.1076.

Cloke, H. L., and F. Pappenberger (2009), Ensemble flood forecasting: a review, *Journal of Hydrology*, 375(3-4), 613–626. doi:10.1016/j.jhydrol.2009.06.005.

Coe, M. T. (2000), Modeling Terrestrial Hydrological Systems at the Continental Scale, Testing the accuracy of an Atmospheric GCM, *Journal of Climate*, 13(4), 686-704, doi:10.1175/1520-0442(2000)013<0686:MTHSAT>2.0.CO;2.

Costa-Cabral, M. C, J. E Richey, G. Goteti, D. P. Lettenmaier, C. Feldkötter, and A. Snidvongs (2008), Landscape structure and use, climate, and water movement in the Mekong River basin, *Hydrological Processes*, 22(12), 1731-1746, doi:10.1002/hyp.6740.

Cuo, L., T. C.Pagano, and Q. J. Wang (2011), A Review of Quantitative Precipitation Forecasts and Their Use in Short- to Medium-Range Streamflow Forecasting, *Journal of Hydrometeorology*, 12(5), 713-728, doi:10.1175/2011JHM1347.1.

Davolio, S., M. M. Miglietta, T. Diomede, C. Marsigli, A. Morgillo, and A. Moscatello (2008), A meteo-hydrological prediction system based on a multi-model approach for precipitation forecasting, *Natural Hazards and Earth System Science*, 8, 143-159, doi:10.5194/nhess-8-143-2008.

Dudhia, J. (1989), Numerical study of convection observed during the Winter Monsoon Experiment using a mesoscale two–dimensional model, *Journal of the Atmospheric Science*, 46(20), 3077-3107, doi:10.1175/1520-0469(1989)046<3077:NSOCOD>2.0.CO;2.

Dulal, H. B. (2014), Governing climate change adaptation in the Ganges basin: assessing needs and capacities, *International Journal of Sustainable Development and World Ecology*, 21(1), 1-14, doi:10.1080/13504509.2013.871657.

Dumenil, L. and E. Todini (1992), A rainfall-runoff scheme for use in the Hamburg climate model, In J. P. O'Kane, ed. *Advances in Theoretical Hydrology: A tribute to James Dooge*, Elsevier Science Publishers B.V., Amsterdam, 129-157.

Durai, V. R., and R. Bhardwaj (2013), Improving precipitation forecasts skill over India using a multi-model ensemble technique, *Geofizika*, 30(2), 119-141.

Dwivedi, S., A. K. Mittal, B. N. Goswami (2006), An empirical rule for extended range prediction of duration of Indian summer monsoon breaks, *Geophysical Research Letters*, 33(18), L18801(1-5), doi:10.1029/2006GL027035.

Dyurgerov, M. B., and M. F. Meier (2005), Glaciers and the changing earth system: a 2004 snapshot, Occasional Paper No. 58, *INSTAAR*, University of Colorado, Boulder, USA.

Ebert, E. E. (2001), Ability of a Poor Man's Ensemble to Predict the Probability and Distribution of Precipitation, *Monthly Weather Review*, 129(10), 2461-2480, doi:10.1175/1520-0493(2001)129<2461:AOAPMS>2.0.CO;2.

Efstathiou, G. A., N. M. Zoumakis, D. Melas, C. J. Lolis, and P. Kassomenos (2013), Sensitivity of WRF to boundary layer parameterizations in simulating a heavy rainfall event using different microphysics schemes. Effect on large-scale processes, *Atmospheric Research*, 132-133, 125-143.

FAO. (2011), *AQUASTAT*, http://www.fao.org/nr/water/aquastat/main/index.stm [accessed 24 September 2017].

FFWC (2014), *Annual Flood Report 2014*, Flood Forecasting and Warning Centre, Bangladesh Water Development Board, Dhaka, Bangladesh, http://www.ffwc.gov.bd/images/annual14.pdf [accessed 24 September 2017].

Freitas, S. R. et al. (2017), The Brazilian developments on the Regional Atmospheric Modeling System (BRAMS 5.2), an integrated environmental model tuned for tropical areas, *Geoscientific Model Development*, 10, 189-222, doi:10.5194/gmd-10-189-2017.

Funk, C., A. Hoell., S. Shukla, I. Bladé, B. Liebmann, J. B. Roberts, F. R. Robertson, and G. Husak (2014), Predicting East African spring droughts using Pacific and Indian Ocean sea surface temperature indices, *Hydrology and Earth System Sciences*, 18, 4965-4978, doi:10.5194/hess-18-4965-2014.

Funk, C., P. Peterson, M. Landsfeld, D. Pedreros, J. Verdin, S. Shukla, G. Husak, J. Rowland, L. Harrison, A. Hoell, and J. Michaelsen (2015), The climate hazards infrared precipitation with stations—a new environmental record for monitoring extremes, *Scientific Data 2*, 150066, doi:10.1038/sdata.2015.66.

Georgakakos, K. P., N. E. Graham, T. M. Modrick, M. J. Murphy Jr., E. Shamir, C. R. Spencer, and J. A. Sperfslage (2014), Evaluation of real-time hydrometeorological ensemble prediction on hydrologic scales in Northern California, *Journal of Hydrology*, 519, 2978–3000, doi:10.1016/j.jhydrol.2014.05.032.

Givati, A., B. Lynn, Y. Liu, and A. Rimmer (2012), Using the WRF Model in an Operational Streamflow Forecast System for the Jordan River, *Journal of Applied Meteorology and Climatology*, 51(2), 285-299, doi:10.1175/JAMC-D-11-082.1.

Grell, G. A. and S. R. Freitas (2014), A scale and aerosol aware stochastic convective parameterization for weather and air quality modeling, *Atmospheric Chemistry and Physics*, 14, 5233-5250, doi:10.5194/acp-14-5233-2014.

Hagedorn, R., F. Doblas-Reyes, and T. Palmer (2005), The rationale behind the success of multi-model ensembles in seasonal forecasting – I. Basic concept, *Tellus*, 57A, 219–233, doi:10.1111/j.1600-0870.2005.00103.x.

Hamlet, A. F., and D. P. Lettenmaier (1999a), Effects of Climate Change on Hydrology and Water Resources in the Columbia River Basin, *Journal of the American Water Resources Association*, 35(6), 1597-1623, doi:10.1111/j.1752-1688.1999.tb04240.x.

Hamlet, A. F., and D. P. Lettenmaier (1999b), Columbia River Streamflow Forecasting Based on ENSO and PDO Climate Signals, *Journal of Water Resources Planning and Management*, 125(6), 333-341, doi:10.1061/(ASCE)0733-9496(1999)125:6(333).

Hapuarachchi, H. A. P., Q. J. Wang, and T. C. Pagano (2011), A review of advances in flash flood forecasting, *Hydrological Process*, 25, 2771-2784.

Hirpa, F.A., T. M. Hopson, T. D. Groeve, G. R. Brakenridge, M. Gebremichael, and P. J. Restrepo (2013), Upstream satellite remote sensing for river discharge forecasting:

Application to major rivers in South Asia, *Remote Sensing of Environment*, 131, 140-151, doi:10.1016/j.rse.2012.11.013.

Hong, S. Y., Y. Noh, and J. Dudhia (2006), A new vertical diffusion package with an explicit treatment of entrainment processes, *Monthly Weather Review*, 134, 2318-2341, doi:10.1175/MWR3199.1.

Hong, S. Y., and J. O. J. Lim (2006), The WRF Single-Moment 6-Class Microphysics Scheme (WSM6), *Journal of Korean Meteorological Society*, 42(2), 129-151.

Hong, S. Y., J. Dudhia, and S. H. Chen (2004), A Revised Approach to Ice Microphysical Processes for the Bulk Parameterization of Clouds and Precipitation, *Monthly Weather Review*, 132, 103-120, doi: 10.1175/1520-0493(2004)132<0103:ARATIM>2.0.CO;2.

Hong, S. Y., and J. W. Lee (2009), Assessment of the WRF model in reproducing a flash-flood heavy rainfall event over Korea, *Atmospheric Research*, 93(4), 818-831.

Hopson, T. M., and P. J. Webster (2010), A 1-10-Day Ensemble Forecasting Scheme for the Major River Basins of Bangladesh: Forecasting Severe Floods of 2003-07, *Journal of Hydrometeorology*, 11, 618-641.

Hossain, F., M. Maswood, A. H. Sidddique-E-Akbor, W. Yigzaw, L. C. Mazumder, T. Ahmed, M. Hossain, S. M. ShahNewaz, A. Limaye, H. Lee, S. Pradhan, B. Shrestha, B. Bajracahrya, S. Biancamaria, C. K. Shum, and F. J. Turk (2014c), A Promising Radar Altimetry Satellite System for Operational Flood Forecasting in Flood-Prone Bangladesh, *IEEE Geoscience and Remote Sensing Magazine*, 2(3), 27-36.

Hossain, F. (2014), The Paradox of Peak Flows in a Changing Climate, *Journal of Hydrologic Engineering*, 19(9), 02514001, doi:10.1061/(ASCE)HE.1943-5584.0001059.

Hossain, F. and N. Katiyar (2006), Improving Flood Forecasting in International River Basins, *EOS (AGU)*, 87(5), 49-60.

Hossain, F., C. K. Shum, F. J. Turk, S. Biancamaria, H. Lee, A. Limaye., L. C. Mazumder, M. Hossain, S. Shah-Newaz, T. Ahmed, W. Yigzaw, A. H. M. Siddique-E-Akbor (2014a), Crossing the "Valley of Death": Lessons Learned from Implementing an Operational Satellite-Based Flood Forecasting System, *Bulletin of American Meteorological Society*, 95(8), 1201-1207, doi:10.1175/BAMS-D-13-00176.1.

Hossain, F., A. H. Siddique-E-Akbor, L. C. Mazumder, S. M. ShahNewaz, S. Biancamaria, H. Lee and C. K. Shum (2014b), Proof of Concept of an Altimeter-Based River Forecasting System for Transboundary Flow Inside Bangladesh. *IEEE Journal of Selected Topics in Applied Remote Sensing*, 7(2), 587-601, doi:10.1109/JSTARS.2013.2283402.

Hossain, F., S. Sikder, N. Biswas, M. Bonnema, H. Lee, N. D. Luong, N. H. Hiep, B. D. Duong and D. Long (2017), Predicting Water Availability of the Regulated Mekong River Basin Using Satellite Observations and a Physical Model, *Asian Journal of Water, Environment and Pollution*, 14(3), 39-48, doi:10.3233/AJW-170024.

Hossain, F., N. Katiyar, Y. Hong, and A. Wolf (2007), The emerging role of satellite rainfall data in improving the hydro-political situation of flood monitoring in the under-developed regions of the world, *Natural Hazards*, 43(2), 199-210.

Houze Jr., R. A., K. L. Rasmussen, S. Medina, S. R. Brodzik, U. Romatschke (2011), Anomalous Atmospheric Events Leading to the Summer 2010 Floods in Pakistan, *Bulletin of American Meteorological Society*, 92(3), 291-298.

Hsiao, L. F., M. J. Yang, C. S. Lee, H. C. Kuo, D. S. Shih, C. C. Tsai, C. J. Wang, L. Y. Chang, D. Y. C. Chen, L. Feng, J. S. Hong, C. T. Fong, D. S. Chen, T. C. Yeh, C. Y. Huang, W. D. Guo, and G. F. Lin (2013), Ensemble forecasting of typhoon rainfall and floods over a mountainous watershed in Taiwan, *Journal of Hydrology*, 506, 55–68.

Huffman, G. J., D. T. Bolvin, D. Braithwaite, K. Hsu, R. Joyce, and P. Xie (2015), *GPM Integrated Multi-Satellite Retrievals for GPM (IMERG) Algorithm Theoretical Basis Document (ATBD) v4.5*, http://pmm.nasa.gov/sites/default/files/document_files/IMERG_ATBD_V4.5_0.pdf [accessed 24 September 2017].

Huffman (2013), *Algorithm 3B42: TRMM Merged HQ/Infrared Precipitation*, http://trmm.gsfc.nasa.gov/3b42.html [accessed 24 September 2017].

Hwang, C. L. and K. Yoon (1981), *Multiple Attribute Decision Making: Methods and Applications*, Springer-Verlag, Berlin-Heidelberg, Germany.

IPCC (2013), *What is a GCM?* Intern-governmental Panel on Climate Change (IPCC), http://www.ipcc-data.org/guidelines/pages/gcm_guide.html [accessed 24 September 2017].

Islam, A. K. M. S., A. Haque, S. K. Bala (2010), Hydrologic characteristics of floods in Ganges–Brahmaputra–Meghna (GBM) delta, *Natural Hazards*, 54(3), 797-811.

Jacques, F. M. B., T. Su, Y. J. Huang, L. Wang, and Z. K. Zhou (2013), A global-scale test for monsoon indices used in palaeoclimatic reconstruction, *Palaeoworld*, 22(3-4), 93-100, doi:10.1016/j.palwor.2013.02.002.

Jang, J., and S. Y. Hong (2014), Quantitative forecast experiment of a heavy rainfall event over Korea in a global model: horizontal resolution versus lead time issues, *Meteorology and Atmospheric Physics*, 124(3), 113-127.

Janjic, Z. I. (1994), The Step–Mountain Eta Coordinate Model: Further developments of the convection, viscous sublayer, and turbulence closure schemes, *Monthly Weather Review*, 122, 927-945, doi:10.1175/1520-0493(1994)122<0927:TSMECM>2.0.CO;2.

Jankov, I., W. A. Gallus Jr., M. Segal, and S. E. Koch (2007), Influence of initial conditions on the WRF-ARW Model QPF response to physical parameterization changes, *Weather Forecast*, 22(3), 501-519, doi:10.1175/WAF998.1.

Jasper, K., J. Gurtz, and H. Lang (2002), Advanced flood forecasting in Alpine watersheds by coupling meteorological observations and forecasts with a distributed hydrological model, *Journal of Hydrology*, 267(1-2), 40-52, doi:10.1016/S0022-1694(02)00138-5.

Jian, J., P. J. Webster, and C. D. Hoyos, (2009), Large-scale controls on Ganges and Brahmaputra river discharge on intraseasonal and seasonal time-scales, *Quarterly Journal of the Royal Meteorological Society*, 135, 353–370, doi:10.1002/qj.384.

Kain, J. S. (2004), The Kain–Fritsch convective parameterization: An update, *Journal of Applied Meteorology and Climatology*, 43, 170-181, doi:10.1175/1520-0450(2004)043<0170:TKCPAU>2.0.CO;2.

Kale, V. S. (2014), Is flooding in South Asia getting worse and more frequent? *Journal of Tropical Geography*, 35(2), 161-178.

Kale, V. (2012), On the link between extreme floods and excess monsoon epochs in South Asia, *Climate Dynamics*, 39(5), 1107-1122.

Kalnay, E. (2003), *Atmospheric modeling, data assimilation, and predictability*, Cambridge University Press, New York, USA.

Katiyar, N., and F. Hossain (2007), An open-book watershed model for prototyping space-borne flood monitoring systems in International River Basins, *Environmental Modelling and Software*, 22(12), 1720-1731.

Khromov, S. P. (1957), Die Geographische Verbreitung der Monsune, *Petermanns Geographische Mitteilungen*, 101, 234-237.

Kirtman, B. P., et al. (2014), The North American Multi-Model Ensemble (NMME): Phase-1 seasonal to inter-annual prediction, phase-2 toward developing intra-seasonal prediction, *Bulletin of American Meteorological Society*, 95(4), 585-601, doi:10.1175/BAMS-D-12-00050.1.

Klein, S. A., B. J. Soden, and N. C. Lau (1999), Remote sea surface temperature variations during ENSO: Evidence for a tropical atmospheric bridge, *Journal of Climate*, 12(4), 917–932, doi:10.1175/1520-0442(1999)012<0917:RSSTVD>2.0.CO;2.

Kumar, P., C. M. Kishtawal, P. K. Pal (2015), Impact of ECMWF, NCEP, and NCMRWF global model analysis on the WRF model forecast over Indian Region, *Theoretical and Applied Climatology*, doi:10.1007/s00704-015-1629-1.

Kumar, P., C. M. Kishtawal, and P. K. Pal (2016), Skill of regional and global model forecast over Indian region, *Theoretical and Applied Climatology*, 123(3), 629-636, doi:10.1007/s00704-014-1361-2.

Kumar, P., M. V. Shukla, P. K. Thapliyal, J. H. Bisht, and P. K. Pal (2012), Evaluation of upper tropospheric humidity from NCEP analysis and WRF Model Forecast with Kalpana

observation during Indian summer monsoon 2010, *Meteorological Applications*, 19, 152–160, doi:10.1002/met.1332.

Kumar, R. A., J. Dudhia, and S. K. R. Bhowmik (2010), Evaluation of Physics options of the Weather Research and Forecasting (WRF) Model to simulate high impact heavy rainfall events over Indian Monsoon region, *Geofizika*, 27(2), 101-125.

Kummu, M., and J. Sarkkula (2008), Impact of the Mekong River flow alteration on the Tonle Sap flood pulse, *AMBIO*, 37(3), 185–192. doi:10.1579/0044-7447(2008)37[185:IOTMRF]2.0.CO;2

Kundzewicz, Z. W., and E. Z. Stakhiv (2010), Are climate models "ready for prime time" in water resources management applications, or is more research needed? *Hydrological Sciences Journal*, 55(7), 1085–1089, doi:10.1080/02626667.2010.513211.

Liang, X., D. P. Lettenmaier, E. F. Wood, and S. J. Burges (1994), A Simple hydrologically based model of land surface water and energy fluxes for GSMs, *Journal of Geophysical Research*, 99(D7), 14,415–14,428, doi:10.1029/94JD00483.

Liguori, S., M. A. R. Ramirez, A. N. A. Schellart, and A. J. Saul (2012), Using probabilistic radar rainfall nowcasts and NWP forecasts for flow prediction in urban catchments, *Atmospheric Research*, 103, 80-95.

Lim, K. S. S., and S. Y. Hong (2010), Development of an Effective Double-Moment Cloud Microphysics Scheme with Prognostic Cloud Condensation Nuclei (CCN) for Weather and Climate Models, *Monthly Weather Review*, 138, 1587-1612, doi:10.1175/2009MWR2968.1.

Liu, J., J. Wang, S. Pan, K. Tang, C. Li, and D. Han (2015), A real-time flood forecasting system with dual updating of the NWP rainfall and the river flow, *Natural Hazards*, 77, 1161-1181.

Liu, J., M. Bray, and D. Han (2012), Sensitivity of the Weather Research and Forecasting (WRF) model to downscaling ratios and storm types in rainfall simulation, *Hydrological Processes*, 26, 3012-3031.

Lohmann, D., E. Raschke, B. Nijssen, and D. P. Lettenmaier (1998), Regional scale hydrology: I. Formulation of the VIC-2L model coupled to a routing model, *Hydrological Sciences Journal*, 43, 131–141.

Lohmann, D., R. N. Holube, and E. Raschke (1996), A large-scale horizontal routing model to be coupled to land surface parametrization schemes, *Tellus*, 48(5), 708-721.

Lorenz, E. (1963), Deterministic non-periodic flows, *Journal of the Atmospheric Sciences*, 20, 130-141.

Lowrey, M. R. K., and Z. Yang (2008), Assessing the Capability of a Regional-Scale Weather Model to Simulate Extreme Precipitation Patterns and Flooding in Central Texas, *Weather and Forecasting*, 23(6), 1102-1126.

Mannan, M. A., M. A. M. Chowdhury, and S. Karmakar (2013), Application of NWP model in prediction of heavy rainfall in Bangladesh, *Procedia Engineering*, 53, 667-675.

Maswood, M., and F. Hossain (2015), Advancing river modelling in ungauged basins using satellite remote sensing: the case of the Ganges-Brahmaputra-Meghna basin, *International Journal of River Basin Management*, 14(1), 103-117, doi:10.1080/15715124.2015.1089250.

Medina, S., R. A. Houze Jr., A. Kumar, D. Niyogi (2010), Summer monsoon convection in the Himalayan region: Terrain and land cover effects, *Quarterly Journal of the Royal Meteorological Society*, 136(648), 593-616.

Memon, A. A., S. Muhammad, S. Rahman, M. Haq (2015), Flood monitoring and damage assessment using water indices: A case study of Pakistan flood-2012, *The Egyptian Journal of Remote Sensing and Space Sciences*, 18(1), 99-106.

Milani, A. S., A. Shanian, R. Madoliat, and J. A. Nemes (2005), The effect of normalization norms in multiple attribute decision making models: a case study in gear material selection, *Structural and Multidisciplinary Optimization*, 29, 312-318, doi:10.1007/s00158-004-0473-1.

Mirza, M. M. Q. (2011), Climate change, flooding in South Asia and implications, *Regional Environmental Change*, 11(Supplement 1), 95-107.

Mirza, M. Q., R. A. Warrick, N. J. Ericksen, and G. J. Kenny (1998), Trends and persistence in precipitation in the Ganges, Brahmaputra and Meghna river basins, *Hydrological Science Journal*, 43(6), 845-858.

Mirza, M. Q. M. (1998), Diversion of the Ganges Water at Farakka and Its Effects on Salinity in Bangladesh, *Environmental Management*, 22(5), 711-722, doi:10.1007/s002679900141.

Misra, A. K., A. Saxena, M. Yaduvanshi, A. Mishra, Y. Bhauduriya, and A. Takur. (2007), Proposed River Linking Project of India: Boon or Bane to Nature? *Environmental Geology*, 51(8), 1361-1376, doi: 10.1007/s00254-006-0434-7.

Miyakoda, K., G. D. Hembree, R. F. Strickler and I. Shulman (1972), Cumulative results of extended forecast experiments: I. Model performance for winter cases, *Monthly weather Review*, 100(12), 836-855.

Mlawer, E. J., S. J. Taubman, P. D. Brown, M. J. Iacono, and S. A. Clough (1997), Radiative transfer for inhomogeneous atmospheres: RRTM, a validated correlated–k model for the longwave, *Journal of Geophysical Research*, 102(D14), 16663-16682, doi:10.1029/97JD00237.

Molden, D. (2007), *Water for Food, Water for Life*, D. Molden, ed., International Water Management Institute, Earthscan, London, UK.

Morrison, H. and G. Thompson (2009), Impact of Cloud Microphysics on the Development of Trailing Stratiform Precipitation in a Simulated Squall Line: Comparison of One– and Two–Moment Schemes, *Monthly Weather Review*, 132, 103-120, doi:10.1175/2008MWR2556.1.

Mukhopadhyay, P., S. Taraphdar, B. N. Goswami, and K. Krishnakumar (2010), Indian Summer Monsoon Precipitation Climatology in a High-Resolution Regional Climate Model: Impacts of Convective Parameterization on Systematic Biases, *Weather and Forecasting*, 25(2), 369-387, doi:10.1175/2009WAF2222320.1.

Müller, W. A., C. Appenzeller, F. J. Doblas-Reyes, and M. A. Liniger. (2005), A debiased ranked probability skill score to evaluate probabilistic ensemble forecasts with small ensemble sizes, *Journal of Climate*, 18, 1513–1523, doi:10.1175/JCLI3361.1.

Murphy, A. H., and E. S. Epstein (1989), Skill Scores and Correlation Coefficients in Model Verification, *Monthly weather Review*, 117, 572–582.

Nam, D. H., D. T. Mai, K. Udo, and A. Mano (2014), Short-term flood inundation prediction using hydrologic-hydraulic models forced with downscaled rainfall from global NWP, *Hydrological Processes*, 28, 5844-5859.

Negri, A. J., N. Burkardt, J. H. Golden, J. B. Halverson, G. J. Huffman, M. C. Larsen, J. A. Mcginley, R. G. Updike, J. P. Verdin, and G. F. Wieczorek (2005), The Hurricane-Flood-Landslide continuum, *Bulletin of American Meteorological Society*, 1241-1247, doi:10.1175/BAMS-86-9-1241.

Nishat, A., and I. M. Faisal (2000), An Assessment of the Institutional Mechanisms for Water Negotiations in the Ganges-Brahmaputra-Meghna System, *International Negotiation*, 5(2), 289-310.

Nishat, B., and M. Rahman (2009), Water Resources Modeling of the Ganges-Brahmaputra-Meghna River Basins Using Satellite Remote Sensing Data, *Journal of the American Water Resources Association*, 45(6), 1313-1327, doi:10.1111/j.1752-1688.2009.00374.x.

NRC (2010), *Assessment of Intraseasonal to Interannual Climate Prediction and Predictability*, National Academies Press, Washington D.C., USA, 192.

Paudyal, G. N. (2002), Forecasting and warning of water-related disasters in a complex hydraulic setting-the case of Bangladesh, *Hydrological Science Journal*, 47, S(5-18).

Paulikas, M. J., and M. K. Rahman (2015), A temporal assessment of flooding fatalities in Pakistan (1950–2012), *Journal of Flood Risk Management*, 8(1), 62-70.

Pennelly, C., G. Reuter, and T. Flesch (2014), Verification of the WRF model for simulating heavy precipitation in Alberta, *Atmospheric Research*, 135-136, 172-192.

Pielke Sr., R. A. (1998), Letters to the editor-Climate Prediction as an Initial Value Problem, *Bulletin of the American Meteorological Society*, 79(12), 2743-2745.

Rajeevan, M., A. Kesarkar, S. B. Thampi, T. N. Rao, B. Radhakrishna, and M. Rajasekhar (2010), Sensitivity of WRF cloud microphysics to simulations of a severe thunderstorm event over Southeast India, *Annales Geophysicae*, 28, 603-619.

Raju, A., A. Parekh, P. Kumar, and C. Gnanaseelan (2015), Evaluation of the impact of AIRS profiles on prediction of Indian summer monsoon using WRF variational data assimilation system, *Journal of Geophysical Research: Atmospheres*, 120(16), 8112-8131, doi:10.1002/2014JD023024.

Rakesh, V., R. Singh, P. K. Pal, and P. C. Joshi (2007), Sensitivity of Mesoscale Model Forecast During a Satellite Launch to Different Cumulus Parameterization Schemes in MM5, *Pure and Applied Geophysics*, 164(8), 1617-1637.

Rakesh, V., R. Singh, P. K. Pal, and P. C. Joshi (2009a), Impacts of Satellite-Observed Winds and Total Precipitable Water on WRF Short-Range Forecasts over the Indian Region during the 2006 Summer Monsoon, *Weather Forecast*, 24(6), 1706-1731.

Rakesh, V., R Singh, D. Yuliya, P. K. Pal, and P. C. Joshi (2009b), Impact of variational assimilation of MODIS thermodynamic profiles in the simulation of western disturbance, *International Journal of Remote Sensing*, 30(18), 4867-4887.

Ramage, C. S. (1971), *Monsoon Meteorology*, Academic Press, London, UK.

Rao, Y. V. R., H. R. Hatwar, A. K. Salah, and Y. Sudhakar (2007), An Experiment Using the High Resolution Eta and WRF Models to Forecast Heavy Precipitation over India, *Pure and Applied Geophysics*, 164, 1593-1615.

Ratnam, J. V., and E. A. Cox (2006), Simulation of monsoon depressions using MM5: sensitivity to cumulus parameterization schemes, *Meteorology and Atmospheric Physics*, 93(1), 53-78.

Reynolds, R. W., T. M. Smith, C. Liu, D. B. Chelton, K. S. Casey, and M. G. Schlax (2007), Daily high-resolution-blended analyses for sea surface temperature, *Journal of Climate*, 20(22): 5473–5496, doi:10.1175/2007JCLI1824.1.

Roberts, N. M., S. J. Cole, R. M. Forbes, R. J. Moore, and D. Boswell (2009), Use of high-resolution NWP rainfall and river flow forecasts for advance warning of the Carlisle flood, north-west England, *Meteorological Applications*, 16, 23–34.

Roberts, N. M., and H. W. Lean (2008), Scale-selective verification of rainfall accumulations from high-resolution forecasts of convective events, *Monthly Weather Review*, 136(1), 78-97.

Roberts, N. M., S. J. Cole, R. M. Forbes, R. J. Moore, and D. Boswell (2009), Use of high-resolution NWP rainfall and river flow forecasts for advance warning of the Carlisle flood, north-west England, *Meteorological Applications*, 16, 23-34.

Routray, A., U. C. Mohanty, S. R. H. Rizvi, D. Niyogi, K. K. Osuri, and D. Pradhan (2010), Impact of Doppler weather radar data on numerical forecast of Indian monsoon depressions, *Quarterly Journal of the Royal Meteorological Society*, 136(652), 1836-1850.

Salas, J. D., B. Rajagopalan, L. Saito, and C. Brown, (2012), Special Section on Climate Change and Water Resources: Climate Nonstationarity and Water Resources Management, *Journal of Water Resources Planning and Management*, 138(5), 385–388.

Shah, R. B. (2001), Ganges-Brahmaputra: The Outlook for the Twenty-first Century, In A. K. Biswas and J. I. Uitto, ed. *Sustainable Development of the Ganges-Brahmaputra-Meghna Basins*, Oxford University Press, New Delhi, India, 17-45.

Sheffield, J., B. Livneh, and E. F. Wood (2012), Representation of Terrestrial Hydrology and Large Scale Drought of the Continental US from the North American Regional Reanalysis, *Journal of Hydrometeorology*, doi:10.1175/JHM-D-11-065.1.

Sheffield, J., G. Goteti, E. F. Wood, (2006), Development of a 50-year high-resolution global dataset of meteorological forcings for land surface modeling, *Journal of Climate*, 19(3): 3088-3111.

Shrestha, K. Y., P. J. Webster, and V. E. Toma (2014), An Atmospheric–Hydrologic Forecasting Scheme for the Indus River Basin, *Journal of Hydrometeorology*, 15, 861–890.

Shrestha, M. S., W. E. Grabs, and V. R. Khadgi (2015), Establishment of a regional flood information system in the Hindu Kush Himalayas: challenges and opportunities, *International Journal of Water Resources Development*, 31(2), 238-252. doi:10.1080/07900627.2015.1023891.

Siddique-E-Akbor, A. H. M., F. Hossain, S. Sikder, C. K. Shum, S. Tseng, Y. Yi, F. J. Turk and A. Limaye (2014), Satellite Precipitation Data Driven Hydrologic Modeling for Water Resources Management in the Ganges, Brahmaputra and Meghna Basins, *Earth Interactions*, doi:10.1175/EI-D-14-0017.1.

Sikder, M. S., and F. Hossain (2015), Understanding the Geophysical Sources of Uncertainty for Satellite Interferometric (SRTM)-Based Discharge Estimation in River Deltas: The Case for Bangladesh, *IEEE Journal of Selected Topics in Applied Earth Observations and Remote Sensing*, 8(2), 523-538.

Sikder, S., X. Chen, F. Hossain, J. B. Roberts, F. Robertson, C. K. Shum and F. J. Turk (2016), Are General Circulation Models Ready for Operational Streamflow Forecasting for Water Management in the Ganges and Brahmaputra River Basins? *Journal of Hydrometeorology*, 17(1), 195-210, doi:10.1175/JHM-D-14-0099.1.

Sikder, S., and F. Hossain (2016), Assessment of the weather research and forecasting model generalized parameterization schemes for advancement of precipitation forecasting in monsoon-driven river basins, *Journal of Advances in Modeling Earth Systems*, 8(3), 1210-1228. doi:10.1002/2016MS000678.

Sikder, S., and F. Hossain (2017a), Sensitivity of Initial Condition and Cloud Microphysics to Forecasting of Monsoon Rainfall in South Asia, *Meteorological Applications* [in revision].

Sikder, S., and F. Hossain (2017b), Improving Operational Flood Forecasting in Monsoon Climates with Bias-corrected Quantitative Forecasting of Precipitation. *International Journal of River Basin Management* [in review].

Sikka, R. D., and P. S. Rao (2008), The use and performance of mesoscale models over the Indian region for two high-impact events, *Natural Hazards*, 44(3), 353-372.

Sinha, I. N. (1995), Opportunity, Delay and Policy Planning Vision in the Synergic Development of Eastern Himalayan Rivers: A Conspectus, *International Journal of Water Resources Development*, 11(3), doi:10.1080/07900629550042254.

Skamarock, W. C., J. B. Klemp, J. Dudhia, D. O. Gill, D. M. Barker, M. G. Duda, X. Y. Hung, W. Wang, and J. G. Powers (2008), *A Description of the Advanced Research WRF Version 3*, National Center for Atmospheric Research Technical Note, NCAR/TN-475+STR.

Sokol, Z. (2009), Effects of an assimilation of radar and satellite data on a very-short range forecast of heavy convective rainfalls, *Atmospheric Research*, 93, 188-206.

Sood, A., and B. K. P. Mathukumalli (2011), Managing international river basins: reviewing India–Bangladesh transboundary water issues, *International Journal of River Basin Management*, 9(1), 43-52.

Sowjanya, K., S. C. Kar, A. Routray, and P. Mali (2013), Impact of SSM/I retrieval data on the systematic bias of analyses and forecasts of the Indian summer monsoon using WRF assimilation system, *International Journal of Remote Sensing*, 34(2), 631-654.

Srinivas, C. V., D. H. Prasad, D. V. B. Rao, R. Baskaran, and B. Venkatraman (2015), Simulation of the Indian summer monsoon onset-phase rainfall using a regional model, *Annales Geophysicae*, 33(9), 1097-1115.

Srinivas, C. V., D. Hariprasad, D. V. B. Rao, Y. Anjaneyulu, R. Baskaran, and B. Venkatraman (2013), Simulation of the Indian summer monsoon regional climate using advanced research WRF model, *International Journal of Climatology*, 33(5), 1195-1210, doi:10.1002/joc.3505.

Stensrud, D. J. (2007), *Parameterization Schemes: Keys to Understanding Numerical Weather Prediction Models*, Cambridge University Press, Cambridge, UK.

Syvitski, J. P. M., et al. (2009), Sinking deltas due to human activities, *Nature Geoscience*, 2, 681-686, doi:10.1038/ngeo629.

Tewari, M., F. Chen, W. Wang, J. Dudhia, M. A. LeMone, K. Mitchell, M. Ek, G. Gayno, J. Wegiel, and R. H. Cuenca (2004), Implementation and verification of the unified NOAH land surface model in the WRF model, in *20th Conference on Weather Analysis and Forecasting/16th Conference on Numerical Weather Prediction*, American Meteorological Society, Seattle, Washington, USA.

Thompson, G., P. R. Field, R. M. Rasmussen, and W. D. Hall (2008), Explicit Forecasts of Winter Precipitation Using an Improved Bulk Microphysics Scheme. Part II: Implementation of a New Snow Parameterization, *Monthly Weather Review*, 136, 5095-5115, doi:10.1175/2008MWR2387.1.

Ulate, M., J. Dudhia, and C. Zhang (2014), Sensitivity of the water cycle over the Indian Ocean and Maritime Continent to parameterized physics in a regional model, *Journal of Advances in Modeling Earth Systems*, 6, 1095–1120, doi:10.1002/2014MS000313.

UN-Water (2008), *Transboundary Waters: Sharing Benefits, Sharing Responsibilities*, http://www.unwater.org/app/uploads/2017/05/UNW_TRANSBOUNDARY.pdf [accessed 24 September 2017].

Upadhyaya, S. and R. Ramsankaran (2014), Multi-Index Rain Detection: A New Approach for Regional Rain Area Detection from Remotely Sensed Data, *Journal of Hydrometeorology*, 15, 2314-2330, doi:10.1175/JHM-D-14-0006.1.

Vaidya, S. S. (2006), The performance of two convective parameterization schemes in a mesoscale model over the Indian region, *Meteorology and Atmospheric Physics*, 92(3), 175-190.

Verbunt, M., M. Zappa, J. Gurtz and P. Kaufmann (2006), Verification of a coupled hydrometeorological modelling approach for alpine tributaries in the Rhine basin, *Journal of Hydrology*, 324, 224-238.

Vogel, R. M. (2011), Hydromorphology, *Journal of Water Resources Planning and Management*, 137(2), 147-149, doi: 10.1061/(ASCE)WR.1943-5452.0000122.

Wang, S. Y., R. E. Davies, W. R. Huang, and R. R. Gillies (2011), Pakistan's two-stage monsoon and links with the recent climate change, *Journal of Geophysical Research: Atmospheres*, 116(D16114), 1-15.

Wardah, T., S. H. A. Bakar, A. Bardossy, and M. Maznorizan (2008), Use of geostationary meteorological satellite images in convective rain estimation for flash-flood forecasting, *Journal of Hydrology*, 356, 283-298.

Webster, P. J. (2013), Improve weather forecasts for the developing world, *Nature*, doi: 10.1038/493017a.

Webster, P.J., et al. (2010), Extended-range probabilistic forecasts of Ganges and Brahmaputra floods in Bangladesh, *Bulletin of the American Meteorological Society*, 91(11), 1493-1514.

Wilby, R. L., T. M. L. Wigley, D. Conway, P. D. Jones, B. C. Hewitson, J. Main, and D. S. Wilks (1998), Statistical downscaling of general circulation model output: A comparison of methods, *Water Resources Research*, 34(11), 2995–3008, doi:10.1029/98WR02577.

Wilks, D. S. (2011), *Statistical Methods in the Atmospheric Sciences*, 3rd edition, Elsevier, Amsterdam.

Wood, A. W., E. P. Maurer, A. Kumar, and D. P. Lettenmaier (2002), Long-range experimental hydrologic forecasting for the eastern United States, *Journal of Geophysical Research: Atmospheres*, 107(20), 4429, doi:10.1029/2001JD000659.

World Bank (2016), *Proceedings of the regional flood early warning system workshop*, Washington D.C., World Bank Group, http://documents.worldbank.org/curated/en/431281468000591916/Proceedings-of-the-regional-flood-early-warning-system-workshop [accessed 24 September 2017].

World Bank (2007), *Pakistan - Cyclone and floods 2007 : preliminary damage and needs assessment - Balochistan and Sindh*, Washington D.C., World Bank, http://documents.worldbank.org/curated/en/606211468058511720/Pakistan-Cyclone-and-floods-2007-preliminary-damage-and-needs-assessment-Balochistan-and-Sindh [accessed 24 September 2017].

Wu, H., R. F. Adler, Y. Hong, Y. Tian, and F. Policelli (2012), Evaluation of Global Flood Detection Using Satellite-Based Rainfall and a Hydrologic Model, *Journal of Hydrometeorology*, 13(4), 1268-1284, doi:10.1175/JHM-D-11-087.1.

Xiaodong, C., and F. Hossain (2016), Revisiting extreme storms of the past 100 years for future safety of large water management infrastructures, *Earth's Future*, 4(7), 306–322, doi:10.1002/2016EF000368

Yatagai, A., K. Kamiguchi, O. Arakawa, A. Hamada, N. Yasutomi, and A. Kitoh (2012), APHRODITE: Constructing a Long-term Daily Gridded Precipitation Dataset for Asia based on a Dense Network of Rain Gauges, *Bulletin of American Meteorological Society*, 93(9), 1401-1415, doi:10.1175/BAMS-D-11-00122.1.

Yuan, X., E. F. Wood, and Z. Ma (2015), A review on climate-model-based seasonal hydrologic forecasting: physical understanding and system development, *WIREs Water*, 2(5), 523–536, doi:10.1002/wat2.1088.

Yucel, I. and A. Onen (2014), Evaluation a mesoscale atmosphere model and a satellite-based algorithm in estimating extreme rainfall events in northwestern Turkey, *Natural Hazards and Earth System Science*, 14, 611-624.

Yucel, I., A. Onen, K. K. Yilmaz, and D. J. Gochis (2015), Calibration and evaluation of a flood forecasting system: Utility of numerical weather prediction model, data assimilation and satellite-based rainfall, *Journal of Hydrology*, 523, 49-66.

Zarfl, C., et al. (2015), A global boom in hydropower dam construction, *Aquatic Sciences*, 77(1), 161–170, doi:10.1007/s00027-014-0377-0.

Zhang D. and R. A. Anthes (1982), A high–resolution model of the planetary boundary layer–sensitivity tests and comparisons with SESAME–79 data, *Journal of Applied Meteorology and Climatology*, 21, 1594-1609, doi:10.1175/1520-0450(1982)021<1594:AHRMOT>2.0.CO;2.

Zhang, S. and B. Wang (2008), Global summer monsoon rainy seasons, *International Journal of Climatology*, 28(12), 1563-1578, doi:10.1002/joc.1659.

Zheng, Y., K. Alapaty, J. A. Herwehe, A. D. D. Genio, and D. Niyogi (2015), Improving High-Resolution Weather Forecasts using the Weather Research and Forecasting (WRF) Model with an Updated Kain-Fritsch Scheme, *Monthly Weather Review*, 144(3), 833-860, doi:10.1175/MWR-D-15-0005.1.

# CURRICULUM VITA

# MD. SAFAT SIKDER

University of Washington
Dept. of Civil & Environmental Engineering, Box 352700, Seattle, WA 98195
E-mail: mssikder@uw.edu; safatbd@gmail.com | Cell: +1-931-284-5729
Web: students.washington.edu/mssikder | www.linkedin.com/in/safatsikder

## EDUCATION

**University of Washington, Seattle, USA**
Ph.D. in Civil & Environmental Engineering (June 2018)
Dissertation: *Advancing Precipitation and Transboundary Flood Forecasting in Monsoon Climates.*

**Tennessee Technological University, USA**
M.S. in Civil & Environmental Engineering (December 2013)
Thesis: *Understanding Geophysical Sources of Uncertainty of Satellite Interferometric Discharge Estimation Using Manning's Approach: A Case Study of GBM Delta.*

**Bangladesh University of Engineering and Technology, Bangladesh**
B.Sc. in Water Resources Engineering (October 2009)

## EMPLOYMENT HISTORY

**Graduate Student Research Assistant,** January 2014 - Present
Civil and Environmental Engineering Dept., University of Washington, Seattle, USA

**Graduate Student Research Assistant,** September 2012 – December 2013
Civil and Environmental Engineering Dept., Tennessee Technological University, USA

**Junior Engineer,** October 2010 – August 2012
Flood Management Division, Institute of Water Modelling (IWM), Bangladesh

**Research Assistant,** October 2009 – July 2010
Research, Development and Training Division, Center for Environmental and Geographic Information Services (CEGIS), Bangladesh

## AWARDS & FELLOWSHIPS

| | | |
|---|---|---|
| NASA Earth and Space Science Fellowship | *University of Washington* | 2016-2017 |
| Ivanhoe Graduate Fellowship | *Tennessee Technological University* | 2012 |
| Vocational Scholarship | *BUET, Bangladesh* | 2004-2008 |

# PUBLICATIONS

- **Sikder, M. S.** and F. Hossain (2018), Improving Operational Flood Forecasting in Monsoon Climates with Bias-corrected Quantitative Forecasting of Precipitation, *International Journal of River Basin Management*, 1-11, doi:10.1080/15715124.2018.1476368.
- **Sikder, M. S.** and F. Hossain (2018), Sensitivity of Initial Condition and Cloud Microphysics to Forecasting of Monsoon Rainfall in South Asia, *Meteorological Applications*, 1-18, doi:10.1002/met.1716.
- **Sikder, S.** and F. Hossain (2016), Assessment of the weather research and forecasting model generalized parameterization schemes for advancement of precipitation forecasting in monsoon-driven river basins, *Journal of Advances in Modeling Earth Systems*, 8(3), 1210-1228, doi:10.1002/2016MS000678.
- **Sikder, S.**, X. Chen, F. Hossain, J. B. Roberts, F. Robertson, C. K. Shum, and F. J. Turk (2016), Are General Circulation Models Ready for Operational Streamflow Forecasting for Water Management in the Ganges and Brahmaputra River Basins? *Journal of Hydrometeorology*, 17(1), 195-210, doi:10.1175/JHM-D-14-0099.1.
- **Sikder, M. S.** and F. Hossain (2015), Understanding the Geophysical Sources of Uncertainty for Satellite Interferometric (SRTM)-Based Discharge Estimation in River Deltas: The Case for Bangladesh, *IEEE Journal of Selected Topics in Applied Remote Sensing*, 8(2), 523-538, doi:10.1109/JSTARS.2014.2326893.
- Hossain, F., **S. Sikder**, N. Biswas, M. Bonnema, H. Lee, N.D. Luong, N. H. Hiep, B. D. Duong and D. Long (2017), Predicting Water Availability of the Regulated Mekong River Basin Using Satellite Observations and a Physical Model, *Asian Journal of Water, Environment and Pollution*, 14(3), 39-48, doi:10.3233/AJW-170024.
- Bonnema, M., **S. Sikder**, F. Hossain, M. Durand, C. Gleason, and D. Bjerklie (2016), Benchmarking Wide Swath Altimetry Based River Discharge Estimation Algorithms for the Ganges River System. *Water Resources Research*, 52(4), 2439-2461, doi:10.1002/2015WR017296.
- Bonnema, M., **S. Sikder**, Y. Miao, X. Chen, F. Hossain, I. A. Pervin, S. M. Rahman, and H. Lee (2016), Understanding Satellite-based Monthly-to-Seasonal Reservoir Outflow Estimation as a function of Hydrologic Controls, *Water Resources Research*, 52(5), 4095-4115, doi:10.1002/2015WR017830.
- Siddique-E-Akbor, A. H. M., F. Hossain, **S. Sikder**, C. K. Shum, S. Tseng, Y. Yi, F. J. Turk, and A. Limaye (2014), Satellite Precipitation Data–Driven Hydrological Modeling for Water Resources Management in the Ganges, Brahmaputra, and Meghna Basins, *Earth Interactions*, 18(17), 1-25, doi:10.1175/EI-D-14-0017.1.
- Hossain, M. M., R. Khan, and **M. S. Sikder** (2010), Floodplain mapping of Arial Khan-Naria Khal River in Bangladesh, *Bangladesh Journal of Water Resource Research*, 22, 21-32.
- Ahmad, S., F. Hossain, A. Gebregiorgis, H. Lee, and **S. Sikder** (2018), Assessing Potential of Quantitative Precipitation Forecasts for Urban Flood Management: The Case for Houston and Harris County Flood Control District (HCFCD), *Urban Water* ***(In review)***.

## POSTER AND PRESENTATION

- **Sikder, M. S.** and F. Hossain (2017), A Generalized Approach for Operational Flood Forecasting System of the Monsoon Driven River Basins of South and Southeast Asia, *97th AMS Annual Meeting*, Seattle, USA.
- Hossain, M. M, R. Khan, and **M. S. Sikder** (2009), Floodplain mapping of Arial khan-Naria Khal River reach in Bangladesh, *IAHS 8th Scientific Assembly & 37th IAH Congress*, Hyderabad, India.

## REVIEWER

- Journal of Hydrometeorology, AMS
- Hydrological Sciences Journal, IAHS
- Journal of Hydrology, Elsevier
- Journal of the American Water Resources Association, AWRA
- Proposal Reviewer for National Geographic Society, 2017

## PROFESSIONAL MEMBERSHIPS

- American Geophysical Union, 2013 - present
- American Meteorological Society, 2013 - present
- Institution of Engineers, Bangladesh, 2011 - present
- Bangladesh Society of Geoinformatics, 2010 - present

## PROFESSIONAL SKILLS

| | |
|---|---|
| Programming language | C++, Shell, Python, MATLAB |
| Platform | Windows, Linux |
| GIS and mapping | ArcGIS, MapWindow |
| Numerical modeling | *Weather Prediction:* WRF<br>*Rainfall-runoff:* VIC, SWAT, NAM, SOBEK-RR<br>*Hydrodynamic:* HEC-RAS, MIEK-11, SOBEK-1D<br>*Integrated:* MIKE-FLOOD, SOBEK-2D |
| Others | Remote Sensing & Climate Data Processing, High Performance Computing (HPC) |

## TRAINING & WORKSHOPS

**As Resource Person:**

- SRTM-2 Regional Training Workshop, International Centre for Integrated Mountain Development (ICIMOD), Kathmandu, Nepal (September 2016).
- Training on Variable Infiltration Capacity (VIC) model at University of Washington, Seattle to person/group from:
  - Asian Disaster Preparedness Center (ADPC), Thailand (February 2018)
  - Bangladesh Water Development Board (BWDB), Bangladesh (November 2017)
  - Institute of Water Modelling (IWM), Bangladesh (March – April 2017)

- National Center for Water Resources Planning and Investigation (NAWAPI), Vietnam (October – November 2016)
- Department of Hydrology and Meteorology (DHM), Nepal (April – May 2016)
- National University of Civil Engineering (NUCE), Vietnam (March – April 2016)
- NASA-SERVIR, Huntsville, USA (December 2015)
- Pakistan Council of Research in Water Resources (PCRWR), Pakistan (May – November 2015)
- International Centre for Integrated Mountain Development (ICIMOD), Nepal (July 2014)

**As Trainee:**

- Training on Climate Modeling and Downscaling Techniques, Institute of Water & Flood Management (IWFM), Bangladesh University of Engineering and Technology, Bangladesh (February 2012).
- Seasonal Forecast Information Development and Applications Training, Asian Disaster Preparedness Center (ADPC) & APEC Climate Center (APCC), at Dept. of Agricultural Extension (DAE), Bangladesh (January 2012).
- Training on MIKE FLOOD, Institute of Water Modelling (IWM), Bangladesh (August 2011).
- Weather Research and Forecasting (WRF) training workshop, Asian Disaster Preparedness Center (ADPC) & The Energy and Resources Institute (TERI), at Institute of Water Modelling (IWM), Bangladesh (April 2011).
- Basic Training Course on Open Channel Hydraulics, Hydrology and Mathematical Modelling, Department of Water Resources Engineering, Bangladesh University of Engineering and Technology, Bangladesh (December 2010 – March 2011).
- Training on River Bank Protection, Asian Development Bank (ADB), at Department of Water Resources Engineering, Bangladesh University of Engineering and Technology, Bangladesh (November-December 2009).
- Internship on Water Resources Engineering, Center for Environmental and Geographic Information Services (CEGIS), Bangladesh (February-March 2009).